

RALOXIFENE DELIVERY SYSTEMS FOR OSTEOPOROSIS TREATMENT

A THESIS SUBMITTED TO  
THE GRADUATE SCHOOL OF NATURAL AND APPLIED SCIENCES  
OF  
MIDDLE EAST TECHNICAL UNIVERSITY

BY

AYŞEGÜL KAVAS

IN PARTIAL FULFILLMENT OF THE REQUIREMENTS  
FOR  
DOCTOR OF PHILOSOPHY  
IN  
ENGINEERING SCIENCES

SEPTEMBER 2014



Approval of the thesis:

**RALOXIFENE DELIVERY SYSTEMS FOR OSTEOPOROSIS TREATMENT**

submitted by **AYŞEGÜL KAVAS** in partial fulfillment of the requirements for the degree of **Doctor of Philosophy in Engineering Sciences Department, Middle East Technical University** by,

Prof. Dr. Gülbin Dural Ünver  
Dean, Graduate School of **Natural and Applied Sciences**

\_\_\_\_\_

Prof. Dr. Murat Dicleli  
Head of Department, **Engineering Sciences**

\_\_\_\_\_

Assoc. Prof. Dr. Ayşen Tezcaner  
Supervisor, **Engineering Sciences Dept., METU**

\_\_\_\_\_

Assoc. Prof. Dr. Dilek Keskin  
Co-Supervisor, **Engineering Sciences Dept., METU**

\_\_\_\_\_

**Examining Committee Members:**

Prof. Dr. Ufuk Gündüz  
Biological Sciences Dept., METU

\_\_\_\_\_

Assoc. Prof. Dr. Ayşen Tezcaner  
Engineering Sciences Dept., METU

\_\_\_\_\_

Assoc. Prof. Dr. Korhan Altunbaş  
Histology and Embryology Dept., Afyon Kocatepe University

\_\_\_\_\_

Assoc. Prof. Dr. Senih Gürses  
Engineering Sciences Dept., METU

\_\_\_\_\_

Assoc. Prof. Dr. Sreeparna Banerjee  
Biological Sciences Dept., METU

\_\_\_\_\_

**Date:** 26.09.2014

**I hereby declare that all information in this document has been obtained and presented in accordance with academic rules and ethical conduct. I also declare that, as required by these rules and conduct, I have fully cited and referenced all material and results that are not original to this work.**

Name, Last name :

Signature :

# **ABSTRACT**

## **RALOXIFENE DELIVERY SYSTEMS FOR OSTEOPOROSIS TREATMENT**

Kavas, Ayşegül

Ph.D., Department of Engineering Sciences

Supervisor : Assoc. Prof. Dr. Ayşen Tezcaner

Co-Supervisor: Assoc. Prof. Dr. Dilek Keskin

September 2014, 144 pages

One of the osteoporosis drugs, Raloxifene (Ral) is systemically administrated in high dose at frequent intervals, causing high risk of side effects which influence all the body. As a solution to such issues, delivery systems providing controlled and sustained drug release at therapeutic level from a carrier have been studied recently. The aim of this study was to develop Ral- or Ral-poly(ethylene glycol) (PEG)-loaded poly( $\epsilon$ -caprolactone) (PCL) or PCL:poly(D,L-lactide-co-glycolide) (PLGA) microspheres and to evaluate their potential usage.

Mean diameters of the microspheres were around 1.5  $\mu\text{m}$ . Ral-loaded PCL microspheres had maximum Ral encapsulation efficiency (%) because of high hydrophobic natures of Ral and PCL. Total amount of Ral released from Ral-PEG-loaded PCL:PLGA microspheres was significantly higher than from other microsphere groups. This finding

can be ascribed to enhanced wettability of Ral and conversion of crystalline nature of Ral to amorphous form provided by Ral-PEG conjugation, resulting in increased water-solubility of Ral. Enhanced wettability of Ral increases degradation rates of PCL and PLGA by allowing more water penetration into the polymer matrix. Related with this outcome, Ral release from Ral-PEG-loaded PCL:PLGA microspheres resulted with significantly higher mineralization of female adipose-derived mesenchymal stem cells than other groups. *In vitro* cytotoxicity studies performed using adipose-derived stem cells demonstrated that all microspheres were non-toxic.

It was demonstrated that Ral-PEG-loaded PCL:PLGA microsphere formulation provided increased Ral release rate and therefore enhanced mineralization of the stem cells compared to the other formulations in this study. This formulation holds promise for osteoporosis therapy as an effective controlled drug delivery system. For forthcoming studies, PEG conjugation to Ral presents the possibility of adjusting rate of Ral release from microspheres readily by changing PEG ratio in the conjugate.

Keywords: Raloxifene, Controlled Drug Release, Osteoporosis

# ÖZ

## OSTEOPOROZ TEDAVİSİ İÇİN RALOKSİFEN TAŞIYICI SİSTEMLER

Kavas, Ayşegül

Doktora, Mühendislik Bilimleri Bölümü

Tez Yöneticisi : Doç. Dr. Ayşen Tezcaner

Ortak Tez Yöneticisi: Doç. Dr. Dilek Keskin

Eylül 2014, 144 sayfa

Osteoporoz ilaçlarından biri olan Raloksifen (Ral), sistemik olarak, yüksek dozda ve sık aralıklarla hastalara verilmektedir. Bu durum, tüm vücudu etkileyen yan etkilerin görülme riskinin artmasına sebep olmaktadır. Bu tür sorunlara çözüm olarak, son yıllarda, bir taşıyıcıdan tedavi edici seviyede, kontrollü ve sürekli ilaç salımı sağlayan taşıma sistemleri üzerinde çalışılmaktadır. Bu çalışmanın amacı Ral- veya Ral-poli(etilen glikol) (PEG)-yükü poli( $\epsilon$ -kaprolakton) (PCL) veya PCL:poli(D,L-laktit-koglikolit) (PLGA) mikrokürelerin geliştirilmesi ve potansiyel kullanımlarının değerlendirilmesidir.

Mikrokürelerin çapları ortalama 1.5  $\mu$ m civarındadır. Ral ve PCL'nin yüksek düzeydeki hidrofobik özelliklerinden dolayı en yüksek Ral yükleme verimliliği (%) Ral-yükü PCL mikrokürelere ait bulunmuştur. Ral-PEG-yükü PCL:PLGA mikrokürelere ortama salınan toplam Ral miktarı, diğer mikroküre gruplarından salınan miktarlar ile

karşılaştırıldığında önemli ölçüde yüksektir. Bu bulgu, Ral-PEG konjugasyonu ile sağlanan, Ral'ın sulu ortamda ıslanabilirliğinin artması ile Ral'ın kristal yapısının amorf bir forma dönüşmesi ve sonucunda Ral'ın sudaki çözünürlüğünün artmasıyla açıklanabilir. Ral'ın sulu ortamda ıslanabilirliğinin artması ise polimer matrisine daha fazla suyun nüfuz etmesine izin vererek PCL ve PLGA'nın bozunum hızlarını artırmaktadır. Bu sonuçla bağlantılı olarak, Ral-PEG-yüklü PCL:PLGA mikrokürelerden ortama salınan Ral, dişi yağ dokusu kaynaklı mezenkimal kök hücreler tarafından oluşturulan matris mineralizasyonunun diğer gruptakine göre belirgin ölçüde yüksek olmasını sağlamıştır. Yağ dokusu kaynaklı kök hücreler ile gerçekleştirilen *in vitro* sitotoksite çalışmaları, tüm mikrokürelerin toksik olmadığını göstermiştir.

Ral-PEG-yüklü PCL:PLGA mikroküre formülasyonunun, bu çalışmadaki diğer formülasyonlara kıyasla, daha yüksek Ral salım hızı sağladığı ve bu sayede kök hücreler tarafından oluşturulan matris mineralizasyonunu artırdığı gösterilmiştir. Bu formülasyon, etkili bir kontrollü ilaç salım sistemi olarak osteoporoz tedavisi için umut vadetmektedir. İlerideki çalışmalar için, PEG'in Ral'a konjuge edilmesi, konjugattaki PEG oranını değiştirerek Ral'ın mikrokürelerden salım hızını kolaylıkla ayarlama imkanı sunmaktadır.

Anahtar Kelimeler: Raloksifen, Kontrollü İlaç Salımı, Osteoporoz

*To My Beloved Family*  
&  
*To the Upcoming Days Full of Hope*

## ACKNOWLEDGEMENTS

I would like to express my sincere gratitude to my supervisor Assoc. Prof. Dr. Ayşen Tezcaner and co-supervisor Assoc. Prof. Dr. Dilek Keskin for their continuous guidance, encouragement, support and advice throughout this study. I would also like to thank my thesis progress and examining committee members, Prof. Dr. Ufuk Gündüz and Assoc. Prof. Dr. Senih Gürses, for their support and suggestions. My special thanks to my examining committee member, Assoc. Prof. Dr. Sreeparna Banerjee, for her helpful comments and valuable input throughout revision stage of my thesis.

I am deeply thankful to my other examining committee member, Assoc. Prof. Dr. Korhan Altunbaş, for his suggestions, valuable support and help especially for the isolation of mesenchymal stem cells and allowing me to study in his laboratory at Afyon Kocatepe University, Veterinary Faculty, Histology and Embryology Department. I would also like to thank Dr. Özlem Özden Akkaya and Dr. M. Volkan Yaprakçı for their help in the experiments.

I owe special thanks to Prof. Dr. M. Ruşen Geçit for encouraging me to begin an academic career in the Department of Engineering Sciences.

My sincere acknowledgements go to our department secretary, Leyla Kaya, for being genial and helpful at all times. I appreciate her behaving with a strong sense of responsibility.

I wish to express my thanks to Hamdi Kömürcü from Graduate School of Natural and Applied Sciences (METU) for his kind help during the thesis submission period.

I would like to thank all my labmates, firstly, Özge Erdemli, Özlem Aydın, Aslı Astarıcı and Parisa Sharafı for their friendship, support and sharings, and (in alphabetical order) Ali Deniz Dalgıç, Alişan Kayabölen, Aydın Tahmasebifar, Bengi Yılmaz, Bora Onat, Burçin Başar, Deniz Atila, Engin Pazarçeviren, Funda Guzey, Hazal Aydoğdu, İdil Uysal, Mert Baki, Merve Güldiken, Merve Nur Kazaroğlu, Mine Toker, Nil Göl, Ömer Aktürk, Pınar Sun, Reza Moonesirad, Selin Yitkin, Serap Güngör, Seylan Aygün, Sibel Ataol, Sina Khoshsima, Yağmur Çalışkan, Yiğit Öcal and Zeynep Barçın for their friendship, support and pleasant memories.

I owe my thanks to my roommate, Ayşe Durucan, for all the moments we shared. I would also like to thank my friends, Yasemin Kaya and Volkan İşbuğa, for their valuable friendship throughout this study.

I would like to express my special thanks to my “garfield”, Ersan Güray, for standing by me and believing in me all the time. His love, continuous support and endless patience are very precious for me.

I owe my deepest thanks to my family for their love, endless support, encouragement, patience and understanding throughout this study and my entire life. Their presence in my life means more than that the words can express. Warmest hugs from me to each of them...

I would like to thank METU-BAP for the financial support they provided to this study (Project Number: BAP-03-10-2011-001).

# TABLE OF CONTENTS

ABSTRACT.....	v
ÖZ.....	vii
ACKNOWLEDGEMENTS.....	x
TABLE OF CONTENTS.....	xii
LIST OF TABLES.....	xvi
LIST OF FIGURES.....	xvii
LIST OF ABBREVIATIONS.....	xxiv
CHAPTERS	
1. INTRODUCTION.....	1
1.1. Function and Structure of Bone.....	1
1.1.1. Composition of Bone.....	1
1.1.2. Classification of Bones.....	3
1.1.2.1. Parts of a Long Bone.....	4
1.1.3. Microscopic Structure of Bone.....	5
1.1.3.1. Compact Bone.....	5
1.1.3.2. Spongy Bone.....	6
1.2. Osteoporosis.....	8
1.2.1. Current Therapy Options for Osteoporosis.....	10
1.2.1.1. Hormone Replacement Therapy.....	11
1.2.1.2. Bisphosphonates.....	12
1.2.1.3. SERMs.....	13
1.2.1.4. Calcitonin.....	15
1.2.1.5. Denosumab.....	17
1.2.1.6. Raloxifene.....	17
1.3. Controlled Drug Delivery.....	21

1.3.1. Ral Delivery Systems .....	21
1.3.2. Biodegradable Polymers: PCL and PLGA .....	23
1.4. Ral-PEG Conjugate .....	25
1.5. Aim of the Study.....	27
2. MATERIALS AND METHODS .....	29
2.1. Materials.....	29
2.2. Methods.....	30
2.2.1. Optimization Studies for Preparation of the Microspheres.....	30
2.2.1.1. Co-precipitation Method .....	30
2.2.1.2. Solid-in-Oil-in-Water Method .....	31
2.2.1.3. Oil-in-Oil-in-Water Method.....	34
2.2.2. Preparation of Ral-PEG Conjugate.....	34
2.2.3. Characterization of Ral-PEG Conjugate.....	36
2.2.3.1. Fourier Transform Infrared Spectroscopy.....	36
2.2.3.2. X-Ray Diffraction Analysis .....	37
2.2.3.3. Morphological Analysis by Scanning Electron Microscopy .....	37
2.2.4. Preparation of Ral- and Ral-PEG Conjugate-Loaded PCL and PCL:PLGA (1:1) Microspheres .....	38
2.2.5. Characterization of Ral- and Ral-PEG-Loaded PCL and PCL:PLGA (1:1) Microspheres .....	40
2.2.5.1. Morphological Analysis by SEM.....	40
2.2.5.2. Particle Size Analysis.....	40
2.2.5.3. Determination of Ral Encapsulation Efficiency and Loading .....	41
2.2.5.4. Ral Release Profiles of the Microspheres .....	41
2.2.5.4.1. HPLC Analysis.....	42
2.2.5.4.2. Spectrophotometric Analysis .....	43
2.2.6. Cell Culture Studies .....	43
2.2.6.1. Isolation and Proliferation of Adipose-Derived Mesenchymal Stem Cells .....	43

2.2.6.2. Human Fetal Osteoblast Cell Line (hFOB) .....	44
2.2.6.3. Dose-Dependent Effects of Ral and Ral-PEG on Adipose- Derived Mesenchymal Stem Cells and hFOB Cells .....	44
2.2.6.3.1. <i>In Vitro</i> Cytotoxicity Studies .....	45
2.2.6.3.2. Alkaline Phosphatase (ALP) Activity Analysis.....	46
2.2.6.4. Effects of Ral- and Ral-PEG-Loaded Microspheres on Adipose-Derived Mesenchymal Stem Cells .....	47
2.2.6.4.1. <i>In Vitro</i> Cytotoxicity Studies .....	48
2.2.6.4.2. Alizarin Red S Staining .....	48
2.2.7. Statistical Analysis .....	49
3. RESULTS AND DISCUSSION .....	51
3.1. Optimization Studies for the Preparation of Ral-Loaded Microspheres .....	51
3.1.1. Co-precipitation Method.....	51
3.1.2. Solid-in-Oil-in-Water Method.....	54
3.1.3. Oil-in-Oil-in-Water Method .....	64
3.2. Characterization of Ral-PEG.....	65
3.2.1. FT-IR Analysis .....	65
3.2.2. XRD Analysis.....	67
3.2.3. Morphological Analysis by SEM.....	69
3.3. Characterization of Ral- and Ral-PEG-Loaded PCL and PCL:PLGA (1:1) Microspheres.....	71
3.3.1. Morphological Analysis by SEM .....	71
3.3.2. Particle Size Analysis .....	78
3.3.3. Ral Encapsulation Efficiency and Loading .....	83
3.3.4. Ral Release Profiles of the Microspheres.....	84
3.3.5. Morphological Analysis of the Microspheres after Release.....	90
3.4. Cell Culture Studies .....	94

3.4.1. Dose-Dependent Effects of Ral and Ral-PEG on Adipose-Derived Mesenchymal Stem Cells and hFOB Cells .....	97
3.4.1.1. <i>In Vitro</i> Cytotoxicity Studies .....	97
3.4.1.2. ALP Activity Analysis .....	99
3.4.2. Effects of Ral- and Ral-PEG-Loaded Microspheres on Adipose-Derived Mesenchymal Stem Cells .....	101
3.4.2.1. <i>In Vitro</i> Cytotoxicity Studies .....	101
3.4.2.2. Alizarin Red S Staining.....	103
4. CONCLUSIONS .....	109
REFERENCES .....	113
APPENDICES	
A. ETHICAL COMMITTEE REPORT.....	133
B. CHROMATOGRAMS & CALIBRATION CURVES USED DURING RELEASE STUDIES.....	135
C. CALIBRATION CURVE USED DURING ENCAPSULATION EFFICIENCY ANALYSES.....	139
D. CALIBRATION CURVE USED DURING ALP ACTIVITY ANALYSES...	141
CURRICULUM VITAE .....	143

## LIST OF TABLES

### TABLES

<b>Table 1.</b> Classification of osteoporosis drugs.....	12
<b>Table 2.</b> Some conventional drugs that decrease the risk of vertebral and hip fractures when used with sufficient calcium and vitamin-D supplementation, and their side-effects.....	20
<b>Table 3.</b> Details related with modifications of the solid-in-oil-in-water method for optimization of microsphere preparation.....	33
<b>Table 4.</b> Details related with modifications of the oil-in-oil-in-water method for optimization of microsphere preparation.....	35
<b>Table 5.</b> Encapsulation efficiency (%), loading (%) and theoretical loading (%) values of Ral-loaded PCL:PLGA (10:4) microspheres belonging to the groups A) - D) in Table 3.....	63
<b>Table 6.</b> Particle size distribution of all microsphere groups.....	79
<b>Table 7.</b> Encapsulation efficiency (%), loading (%) and theoretical loading (%) values of Ral- and Ral-PEG-loaded microspheres prepared by the optimized oil-in-oil-in-water method (n=3).....	84

# LIST OF FIGURES

## FIGURES

<b>Figure 1.</b> Composition of bone.....	2
<b>Figure 2.</b> Major parts of a long bone.....	5
<b>Figure 3.</b> The microscopic structure of compact and spongy bones .....	7
<b>Figure 4.</b> Activation-resorption-formation (A-R-F) sequence of bone remodelling.....	8
<b>Figure 5.</b> Variations in bone mass with age, and factors influencing peak bone mass and decrease of bone mass after mid-life.....	10
<b>Figure 6.</b> The structure of bisphosphonates.....	13
<b>Figure 7.</b> The structure of alendronate.....	13
<b>Figure 8.</b> Comparative ER agonist or antagonist activities of bazedoxifene (BZA), lasofoxifene (LAS), Ral (RLX), tamoxifen and estrogen in (a) bone, (b) endometrium, (c) breast.....	15
<b>Figure 9.</b> Salmon calcitonin.....	16
<b>Figure 10.</b> Chemical structure of Ral hydrochloride.....	18
<b>Figure 11.</b> Concentration profile of conventional drugs and drug delivery systems.....	22
<b>Figure 12.</b> Chemical structure of PLGA (75:25).....	24
<b>Figure 13.</b> Chemical structure of PCL.....	24
<b>Figure 14.</b> Chemical structure of PEG.....	26
<b>Figure 15.</b> Possible hydrogen bondings (- - -) formed between amine and phenolic-OH groups of Ral and hydroxyl groups of PEG during conjugate reaction.....	36
<b>Figure 16.</b> Procedure for preparation of microspheres.....	39
<b>Figure 17.</b> Hydrolysis of <i>p</i> -nitrophenyl phosphate into an organic radical ( <i>p</i> -nitrophenol) and inorganic phosphate.....	47

<b>Figure 18.</b> SEM micrographs of Ral-loaded PCL microstructures obtained by co-precipitation method (stirring rate: 800 rpm) (a) 300X and b) 1400X).....	52
<b>Figure 19.</b> SEM micrographs of Ral-loaded PLGA microstructures obtained by co-precipitation method(stirring rate: 800 rpm) (a) 1000X and b) 1000X).....	52
<b>Figure 20.</b> SEM micrographs of empty PLGA microstructures obtained by co-precipitation method (stirring rate: 1100 rpm) (a) 1000X and b) 1400X).....	53
<b>Figure 21.</b> SEM micrograph of empty PLGA microstructures obtained by co-precipitation method (stirring rate: 8000 rpm) (1000X).....	54
<b>Figure 22.</b> SEM micrographs of Ral-loaded PCL microspheres obtained by solid-in-oil-in-water method (PVA concentration: 2% and stirring rate: 14000 rpm) (a) 1500X and b) 6000X).....	55
<b>Figure 23.</b> SEM micrographs of Ral-loaded PCL microspheres obtained by solid-in-oil-in-water method (PVA concentration: 2% and stirring rate: 18000 rpm). At c), the microspheres attached onto polymer structures are shown (a) 1000X, b) 5000X and c) 500X).....	56
<b>Figure 24.</b> Ral release profiles (a) $\mu\text{g}$ and b) %) of PCL microspheres (obtained by solid-in-oil-in-water method, PVA concentration: 2% and stirring rate: 18000 rpm) incubated in PBS (0.1 M, pH 7.4) at 37°C for 60 days (n=4).....	57
<b>Figure 25.</b> SEM micrographs of Ral-loaded PCL microspheres (obtained by solid-in-oil-in-water method, PVA concentration: 2% and stirring rate: 18000 rpm) after 60 days of release in PBS (0.1 M, pH 7.4) at 37°C (a) 3000X and b) 500X).....	59
<b>Figure 26.</b> SEM micrographs of Ral-loaded PCL:PLGA (9.1:1, w/w) microspheres obtained by solid-in-oil-in-water method (a) 3000X and b) 4000X).....	60

<b>Figure 27.</b> Ral release profiles (a) $\mu\text{g}$ and b) % of PCL:PLGA (9.1:1, w/w) microspheres (obtained by solid-in-oil-in-water method) incubated in PBS (0.1 M, pH 7.4) at 37°C for 60 days (n=3).....	61
<b>Figure 28.</b> SEM micrograph of Ral-loaded PCL:PLGA (9.1:1, w/w) microspheres (obtained by solid-in-oil-in-water method) after 60 days of release in PBS (0.1 M, pH 7.4) at 37°C (4000X).....	62
<b>Figure 29.</b> SEM micrographs of Ral from two different stock batches as obtained from the producer a) Batch 1 (200X) and b) Batch 2 (200X).....	64
<b>Figure 30.</b> FT-IR spectra of a) PEG, b) Ral-PEG and c) Ral.....	66
<b>Figure 31.</b> XRD diffractogram of Ral.....	68
<b>Figure 32.</b> XRD diffractogram of PEG.....	68
<b>Figure 33.</b> XRD diffractograms of a) the physical mixture of Ral and PEG and b) Ral-PEG. $\square$ refers to the peaks of Ral and $\bullet$ refers to the peaks of PEG.....	69
<b>Figure 34.</b> SEM micrograph Ral powders before conjugation reaction with PEG (30X).....	70
<b>Figure 35.</b> SEM micrographs of Ral-PEG (a) 150X and b) 600X).....	71
<b>Figure 36.</b> SEM micrographs of empty PCL microspheres prepared by the optimized oil-in-oil-in-water method (a) 5000X, b) 4000X and c) 2500X).....	73
<b>Figure 37.</b> SEM micrographs of Ral-loaded PCL microspheres prepared by the optimized oil-in-oil-in-water method (a) 5000X, b) 3000X, c) 3000X and d) 4000X).....	74
<b>Figure 38.</b> SEM micrographs of Ral-loaded PCL:PLGA (1:1) microspheres prepared by the optimized oil-in-oil-in-water method (a) 6000X, b) 5000X, c) 3000X and d) 2100X).....	75
<b>Figure 39.</b> SEM micrographs of Ral-PEG-loaded PCL microspheres prepared by the optimized oil-in-oil-in-water method (a) 8000X, b) 6000X, c) 4000X and d) 2800X).....	76

<b>Figure 40.</b> SEM micrographs of Ral-PEG-loaded PCL:PLGA (1:1) microspheres prepared by the optimized oil-in-oil-in-water method (a) 5000X, b) 4000X, c) 2500X, d) 4000X and e) 5000X).....	77
<b>Figure 41.</b> Particle size distribution of empty PCL microspheres (prepared by the optimized oil-in-oil-in-water method) presented as a histogram and a cumulative arithmetic curve.....	80
<b>Figure 42.</b> Particle size distribution of a) Ral-loaded PCL and b) Ral-loaded PCL:PLGA (1:1) microspheres (prepared by the optimized oil-in-oil-in-water method) presented as a histogram and a cumulative arithmetic curve.....	81
<b>Figure 43.</b> Particle size distribution of a) Ral-PEG-loaded PCL and b) Ral-PEG-loaded PCL:PLGA (1:1) microspheres (prepared by the optimized oil-in-oil-in-water method) presented as a histogram and a cumulative arithmetic curve.....	82
<b>Figure 44.</b> Ral release profiles (a) $\mu\text{g}$ and b) %) of Ral-loaded PCL:PLGA (1:1) and Ral-loaded PCL microspheres (prepared by the optimized oil-in-oil-in-water method) incubated in PBS (0.1 M, pH 7.4) at 37°C for 60 days (n=3).....	88
<b>Figure 45.</b> Ral release profiles (a) $\mu\text{g}$ and b) %) of Ral-PEG-loaded PCL:PLGA (1:1) and Ral-PEG-loaded PCL microspheres (prepared by the optimized oil-in-oil-in-water method) incubated in PBS (0.1 M, pH 7.4) at 37°C for 60 days (n=3) (Ral to PEG ratio is 1:2).....	89
<b>Figure 46.</b> SEM micrographs of Ral-loaded PCL microspheres (prepared by the optimized oil-in-oil-in-water method) after 60 days of release in PBS (0.1 M, pH 7.4) at 37°C (a) 4000X, b) 6000X, c) 4000X and d) 4000X).....	91

<b>Figure 47.</b> SEM micrographs of Ral-loaded PCL:PLGA: (1:1) microspheres (prepared by the optimized oil-in-oil-in-water method) after 60 days of release in PBS (0.1 M, pH 7.4) at 37°C (a) 5000X, b) 5000X, c) 5000X and d) 5000X).....	92
<b>Figure 48.</b> SEM micrographs of Ral-PEG-loaded PCL microspheres (prepared by the optimized oil-in-oil-in-water method) after 60 days of release in PBS (0.1 M, pH 7.4) at 37°C (a) 8000X, b) 5000X, c) 4000X and d) 5000X) (Ral to PEG ratio is 1:2).....	93
<b>Figure 49.</b> SEM micrographs of Ral-PEG-loaded PCL:PLGA (1:1) microspheres (prepared by the optimized oil-in-oil-in-water method) after 60 days of release in PBS (0.1 M, pH 7.4) at 37°C (a) 5000X and b) 5000X) (Ral to PEG ratio is 1:2).....	94
<b>Figure 50.</b> Phase contrast micrographs of adipose-derived mesenchymal stem cells isolated from Sprague-Dawley rats (10X) (a) and b) primer, c) and d) 1 <sup>st</sup> passage, e) and f) 2 <sup>nd</sup> passage).....	95
<b>Figure 51.</b> Phase contrast micrographs of hFOB cells (10X) (9 <sup>th</sup> passage).....	96
<b>Figure 52.</b> Relative cell viabilities of adipose-derived mesenchymal stem cells presented as percentages of cell viability of the control group. The cells were cultivated in growth medium and data were obtained after 3, 7 and 14 days of Ral and Ral-PEG treatment at the doses of 0.1, 1 and 10 µM. *, ✕ and & represent statistically significant differences relative to 0.1 µM Ral-treated cells at day 3, 7 and 14, respectively. #, ▣ and + represent statistically significant differences relative to 0.1 µM Ral-PEG-treated cells at day 3, 7 and 14, respectively.....	98

- Figure 53.** Relative cell viabilities of hFOB cells presented as percentages of cell viability of the control group. The cells were cultivated in growth medium and data were obtained after 1, 4, 7 and 14 days of Ral and Ral-PEG treatment at the doses of 0.01, 0.1, 1 and 10  $\mu\text{M}$ . \* and # represent statistically significant differences relative to 0.1  $\mu\text{M}$  Ral- and 0.1  $\mu\text{M}$  Ral-PEG-treated cells at day 14, respectively.....99
- Figure 54.** ALP activity (nmol/min) results of hFOB cells after 7 days of Ral and Ral-PEG treatment at the doses of 0.01, 0.1, 1 and 10  $\mu\text{M}$ . \* and # represent statistically significant differences relative to 0.1  $\mu\text{M}$  Ral- and 1  $\mu\text{M}$  Ral-PEG-treated cells, respectively.....100
- Figure 55.** Relative cell viabilities of female adipose-derived mesenchymal stem cells presented as percentages of cell viability of the control group. Data were obtained after 1, 4 and 7 days of incubations of the cells in release media of various microsphere groups. \* refers to statistically significant difference relative to the cells cultivated in release medium of empty PCL:PLGA (1:1) microsphere group at day 1. # and  $\varpi$  refer to statistically significant differences relative to the cells cultivated in release medium of Ral-loaded PCL microsphere group at days 1 and 4, respectively.  $\varpi$  refers to statistically significant difference relative to the cells cultivated in release medium of empty PCL microsphere group at day 4.....102
- Figure 56.** Phase contrast micrographs of the female adipose-derived mesenchymal stem cells stained with Alizarin red S after 7 days of cultivation in the release medium of various microsphere groups (a) and b) Empty PCL:PLGA (1:1) microspheres, c) and d) Empty PCL microspheres, e) and f) Ral-loaded PCL microspheres, (g) and h) Ral-PEG-loaded PCL microspheres, i) and j) Ral-loaded PCL:PLGA (1:1) microspheres, k) and l) Ral-PEG-loaded PCL:PLGA (1:1) microspheres).....104

<b>Figure 57.</b> Mineral content of female adipose-derived mesenchymal stem cells incubated in the release media of various microsphere groups for 7 days. * refers to statistically significant differences between the cells cultivated in release medium of Ral-PEG-loaded PCL:PLGA (1:1) microsphere group and the cells cultivated in release media of the other microsphere groups.....	107
<b>Figure 58.</b> Chromatogram of 5 µg/mL Ral in MeOH:PBS (1:1) obtained by HPLC...	135
<b>Figure 59.</b> Calibration curve of Ral in MeOH:PBS (1:1) obtained by HPLC for release studies.....	136
<b>Figure 60.</b> Calibration curve of Ral in MeOH:PBS (1:1) obtained by spectrophotometry for release studies.....	137
<b>Figure 61.</b> Calibration curve of Ral in DCM:MeOH (1:1) obtained by spectrophotometry for determination of Ral encapsulated in the microspheres.....	139
<b>Figure 62.</b> Calibration curve of <i>p</i> -nitrophenol (nmol/well) for determination of ALP activity of the cells.....	141

## LIST OF ABBREVIATIONS

$\alpha$ -MEM	Alpha-Minimal Essential Medium
ALP	Alkaline Phosphatase
A-R-F	Activation-Resorption-Formation
BDDCS	Biopharmaceutics Drug Disposition Classification System
BMD	Bone Mineral Density
CTR	Calcitonin Receptor
DCM	Dichloromethane
DMSO	Dimethyl Sulfoxide
DMEM	Dulbecco's Modified Eagle's Medium
ER	Estrogen Receptor
FBS	Fetal Bovine Serum
FDA	Food and Drug Administration
FT-IR	Fourier Transform Infrared Spectroscopy
hFOB	Human Fetal Osteoblast
HPLC	High Performance Liquid Chromatography
HRT	Hormone Replacement Therapy
M-CSF	Macrophage-Colony Stimulating Factor
MeOH	Methanol
M <sub>w</sub>	Molecular weight
PBS	Phosphate Buffered Saline
PTH	Parathyroid Hormone
PCL	Poly( $\epsilon$ -caprolactone)
PEG	Poly(ethylene glycol)
PLA	Poly lactide
PLGA	Poly(D,L-lactide-co-glycolide)

PVA	Poly(vinyl alcohol)
Ral	Raloxifene
Ral-PEG	Ral-PEG (1:2) conjugate
RANKL	Receptor Activator of NF- $\kappa$ B Ligand
SEM	Scanning Electron Microscopy
SERM	Selective Estrogen Receptor Modulator
TNF	Tumour Necrosis Factor
Trypsin-EDTA	Trypsin-Ethylenediamine Tetraacetic Acid
UV/VIS	Ultraviolet/Visible
XRD	X-Ray Diffraction



# CHAPTER 1

## INTRODUCTION

### 1.1. Function and Structure of Bone

Bone serves as an internal support system for the body and provides areas of muscle attachment for motion. Additionally, it functions in calcium and phosphorus homeostasis, being the main source of minerals, (Rodan, 1992; Sommerfeldt & Rubin, 2001; Marks & Odgren, 2002), resists loads applied on the body and saves internal organs (Rodan, 1992; Sommerfeldt & Rubin, 2001).

#### 1.1.1. Composition of Bone

Mineralized organic components constitute the extracellular matrix of bone (Marks & Odgren, 2002). The main components of bone are minerals (70 wt %), organic constituents (20 wt %) and water (10 wt %). Hydroxyapatite comprises 95% of mineral part and collagen comprises about 95% of organic part. Non-collagenous proteins, polysaccharides and lipids are the other organic constituents in low amounts (Figure 1). Collagen is composed of tiny filaments, having diameter varying from 0.1 to 2  $\mu\text{m}$ . The fundamental roles of collagen are providing elasticity and structural support to the bone. Hydroxyapatite crystals, which are in the shape of needles and plates, exist in parallel to the collagen filaments. The major role of hydroxyapatite is providing stiffness to the bone (Weiner & Wagner, 1998; Shi & Wen, 2006).

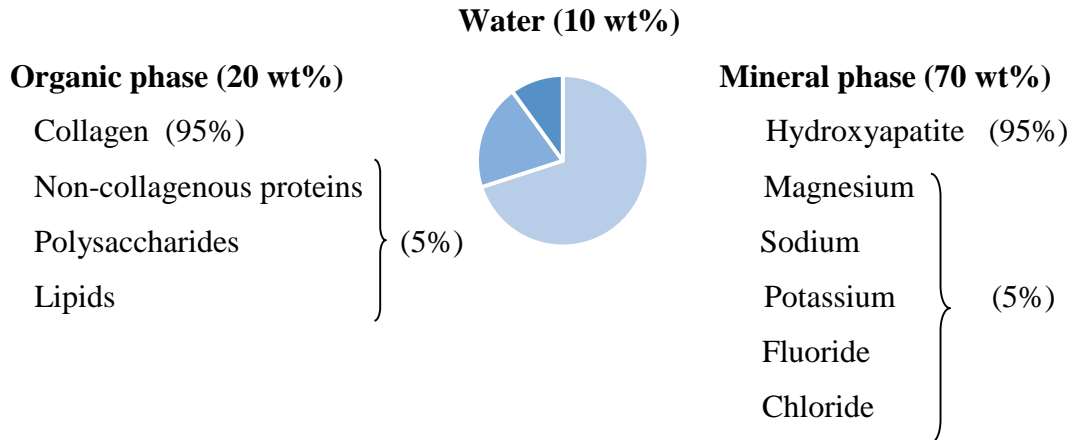


**Figure 1.** Composition of bone (Shi & Wen, 2006).

Bone is made up of four main types of cells:

**1) Osteoblasts:** They are bone-forming cells originating from mesenchymal stem cells. At resorption sites, these cells synthesize organic matrix components, collagen type I and non-collagenous proteins like osteopontin, osteocalcin, osteonectin and etc. Calcium, phosphate and vitamin D play role in mineralization of this organic matrix. Functions of osteoblasts are enhanced by binding of parathyroid hormone to receptors on the osteoblasts (Rachner et al., 2011). Activation of Wnt/ $\beta$ -catenin pathway is the key switch for differentiation of osteoblasts (Baron & Rawadi, 2007).

**2) Osteoclasts:** They are large and multinucleated bone-resorbing cells (Wang et al., 2005) derived from haemopoietic stem cells. Especially receptor activator of NF- $\kappa$ B ligand (RANKL) belonging to the tumour necrosis factor (TNF) family and macrophage-colony stimulating factor (M-CSF) regulate the differentiation of osteoclast precursors to active multinucleated osteoclasts. Osteoclasts attach to bone surfaces by adhesion molecules like integrins, motile cytoskeleton and jelly-fish-like cell extensions,

and produce a highly acidic microenvironment (Rachner et al., 2011). These cells resorb bone by removing minerals with acid and degrading collagen with enzymes (Bigham-Sadegh & Oryan, 2014).

**3) Bone lining cells:** They are inactive osteoblasts and are activated by chemical and/or mechanical stimuli (Miller & Jee, 1992).

**4) Osteocytes:** They are the most abundant bone cells, constituting more than 90% of all bone cells and they present in the mineralized bone matrix (Wang et al., 2005; Rachner et al., 2011). They are former osteoblasts (Bigham-Sadegh & Oryan, 2014) and it is indicated that these cells play role as mechanosensors which regulate bone remodelling (Cowin et al., 1991; Doblaré et al., 2004; Skerry et al., 1989). Additionally, a number of factors regulating phosphate metabolism are expressed by these star-shaped cells which resemble to neural cells (Rachner et al., 2011). Sclerostin, inhibitor of the Wnt-signalling pathway, is also produced and secreted by osteocytes (Poole et al., 2005).

All osteoblasts, osteoclasts and bone lining cells are present only on the bone surfaces (Wang et al., 2005; Miller & Jee, 1992).

### **1.1.2. Classification of Bones**

Bones can be divided into five groups according to their shapes (Shier et al., 1996):

**a) Long bones:** They have long longitudinal axes and expanded ends like the forearm and thigh bones.

**b) Short bones:** Their lengths and widths are approximately equal. Examples are the bones of the wrists and ankles.

c) **Flat bones:** They are platelike structures with broad surfaces. The ribs and some bones of the skull are examples of this kind.

d) **Irregular bones:** They have variety of shapes and are usually connected to several other bones. Many facial bones are the main examples.

e) **Round bones:** These bones, which are usually small and nodular, are embedded within tendons adjacent to joints. The patella is an example of round bones.

### **1.1.2.1. Parts of a Long Bone**

The structure of a long bone can be illustrated by the structure of a femur (Figure 2). At each end of such a bone, there is an expanded portion called epiphysis, which forms a joint with another bone. The articulating portion of the epiphysis is coated with a layer of hyaline cartilage called articular cartilage. The shaft of the bone, which is located between the epiphyses, is called the diaphysis. The wall of the diaphysis is mainly composed of tightly packed tissue called compact bone. The epiphyses, on the other hand, are largely composed of spongy bone with thin layers of compact bone on their surfaces (Figure 2). Compact bone in the diaphysis of a long bone forms a semirigid tube with a hollow chamber called the medullary cavity (Figure 2). This cavity is continuous with the spaces of the spongy bone. All of these areas are lined with a thin layer of epithelial cells called endosteum (Figure 3) and are filled with a specialized type of soft connective tissue called marrow (Figure 2) (Shier et al., 1996).

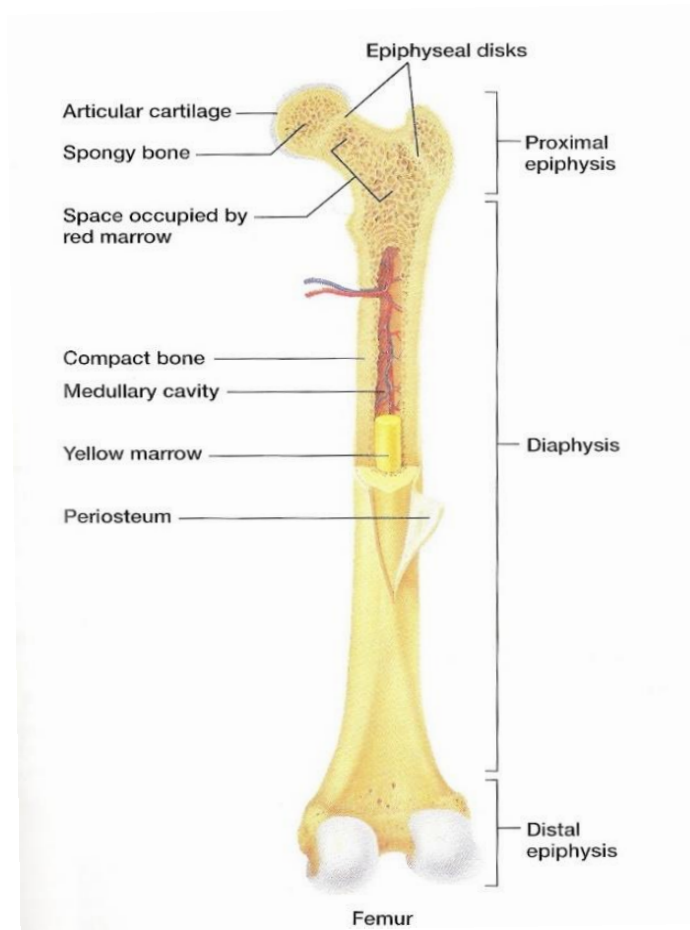


**Figure 2.** Major parts of a long bone (Shier et al., 1996).

### **1.1.3. Microscopic Structure of Bone**

#### **1.1.3.1. Compact Bone**

Compact bone, also called cortical bone, constitutes about 80% of the total skeleton and is 10% porous (Recker, 1992; Buckwalter et al., 1995). This type of bone is solid and strong, and resists bending. In compact bone, the osteocytes and layers of intercellular

material which are grouped concentrically around an osteonic canal form a cylinder-shaped unit called osteon (Haversian system). Many of these units cemented together constitute the substance of compact bone (Figure 3). The orientation of the osteons provides to withstand compressive forces. Each osteonic canal contains one or two small blood vessels including capillaries and nerve fibers surrounded by some loose connective tissue. Blood in these vessels nourishes bone cells associated with the osteonic canal by gap junctions between osteocytes. Osteocytes are located in bony chambers called lacunae existing in concentric circles around osteonic canals. These canals travel longitudinally through bone tissue and are interconnected by transverse perforating canals (Volkmann's canals). Volkmann's canals contain larger blood vessels and nerves by which the vessels and nerve fibers in the osteonic canals communicate with the surface of the bone and the medullary cavity (Figure 3) (Shier et al., 1996).

### **1.1.3.2. Spongy Bone**

Spongy bone, also named cancellous or trabecular bone, forms about 20% of the total skeleton and is 50-90% porous (Recker, 1992; Buckwalter et al., 1995). This higher value relative to that of the compact bone causes modulus of elasticity and ultimate compressive strength of spongy bone to be approximately 10 times lower than those of the cortical bone (Currey, 1984; Buckwalter et al., 1995). Spongy bone is composed of many branching bony plates called trabeculae (Figure 3). Irregular interconnecting spaces between these plates help reduce the weight of the bone. Spongy bone provides strength and its bony plates are most highly developed in the zones of the epiphyses that are subjected to compressive forces. Spongy bone also includes osteocytes and intercellular material. Osteocytes exist within the trabeculae and they are nourished by substances diffusing into the canaliculi that extend to the surface of the thin bony plates (Figure 3) (Shier et al., 1996).

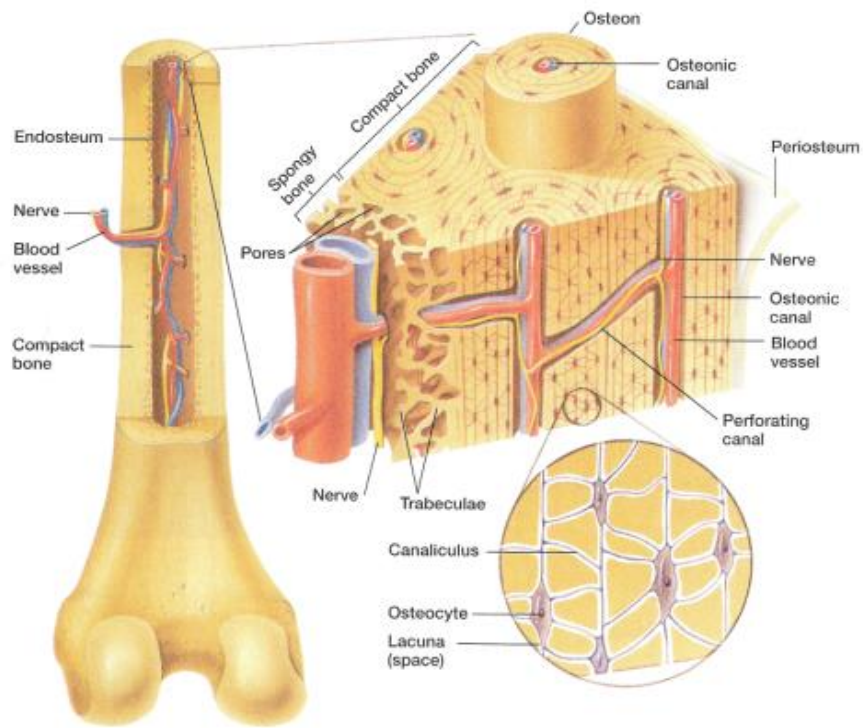


**Figure 3.** The microscopic structure of compact and spongy bones (Shier et al., 1996).

In the body, bone is continuously resorbed and rebuilt. This process is known as bone remodelling (Rodan & Martin, 2000). This process occurs through different cells functioning in collaboration (Frost, 1966). Remodelling takes place in an order of definite steps, as known as activation-resorption-formation (A-R-F) sequence (Frost, 1966; Bigham-Sadegh & Oryan, 2014) (Figure 4). Remodelling sequence starts with the osteoclast activation. The resorptive phase of the remodelling lasts approximately 10 days. Osteoblasts are then attracted to the region of the resorption defect and begin to repair the defect. This process of rebuilding takes about 3 months (Mundy, 2000). In the study of Rodan & Martin (2000), the resorptive and rebuilding phases were stated to take about 3 weeks and 3 to 4 months, respectively, and it was also indicated that, in

healthy people, this process cycle is well arranged which preserves bone mass and microstructure integrity of the skeleton in a steady-state.

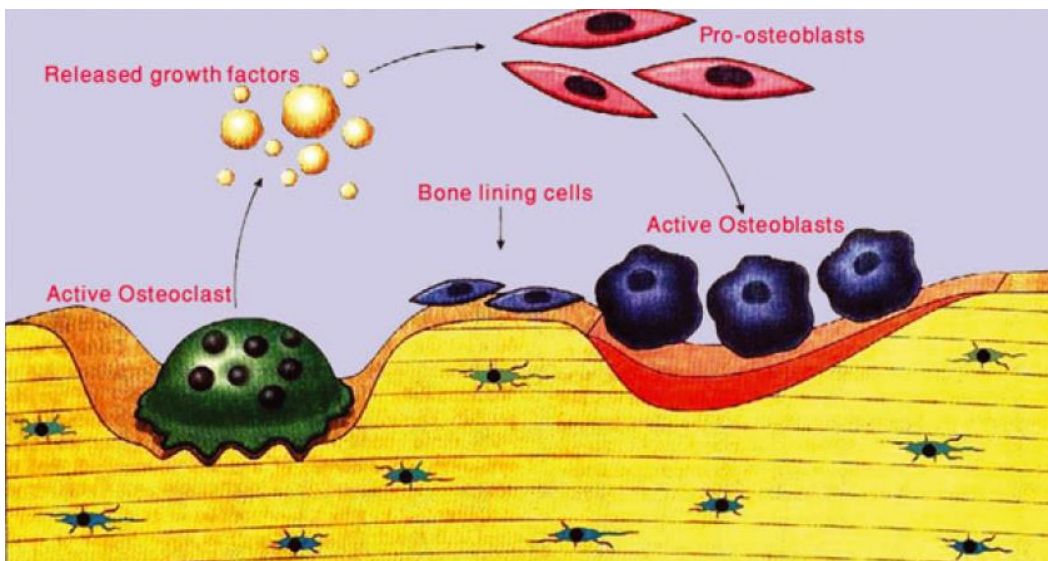


**Figure 4.** Activation-resorption-formation (A-R-F) sequence of bone remodelling (Bigham-Sadegh & Oryan, 2014).

## 1.2. Osteoporosis

Many bone diseases depend on the changes occurring in the bone remodelling sequence. In elderly patients with osteoporosis, osteoblasts are unable to repair sufficiently the defects formed during osteoclastic resorption in the A-R-F sequence (Darby & Meunier, 1981). It should also be noted that progressive bone loss, beginning at about 35 years of age, is seen in all humans and it is an indication of a physiological imbalance between resorption and formation (Mundy, 2000).

The changes in total body bone mass which occur with age are demonstrated in Figure 5. Bone mass reaches a maximum after linear growth stops, then begins to decrease and declines to half of its maximum value at the age of 80. Peak bone mineral density, in other words peak bone mass, is less in women than it is in men. Women show an additional accelerated phase of bone loss that occurs for about 10 years following the termination of ovarian function (Smith et al., 1975; Riggs et al., 1981; Mazess, 1982). In Figure 5, the factors which influence peak bone mass (genetic and environmental factors) and the factors which cause progressive loss of bone mass after mid-life (aging, menopause, environmental factors) can also be seen. The main factors causing bone loss after mid-life are sex hormone deficiency, disuse as well as calcium and vitamin D deficiency. The rates of bone loss subsequent to sudden hormonal withdrawal are exponential while the rates of loss owing to disuse or calcium and vitamin deficiency are more gradual (Heaney, 1993).

Osteoporosis is a skeletal disease characterized by a decrease in bone strength and bone mass, accompanied by an increase in fragility of bones and risk of fractures (NIH Consensus, 2001). It is a significant public health issue, as one of the most prevalent diseases in elderly people, affecting up to 40% of postmenopausal women and 15% of men (Melton et al., 1992). Worldwide, osteoporosis is estimated to be seen in over 200 million people (Reginster & Burlet, 2006). In osteoporosis, fractures especially at the forearm, the vertebral bodies and the hip occur, however patients have also risk of fractures at other sites (Riggs & Melton, 1995). Osteoporotic fractures cause substantial mortality, morbidity, reduced mobility and thus, decreased quality of life (Barrett-Connor, 1995).

Bone mineral density (BMD) is the main determinant of bone strength and osteoporotic fracture risk (NIH Consensus, 2001). Many studies indicate that the risk of fractures increases in an accelerative manner as BMD reduces (Cummings et al., 1990; Cummings et al., 1993). However, several other skeletal characteristics are also

effective in detection of the fracture risk. These are matrix and mineral composition, shape and geometry, and microarchitecture of bone, besides the rate of bone turnover and the degree of mineralization (Sambrook & Cooper, 2006; Seeman & Delmas, 2006).

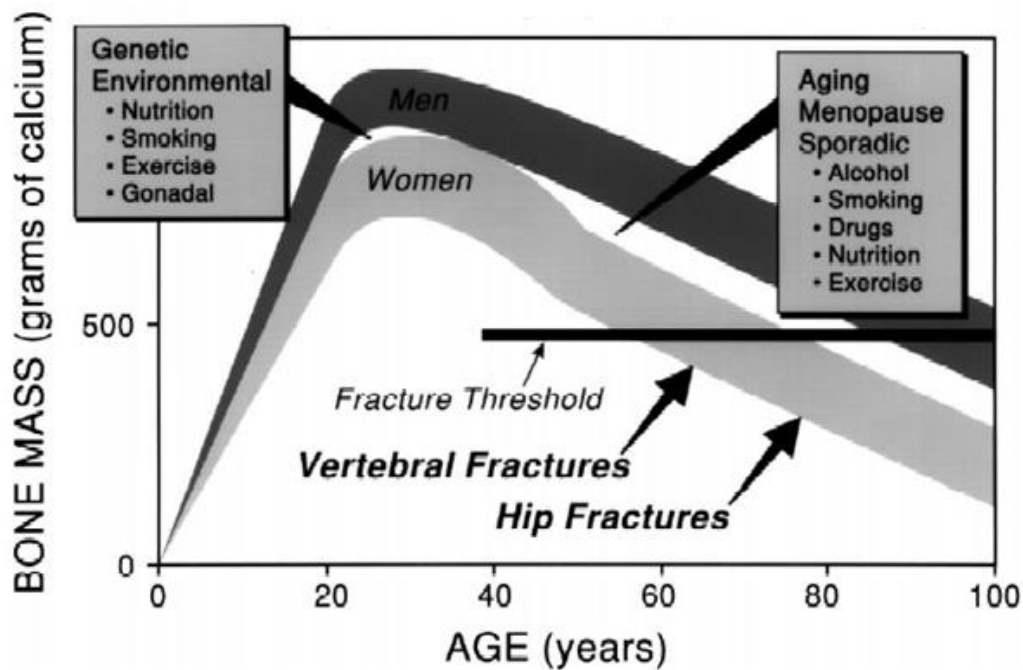


**Figure 5.** Variations in bone mass with age, and factors influencing peak bone mass and decrease of bone mass after mid-life (Mundy, 2000).

### 1.2.1. Current Therapy Options for Osteoporosis

Besides lifestyle modifications such as giving up smoking, decreasing alcohol consumption and enhancing physical activity, vitamin D and calcium administration is suggested as baseline treatment for every osteoporosis patient. It has been noted that the

benefits of osteoporosis drugs can be only seen if these supplements are taken at the same time (Rachner et al., 2011).

Osteoporosis drugs can be classified into two basic groups according to their mechanism of action and their effects on osteoblasts and/or osteoclasts: Antiresorptive (inhibiting/slowing down bone resorption) or anabolic (inducing bone formation) agents (Table 1). Antiresorptive drugs contain estrogens, bisphosphonates, selective estrogen receptor modulators (SERMs), calcitonin, strontium ranelate and denosumab. The only available compounds with clear anabolic effects are full-length parathyroid hormone (PTH 1-84) and its N-terminal fragment, teriparatide (PTH 1-34) (Sambrook & Cooper, 2006; Gennari et al., 2009; Rachner et al., 2011).

#### **1.2.1.1. Hormone Replacement Therapy**

Among the several therapeutical interventions in osteoporosis, hormone replacement therapy (HRT) – namely estrogen replacement – has been regarded as the main standard method for preventing osteoporotic fractures in postmenopausal women as well as for the management of menopausal symptoms. Its other possible benefits are prevention of colon cancer and neuroprotective effects (Chlebowski et al., 2004). Estrogen replacement, especially if administered long-term, may increase risk of breast cancer and also endometrial cancer when unopposed by progestins (Vassilopoulou-Sellin, 2003). Other adverse effects of HRT are breast pain, headache and resumption of menstrual cycle. Consequently, the researchers suggest that the use of HRT needs to be considered as a short-term therapy for menopausal symptom management (Anon, 2004). On the other hand, estrogen replacement must be long-term, possibly lifelong to have continuous influence on bone health.

**Table 1.** Classification of osteoporosis drugs (Sambrook & Cooper, 2006; Gennari et al., 2009; Rachner et al., 2011).

Antiresorptive drugs	Estrogens
	Bisphosphonates
	SERMs
	Calcitonin
	Strontium ranelate
	Denosumab
Anabolic drugs	Parathyroid hormone
	Teriparatide

### 1.2.1.2. Bisphosphonates

The bisphosphonates (alendronate, risedronate, ibandronate and zoledronate) possess high affinity for bone and are the most prescribed medications for osteoporosis therapy since they can be inexpensive and used across a broad spectrum of osteoporosis kinds including postmenopausal, male and steroid-induced osteoporosis, and Paget's disease. Their benefits are restricted to the skeleton where they decrease the risk of vertebral and non-vertebral fractures (Gennari et al., 2009; Rachner et al., 2011). The effects of bisphosphonates on osteoclasts are exhibited in four different ways: (1) Inhibition of osteoclast recruitment, (2) inhibition of osteoclast adhesion to the mineral matrix, (3) shortening of the osteoclast lifespan and (4) direct inhibition of osteoclast activity (Fleisch et al., 2002). Bisphosphonates have a structure of P–C–P (Figure 6). The P–C bond is resistant to most chemical reagents and inert to enzymatic degradation. Generally, bisphosphonates are classified into two types: Those having nitrogen-

containing functional groups at the R<sub>2</sub> position are termed N-BPs and those without nitrogen are termed non-N-BPs (Wang et al., 2005). For example, alendronate belongs to the group N-BPs and its structure is shown in Figure 7.

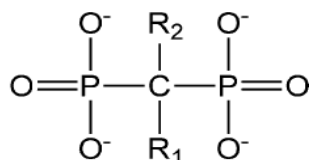


**Figure 6.** The structure of bisphosphonates (Wang et al., 2005).



**Figure 7.** The structure of alendronate (Guénin et al., 2007).

### 1.2.1.3. SERMs

SERMs represent a group with an increasing number of compounds which function as either estrogen receptor (ER) agonists or antagonists in a tissue-specific manner (Cho & Nuttall, 2001; Nilsson & Koehler, 2005). As it is known, SERMs bind to ERs  $\alpha$  and  $\beta$ . After binding, ERs get different conformations and dimerize. This dimerization enables ER complex to regulate gene transcription depending on agonist or antagonist binding. Gene transcription is induced by agonist binding whereas transcription is repressed by

antagonist binding (McDonnell, 2005). Different SERMs display different gene expressions (Berrodin et al., 2009) and SERM-ER complexes behave distinctly in different tissues (McDonnell, 2005). In general, SERMs activate as estrogen agonists in bone (McDonnell, 2005). In a study in which *in vitro* culture of bone marrow from neonatal mice was used, it was found that osteoclast differentiation and bone resorption was declined whereas osteoblast proliferation and activity was increased by SERMs (Taranta et al., 2002).

Currently, there are three major classes of SERMs. First-generation SERMs are triphenylethylene derivatives, tamoxifen and toremifene both of which have been used in clinics. Tamoxifen (Davies et al., 2011) and toremifene (Sawaki et al., 2012) are effective in treatment of breast cancer and tamoxifen is also effective in prevention (Fisher et al., 1998) of the disease. The second-generation SERM, Raloxifene (Ral) (about which detailed information is given in Section 1.2.1.6) is a benzothiopyene derivative used in clinics. This compound is used for osteoporosis treatment and prevention (Ettinger et al., 1999). In a study, it was demonstrated that its use decreased breast cancer incidence in high risk postmenopausal women (Vogel et al., 2006). Moreover, ER antagonist effect of Ral in uterus was reported in animal studies (Sato et al., 1996; Kleinman et al., 1996) and Ral did not increase the risk of endometrial cancer in postmenopausal women (Cummings et al., 1999). However, tamoxifene was documented to increase the risk of endometrial cancer in women with high risk for breast cancer (Fisher et al., 1998) and in breast cancer patients (Fisher et al., 1994). In order to improve the efficacy of SERMs, researches have been continued and recently newer, third generation SERMs have been produced such as ospemifene (Rutanen et al., 2003), lasofoxifene (Gennari, 2006), bazedoxifene (Silverman et al., 2008) and arzoxifene (Deshmane et al., 2007) that are in Phase III clinical trials. Comparative ER agonist or antagonist activities of bazedoxifene, lasofoxifene, Ral, tamoxifen and estrogen in various tissues are shown in Figure 8. Besides many benefits for different

tissues, all SERMS have adverse effects of hot flushes and venous thromboembolism (Cummings et al., 1999; Cummings et al., 2010; Christiansen et al., 2010).

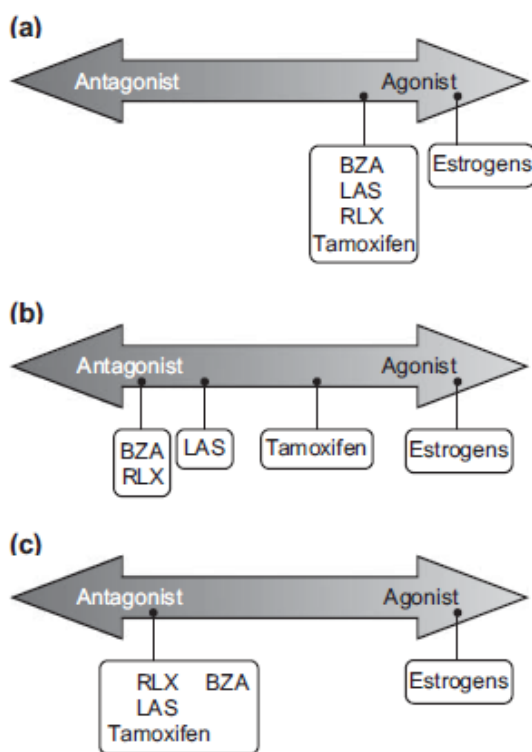


**Figure 8.** Comparative ER agonist or antagonist activities of bazedoxifene (BZA), lasofoxifene (LAS), Ral (RLX), tamoxifen and estrogen in (a) bone, (b) endometrium and (c) breast (Hadji, 2012).

#### 1.2.1.4. Calcitonin

Of the antiresorptive drugs, calcitonin is an endogenous polypeptide hormone which consists of 32 amino acids. It has an important role in calcium homeostasis and bone

remodelling (McDermott and Kidd, 1987; Patel et al., 1993). A primary obstacle for improving bone health through medical intervention is the decreased bone formation seen that is secondary to the effects of the treatments on bone resorption. Most antiresorptive agents reduce bone formation as a secondary effect owing to the coupling between bone resorption and formation (Ravn et al., 1999). However, recent lines of evidence indicate that bone resorption can be attenuated without effects on bone formation as long as the numbers of osteoclasts are maintained (Karsdal et al., 2007; Tankó et al., 2004). Calcitonin is the one that decreases osteoclast activity, but not osteoclast numbers *in vivo* (Ikegame et al., 2004; Chesnut et al., 2005). In clinics, four types of calcitonin are used: Synthetic human calcitonin, synthetic salmon calcitonin (Figure 9), natural porcine calcitonin and a synthetic analogue of eel calcitonin. Calcitonin is administered parenterally or nasally (Stevenson and Evans, 1981).

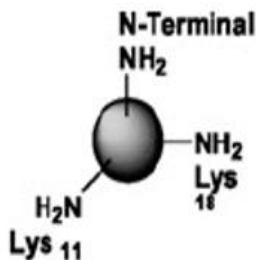


**Figure 9.** Salmon calcitonin (Bhandari et al., 2010).

The therapeutic use of exogenously administered calcitonin is severely hindered by its rapid elimination from the body and its short half-life (approximately 43 min), which in combination contribute to its poor and variable systemic bioavailability (Lee et al., 2003; Shin et al., 2004). Calcitonin elicits its antiresorptive effect by acting on calcitonin receptor (CTR) which exist on osteoclasts (Naot and Cornish, 2008).

However, CTRs are widely distributed in nonskeletal tissues as well, even though calcitonin function has been well defined in osteoclasts. Calcitonin binding was exhibited in tissues such as kidney (Warshawsky et al., 1980), lung (Fouchereau-Peron et al., 1981), placenta (Nicholson et al., 1988), ovaries (Gorn et al., 1992) and spermatozoa (Silvestroni et al., 1987). Therefore, the competitive uptake of available calcitonin among such CTRs likely further reduces calcitonin availability to osteoclasts, especially if the drug is administered systemically and not specifically targeted to bone. Recently, calcitonin was removed from Europe market owing to concerns about causing cancer in its long-term administration (Lim & Clarke, 2012).

#### **1.2.1.5. Denosumab**

In recent years, the studies related with denosumab, a human monoclonal antibody against RANKL which is significant in osteoclastogenesis, have been increased (Bekker et al., 2004; Brown et al., 2009; Cummings et al., 2009). It has been indicated that denosumab has a high specificity and affinity for RANKL (Bekker et al., 2004). After finalization of phase-3 studies (Brown et al., 2009; Cummings et al., 2009), denosumab has been stated to be the most improved one among all investigational compounds and it has recently been approved for osteoporosis in Europe as well as for osteoporosis and bone metastases in the USA (Rachner et al., 2011).

#### **1.2.1.6. Raloxifene**

Raloxifene (Ral) hydrochloride, a nonsteroidal benzothiophen derivative (Figure 10), is a second-generation SERM. It is a light yellow solid with a molecular formula of  $C_{28}H_{27}NO_4S \cdot HCl$  and a molecular weight of 510.05 g/mol. Synonyms of Ral hydrochloride are keoxifene and [6-hydroxy-2-(4-hydroxyphenyl)-benzo[b]thien-3-yl][4-[2-(1-piperidinyl) ethoxy]phenyl] (product information, [www.sigmaaldrich.com](http://www.sigmaaldrich.com)).

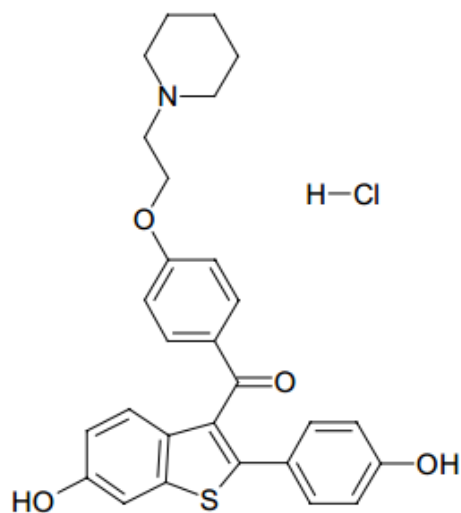


**Figure 10.** Chemical structure of Ral hydrochloride (product information, [www.sigmaaldrich.com](http://www.sigmaaldrich.com)).

Ral is stated for osteoporosis treatment and prevention (Ettinger et al., 1999). Its effects on bone are well established. One clinical trial of Ral at doses of 30 mg, 60 mg and 150 mg demonstrated that these daily doses increased bone mineral density and decreased bone turnover for postmenopausal women (Delmas et al., 1997). In breast and endometrium, Ral binds to ERs to prevent estrogen-induced DNA transcription (Grese et al., 1997; Brzozowski et al., 1997) and therefore activates as an ER antagonist on breast and uterus. In parallel with this phenomena, Ral was found to decrease breast cancer incidence in high risk postmenopausal women (Vogel et al., 2006) and not to increase the risk of endometrial cancer in postmenopausal women (Cummings et al., 1999). In the study of Delmas et al. (1997), in addition to its positive effects on bone, Ral was stated to reduce serum concentrations of total and low-density-lipoprotein cholesterol without endometrial stimulation in postmenopausal women. By Food and Drug Administration (FDA), Ral was approved in 1998 for treatment and prevention of

osteoporosis, and in 2007 for reduction of breast cancer risks (Maximov et al., 2013). It has been used in clinics and available in the markets with the trade name of Evista (Eli Lilly, Indianapolis, IN) as tablets of 60 mg. Moreover, it has been shown that Ral may be more preferable than tamoxifen in terms of the fact that Ral has fewer serious adverse effects while both agents are equally efficient in the prevention of breast cancer. Besides, Ral has been reported to be equally efficient with alendronate in preventing osteoporosis-related fractures and it has been found to have lower side effects than alendronate (Lee et al., 2008).

Although about 60% of Ral administrated orally is absorbed, absolute bioavailability of the drug is just 2%. Ral belongs to class II of Biopharmaceutics Drug Disposition Classification System (BDDCS) since it has the characteristics of high permeability, poor water solubility and high metabolism together. Besides low solubility and dissolution, high presystemic clearance is the other reason for the poor bioavailability of such drugs (Elsheikh et al., 2012). Consequently, when Ral is administrated orally, patients have to take the drug daily and at a high dose of 60 mg. Administration of high dose of Ral systemically would cause to increase risk of Ral side effects influencing many sites of the body. Possible side effects of Ral are venous thromboembolism, pulmonary embolism, hot flushes and leg cramps (Goodman and Gilman's, 2001; Maximov et al., 2013).

In order to summarize the benefits of many osteoporosis drugs along with their side-effects which affect their long-term usages, Table 2 was constructed by Rachner et al. (2011), considering the studies of Black et al. (1996), Cummings et al. (1998), McClung et al. (2001), Harris et al. (1999), Chesnut et al. (2004), Black et al. (2007), Delmas et al. (2002), Reginster et al. (2005), Meunier et al. (2004), Neer et al. (2001) and Greenspan et al. (2007).

**Table 2.** Some conventional drugs that decrease the risk of vertebral and hip fractures when used with sufficient calcium and vitamin-D supplementation, and their side-effects (Rachner et al., 2011).

	Dose	Interval	Route	Efficacy against		Side-effects
				Hip fractures	Vertebral fractures	
<b>Bisphosphonates</b>						Osteonecrosis of the jaw, subtrochanteric femur fractures
<b>Alendronate</b>	70 mg	Weekly	Oral	✓	✓	Oesophageal irritation
<b>Risedronate</b>	35 mg or 150 mg	Weekly or monthly	Oral	✓	✓	Oesophageal irritation
<b>Ibandronate</b>	150 mg	Monthly	Oral	No data	✓	Oesophageal irritation
<b>Ibandronate</b>	3 mg	Every 3 months	Intravenous	No data	No data	Acute-phase reaction
<b>Zoledronic acid</b>	5 mg	Yearly	Intravenous	✓	✓	Acute-phase reaction, hypocalcaemia, potential renal toxic effects
<b>Raloxifene</b>	60 mg	Daily	Oral	No effect	✓	Thromboembolic disease
<b>Strontium ranelate</b>	2 g	Daily	Oral	✓	✓	Thromboembolic disease; drug rash with eosinophilia systemic syndrome, abdominal discomfort
<b>Teriparatide</b>	20 µg	Daily	Subcutaneous	No effect	✓	Hypercalcaemia, nausea, diarrhoea
<b>PTH (1-84)</b>	100 µg	Daily	Subcutaneous	No effect	✓	Hypercalcaemia, nausea, diarrhoea

✓ denotes positive effect of the corresponding drug.

### **1.3. Controlled Drug Delivery**

There are many conventional routes of drug administration such as intravenous and intramuscular ways. Oral administration is the one used mostly since it presents some advantages like being less invasive, self-administrable providing higher patient compliance and lower cost of manufacture. In either way, free drug administration may cause various side effects. For example in *in vivo* environment, drug bioavailability may be very low owing to low solubility and dissolution of drug and/or high presystemic drug clearance. Therefore, drug amount has to be increased to be able to reach the therapeutic dose. However, this results in high dosage use of the drug, and because of that increased risk of side effects occurs. If the drug is administered systemically, many parts of the body would expose to these side effects. Ideally, the drug should be delivered at a required concentration within the therapeutic dose at the right time to a specific target in a safe way. In Figure 11, behaviour of a conventionally administered oral drug after its entrance into the blood plasma is shown. Initially, the concentration of the delivered drug sharply increases, possibly exceeding a toxic level beyond the therapeutic window. Then the concentration decreases to a sub-therapeutic level making the therapy duration dependent on the frequency of administration and the half life of the drug. This inappropriate concentration change along with the low bioavailability obstruct efficacy of the related drug. Hence, there is a need for alternative systems. An example is the controlled drug delivery system enabling a sustained drug release in the therapeutic dose at a rate equivalent to the rate of drug degradation and elimination over an extended period of time (Chirra & Desai, 2012) (Figure 11).

#### **1.3.1. Ral Delivery Systems**

The adverse effects mentioned in Section 1.2.1.6 and the administration frequency of Ral can be lowered provided that long-term, controlled and sustained release of Ral from drug delivery systems is accomplished. Furthermore, total amount of Ral

consumed can be decreased since lower dose of the drug will be sufficient in comparison to the free drug. The dose of the Ral can be even more decreased if the drug is targeted to bone when administrated systemically.

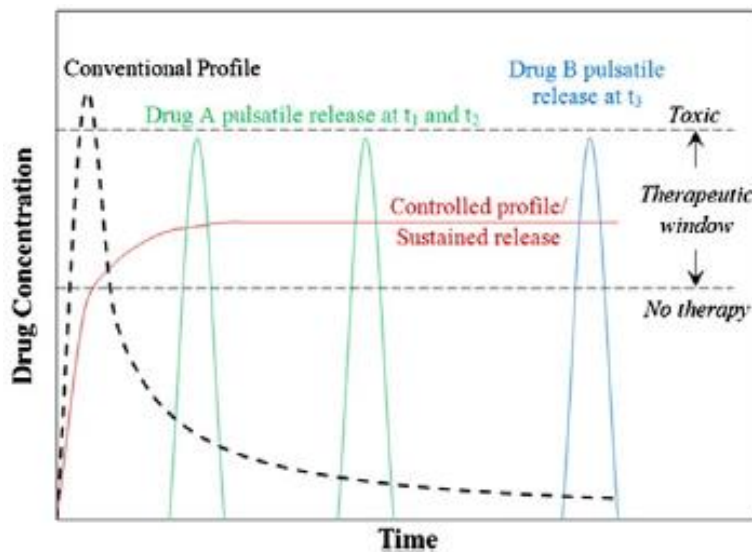


**Figure 11.** Concentration profile of conventional drugs and drug delivery systems (Chirra & Desai, 2012)

In recent years, researches on Ral delivery systems have been increasing. In a study of Burra et al. (2013), triglyceride-based solid lipid nanoparticles containing Ral were prepared and twofold increase in bioavailability was found for oral delivery of the drug. Additionally, Ral-loaded nanoparticles prepared by spray-drying technique (Tran et al., 2013) and by rapid expansion of supercritical system (Keshavarz et al., 2012) were also reported. (Bikiaris et al., 2009) prepared Ral-loaded carriers using aliphatic polyesters by co-precipitation method and investigated the dissolution behavior of the drug from

these nanoparticles. As another example, Ral-loaded gellan gum nanoparticles were examined with *in vitro* drug release and *in vitro* cytotoxicity (human breast carcinoma cell line *MCF-7*) studies (Prakash et al., 2014). Differently from general routes, Mahmood et al. (2014) followed a different strategy by preparing transfersome vesicles for transdermal delivery of Ral and mentioned that this formulation has great potential for delivery of the drug. Other studies involve nanoparticulate Ral delivery system based on biodegradable carboxylated polyurethane (Babanejad et al., 2014), Ral-loaded PLGA microspheres prepared by double-emulsion solvent evaporation method (Park et al., 2009), and injectable and Ral-loaded PCL microspheres (Öcal et al., 2014). Biodegradable polymers of which degradation products are non-toxic have been used widely in drug delivery systems. In this study, Ral-loaded microspheres were prepared by using poly( $\epsilon$ -caprolactone) (PCL) and poly(D,L-lactide-co-glycolide) (PLGA).

### **1.3.2. Biodegradable Polymers: PCL and PLGA**

Biodegradable polymers are categorized into natural and synthetic polymers. Natural polymers include polypeptides, proteins, polysaccharides, and synthetic polymers contain polylactide (PLA), PLGA, PCL and polyorthoesters (Uhrich et al., 1999; Cho et al., 2000; Cohen et al., 1991). Among these, the polyesters PLA, poly(glycolide) (PGA) and PLGA have been extensively used because their dissolution characteristics can be easily adjusted and these polymers possess outstanding physical strength, can be easily synthesized, are susceptible to ready adjustment of molecular weights, are effective in lactide copolymerization and have received FDA approval (Shive and Anderson, 1997; Kang and Schwendeman, 2007; Taluja and Bae, 2007). In this study, PLGA (75:25) with the chemical formula of  $[(C_6H_8O_4)_x(C_4H_4O_4)_y]_n$  (specification sheet of Resomer, Boehringer Ingelheim) was used and its chemical structure is demonstrated in Figure 12.

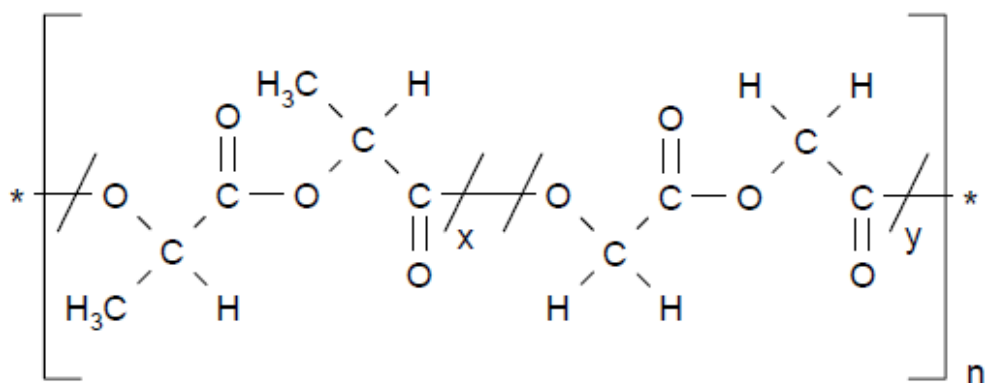


**Figure 12.** Chemical structure of PLGA (75:25) (specification sheet of Resomer, Boehringer Ingelheim).

Another biodegradable polymer is the FDA-approved polyester, PCL, which has a very slow degradation rate relative to many other polymers (Pitt, 1990). Mechanism of drug release from PCL microspheres is often dominated by drug diffusion from microsphere matrix. Therefore, PCL microspheres are suitable for long-term drug release systems (Sinha et al., 2004). Chemical structure of PCL with the formula of  $(C_{10}H_{18}O_2)_n$  (product information, [www.sigmaaldrich.com](http://www.sigmaaldrich.com)) is shown in Figure 13.

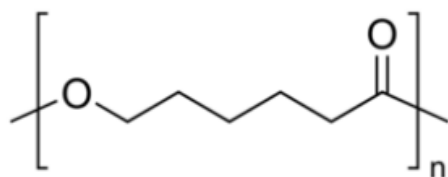


**Figure 13.** Chemical structure of PCL (product information, [www.sigmaaldrich.com](http://www.sigmaaldrich.com)).

PLGA and PCL are biocompatible polymers having the degradation products – lactic acid and glycolic acid – which are easily eliminated in the body (Singh et al., 2006). In this study, in addition to PCL, blends of PCL and PLGA with various ratios were used for microsphere preparation in order to benefit from the advantages of both polymers. In literature, it was indicated that particles/spheres prepared from only PLGA has some disadvantages. For example, Murillo et al. (2002) prepared microspheres of PLGA (100%) or PLGA:PCL (at 75:25 and 50:50 ratios) and loaded with antigenic extract *Hot Saline* from *Brucella ovis*. Their results showed that the pH of the medium during release dropped from 7.4 to 3.5 in the formulation based on PLGA whereas the presence of PCL declined the pH drop. Moreover, Cao & Schoichet (1999) indicated that the microspheres prepared from a blend of PCL and PLGA (50/50) had a degradation profile intermediate between those of PCL and PLGA (50/50), therefore providing a method to further control degradation rate.

#### **1.4. Ral-PEG Conjugate**

Ral possesses very low bioavailability owing to its features of low solubility and dissolution as well as its extensive first-pass metabolism (Elsheikh et al., 2012) as mentioned in Section 1.2.1.6. Considering controlled delivery system of Ral in this study, profile of Ral release from the microspheres of biodegradable polymers, PCL and PLGA, is highly dependent on low solubility and dissolution characteristics of Ral. If Ral turns into a form with higher water solubility, the release rate of Ral from the microspheres would increase.

In order to enhance solubility and dissolution characteristics of poorly water-soluble drugs, many methods have been documented in literature, such as co-grinding (Friedrich et al., 2005; Garg et al., 2009; Patil et al., 2013), spray drying (Rogers et al., 2002), micronization (Chaumeil, 1998), solid dispersion (Khan et al., 2011; Ahuja et al., 2007), super critical fluid technology (Van Nijlen et al., 2003), complexation (Patil et al., 2013;

(Bandela & Anupama, 2009) and lipid-based drug delivery (Attama & Mpamaugo, 2006). Conjugation of the corresponding drug to PEG, which is the technique belonging to the complexation method, can be generated through covalent or non-covalent bondings (Elva et al., 2005).

PEG has been used commonly in the area of polymer-based drug delivery systems due to the fact that it presents many advantages such as high solubility in water and in many organic solvents, lack of immunogenicity, antigenicity and toxicity, and elimination by a combination of renal and hepatic pathways, hence making it ideal to be used in the field of pharmaceuticals. Additionally, PEG has been approved by FDA for human intravenous, oral and dermal applications (Greenwald et al., 2003). Chemical structure of PEG with the formula of  $H(OCH_2CH_2)_nOH$  (product information, [www.sigmaaldrich.com](http://www.sigmaaldrich.com)) is shown in Figure 14:

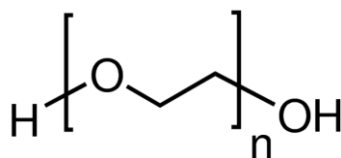


**Figure 14.** Chemical structure of PEG (product information, [www.sigmaaldrich.com](http://www.sigmaaldrich.com)).

Through conjugation of PEG to the relevant drug, PEG molecules shield the drug surface toward the periphery, increasing hydrodynamic radius of the drug. The water solubility of the drug is enhanced by the increased hydrodynamic radius (Bandela & Anupama, 2009). In other words, water solubility of the drug is increased by wettability offered by the hydrophilic polymer, PEG. If the drug is crystalline, PEG conjugation may provide conversion of crystalline nature of the drug to amorphous form, further

increasing the solubility of the drug (Khan et al., 2011; Garg et al., 2009). Because a highly disordered amorphous material has a lower energetic barrier to overcome to enter a solution than a regularly structured crystalline solid (Garg et al., 2009). Additionally, it has been stated that hydrophilic drugs, especially if they are loaded in high amounts, provide water penetration into drug-loaded polymeric systems and generate highly porous polymer structures by drug exit (Klose et al., 2008). Thus, PEG conjugated-drugs can increase degradation rate of polymers owing to their hydrophilic natures, thereby drug release rate can be enhanced.

Considering this study, by means of Ral-PEG (1:2) conjugation, introducing PEG into Ral-loaded PCL:PLGA (1:1) microspheres, of which three components have low water solubility, presents the possibility of increasing water solubility of Ral as well as accelerating degradation rate of the polymers (PCL and PLGA), and thus, enhancing rate of Ral release from the microspheres. As an ultimate advantage, this approach can enable to benefit from more amount of Ral encapsulated in the microspheres as well as to increase treatment efficacy of Ral. Additionally, in the forthcoming studies, this method may provide to adjust release rate of Ral by changing PEG ratio in the conjugate and aid to obtain the optimum composition of the microspheres.

## **1.5. Aim of the Study**

Osteoporosis is a skeletal disease characterized by a decrease in bone strength and bone mass, accompanied by an increase in fragility of bones and risk of fractures seen mostly in elderly people. There are many therapeutic agents used for treatment of osteoporosis in clinics, most of which are administrated systemically. Ral is one of these drugs, having poor bioavailability. Thus, it has to be administrated in high dosage forms and at frequent intervals to maintain the therapeutic level, causing the patients to be at high risk of side effects which influence all the body. Additionally, the treatment method costs highly and the patients have to put up with the tiresome therapy period.

As a solution to such issues, controlled drug delivery systems have been investigated recently. The main principle behind this strategy is that it provides controlled and sustained release of the drug at the therapeutic level from a specified carrier. With this method, many side effects due to use of high dose and the administration frequency of the drug can be lowered, total amount of the sufficient drug can be reduced and efficacy of the treatment can be enhanced. In this study, it was aimed to prepare PCL or PCL:PLGA (1:1) microspheres loaded with Ral or Ral-PEG (1:2) conjugate. Ral-PEG (1:2) conjugate was used to increase Ral water solubility and degradation rate of the polymers (PCL and PLGA), in turn to enhance rate of Ral release from the microspheres for the aim of benefiting from more amount of Ral encapsulated in the microspheres and enhancing treatment efficacy of Ral. For the forthcoming studies, this approach also presents the possibility of adjusting release rate of Ral by changing PEG ratio in the conjugate and thereby reaching the optimum composition of the microspheres. The targets of this study can be summarized as:

- Development of a long-term controlled Ral delivery system with high encapsulation efficiency.
- *In situ* characterizations such as evaluation of Ral release profile of the microspheres as well as size and morphology analyses of the microspheres.
- Usage of Ral-PEG (1:2) conjugate to improve the controlled delivery system by increasing the release rate of Ral from the microspheres.
- Evaluation of the effects of Ral-loaded microspheres on viability and osteogenic differentiation of the cells to determine the functionality of the system.

## CHAPTER 2

### MATERIALS AND METHODS

#### 2.1. Materials

Poly(D,L-lactide-co-glycolide) (PLGA,  $M_w$ : 8000-15000 g/mol, 75:25) was purchased from Boehringer Ingelheim (Germany). Poly( $\epsilon$ -caprolactone) (PCL,  $M_w$ : 14000 and 65000 g/mol) and poly(vinyl alcohol) (PVA,  $M_w$ : ~27000 g/mol) were obtained from Aldrich (Germany). Poly(ethylene glycol) (PEG,  $M_w$ : 3500-4500 g/mol) was purchased from Fluka (Germany). Dichloromethane (DCM) was the product of Merck (Germany). Raloxifene (Ral) hydrochloride, dimethyl sulfoxide (DMSO),  $\beta$ -glycerophosphate, dexamethasone, L-ascorbic acid (99%), methanol (MeOH), Alizarin Red S, paraformaldehyde, acetone and collagenase from *Clostridium histolyticum* were purchased from Sigma-Aldrich (USA). Alpha-Minimal Essential Medium ( $\alpha$ -MEM) was obtained from Lonza (Belgium). Dulbecco's Modified Eagle's Medium/Ham's F-12 Medium (DMEM/F-12) (1:1) was obtained from Thermo Scientific (Utah, USA). Human fetal osteoblast cell line (hFOB 1.19 (ATCC<sup>®</sup> CRL-11372<sup>TM</sup>)) was purchased from American Type Culture Collection (USA). Trypsin-EDTA, fetal bovine serum (FBS) and penicillin/streptomycin were the products of Biochrom (Germany). Plastic ware used for cell culture studies was obtained from Greiner Bio-One GmbH (Germany). Alkaline Phosphatase (ALP) assay kit was the product of Abcam Inc. (USA). PrestoBlue<sup>®</sup> cell viability reagent was purchased from Invitrogen (USA).

## **2.2. Methods**

### **2.2.1. Optimization Studies for Preparation of the Microspheres**

Preparation method of microspheres was optimized with initial studies. During optimization studies, different preparation methods (co-precipitation, solid-in-oil-in-water and oil-in-oil-in-water) were conducted.

#### **2.2.1.1. Co-precipitation Method**

Firstly, co-precipitation method which was proposed for poorly water-soluble drugs like Ral (Bikiaris et al., 2009) was used in this study. Briefly, 5 mg Ral was added into in 2 mL of the solvent system containing acetone:distilled water (15:1, v/v). The resulting mixture was sonicated for 1 min by a sonicator (Sonorex, Bandelin, Germany). Then, PCL or PLGA (50 mg) was added into the same solvent mixture and sonication was performed for another 1 min. The mixture was transferred slowly to 10 mL distilled water in 30 min by a syringe pump (New Era Pump Systems, Inc., New York, USA). The system was gently stirred at 800 rpm with a magnetic stirrer (Schott, Mainz, Germany) until the evaporation of the organic solvent was complete. Finally, the suspension was lyophilized by a freeze-dryer (Heto-Holten Model Maxi-Dry LYO) at METU Central Laboratory. This method was also used in order to prepare empty PLGA microspheres. In this case, 10 mL distilled water was poured into a beaker with a higher surface area and stirred at 1100 rpm continuously throughout the experiment. Except these steps, the same procedure described above was followed. In the next trial, the solvent in the beaker was stirred at a higher rate of 8000 rpm by a homogenizer (T-25 Ultra-Turrax, IKA, Germany) continuously during all the experiment.

### **2.2.1.2. Solid-in-Oil-in-Water Method**

Solid-in-oil-in-water method was also used by following modified version of the methods described by Sinha et al. (2004) and Arias et al. (2010). For the preparation of Ral-loaded PCL microspheres, 100 mg PCL was dissolved in DCM (3 mL). Then, 10 mg Ral was added into PCL solution and stirred. The organic phase was added dropwise into PVA aqueous solution (40 mL, 1%) while stirring at 1100 rpm with the magnetic stirrer (Schott, Mainz, Germany). After 25 min of stirring, the mixture of organic phase and PVA was poured slowly into the remaining PVA solution (140 mL) while stirring at 14000 rpm by the homogenizer (T-25 Ultra-Turrax, IKA, Germany). The mixing was continued for 3 min. DCM was removed by stirring the mixture with the magnetic stirrer (Schott, Mainz, Germany) at 25°C for 2 h. The microspheres were precipitated by centrifugation (Ultracentrifuge, Hitachi, Japan) at 20000  $\times$  g for 20 min at METU Central Laboratory and washed with distilled water two times. The obtained suspension was dried at 37°C to get the microspheres as powder form. Microspheres could not be obtained appropriately with this procedure and some modifications were done as described below.

As the first modification, the volume of DCM was lowered to 1.5 mL to dissolve 100 mg PCL and the same procedure was followed. However, this trial was also not successful. Secondly, the concentration of PVA was increased to 2% and minor changes in the preparation steps were done. For this purpose, after the organic phase was added dropwise into 40 mL of PVA solution, the mixing was continued only for 5 min. Mixture of organic phase and PVA was then poured slowly into the remaining PVA solution (140 mL). After all the mixture was added, stirring at 14000 rpm was carried out with the homogenizer for 3 min. At the end of the process, the microspheres were precipitated by centrifugation (Hettich Zentrifugen, EBA 20, Germany) at 6000 rpm for 10 min and washed with distilled water two times. In another attempt, as the only difference from the latter method, the stirring rate of the homogenizer was increased to

18000 rpm, the microspheres were precipitated by centrifugation at 6000 rpm for 20 min and washed with distilled water three times. At the end, the obtained suspension was dried in a vacuum dryer (Nüve-EV060, Turkey) at room temperature.

Using solid-in-oil-in-water method, Ral-loaded microspheres consisting of a blend of PCL:PLGA (9.1:1, w/w) were also prepared. Shortly, 5.5 mg PLGA was dissolved in DCM (3 mL) and 50.3 mg PCL was added into the solution and stirred. Then, 5.3 mg Ral was added into the polymer solution. With change from the former method, 180 mL aqueous solution of 2% PVA was put into a beaker and foamed by stirring with the homogenizer. The organic phase was then added dropwise into foamed PVA solution while not stirring. After adding all the organic phase, the stirring was initiated with the homogenizer set at 20000 rpm and continued for 10 min. DCM was removed by stirring the mixture with the magnetic stirrer (Schott, Mainz, Germany) at 25°C for 2 h. The microspheres were precipitated by centrifugation at 6000 rpm for 25 min and washed with distilled water three times. The obtained suspension was dried in the vacuum dryer at room temperature. Additionally, some other modifications related with the method were performed and different groups of the microspheres were prepared as summarized in Table 3.

**Table 3.** Details related with modifications of the solid-in-oil-in-water method for optimization of microsphere preparation.

<b>Group</b>	<b>PCL:PLGA (w/w)</b>	<b>Theoretical Ral loading (%)</b>	<b>Modifications</b>
A)	10:4 (PCL, M <sub>w</sub> : 14000)	10	Organic phase including PCL, PLGA and Ral in DCM was sonicated for 1 min and then added directly into 1% PVA solution. In the homogenizer, stirring was performed at 20x10 <sup>3</sup> rpm for 5 min.
B)	10:4 (PCL, M <sub>w</sub> : 14000)	10	Organic phase including PCL, PLGA and Ral in DCM was sonicated for 1 min and then added directly into 2% PVA solution. In the homogenizer, stirring was performed at 17.8x10 <sup>3</sup> rpm for 3 min.
C)	10:4 (PCL, M <sub>w</sub> : 14000)	10	Organic phase including PCL, PLGA and Ral in DCM was sonicated for 1 min and then added dropwise into 2% PVA solution while not stirring. In the homogenizer, stirring was performed at 18.6x10 <sup>3</sup> rpm for 3 min.
D)	10:4 (PCL, M <sub>w</sub> : 14000)	9	Organic phase including PCL, PLGA and Ral in DCM was sonicated for 1 min and then added directly into 2% PVA solution. In the homogenizer, stirring was performed at 18.2x10 <sup>3</sup> rpm for 3 min.

### **2.2.1.3. Oil-in-Oil-in-Water Method**

In order to obtain homogeneous drug dispersion in the organic phase and hence, in the polymer mixture, leading to high drug encapsulation efficiency (Wischke & Schwendeman, 2008), oil-in-oil-in-water method was also used for preparation of microspheres. In initial studies for this method, Ral was dissolved in DMSO or MeOH and the modifications described in Table 4 were applied. As the first trial, Ral was dissolved in its best solvent, DMSO, and added into the polymer solution. For this group, the organic phase was very clear showing homogeneous mixing of Ral and polymer. However, Ral floccules were seen after solvent evaporation, which resulted with low Ral amount entrapped in the polymer matrix of the microspheres. After all optimization studies, MeOH was chosen for the solvent of Ral and the oil-in-oil-in-water (O<sub>1</sub>/O<sub>2</sub>/w) method with the parameters mentioned in Section 2.2.4 was selected to be used for the preparation of the microspheres.

### **2.2.2. Preparation of Ral-PEG Conjugate**

In order to enable Ral to have less hydrophobic and less crystalline nature and to increase degradation rates of PCL and PLGA, and therefore, to increase rate of Ral release from the microspheres, conjugation reaction between Ral and PEG was performed (Figure 15). During reaction, hydrogen bondings are expected to be formed between amine and phenolic-OH groups of Ral and hydroxyl groups of PEG. For preparation of the conjugate, solvent evaporation method described by Bandela & Anupama (2009) was modified and used. Briefly, Ral and PEG at a weight ratio of 1:2 were dissolved in MeOH and stirred for 6 h at room temperature by an orbital shaker (BIOSAN, OS-10, Turkey). The mixture was then dried in the vacuum dryer (Nüve-EV060, Turkey). Resulting Ral-PEG conjugate was kept at 4°C until use.

**Table 4.** Details related with modifications of the oil-in-oil-in-water method for optimization of microsphere preparation.

<b>Method</b>	<b>PCL:PLGA (w/w)</b>	<b>Theoretical Ral loading (%)</b>	<b>Modifications</b>
(o/o/w)	10:4 (PCL, Mw: 65000)	8	Organic phase including PCL, PLGA and Ral in MeOH was sonicated for 1 min and added dropwise into 40 mL of 1% PVA, then poured directly into remaining PVA. In the homogenizer, stirring was performed at $15 \times 10^3$ rpm for 3 min.
(o/o/w)	10:4 (PCL, Mw: 14000)	8	Organic phase including PCL, PLGA and Ral in DMSO was sonicated for 1 min and added dropwise into 40 mL of 1% PVA, then poured directly into remaining PVA. In the homogenizer, stirring was performed at $21.2 \times 10^3$ rpm for 5 min.

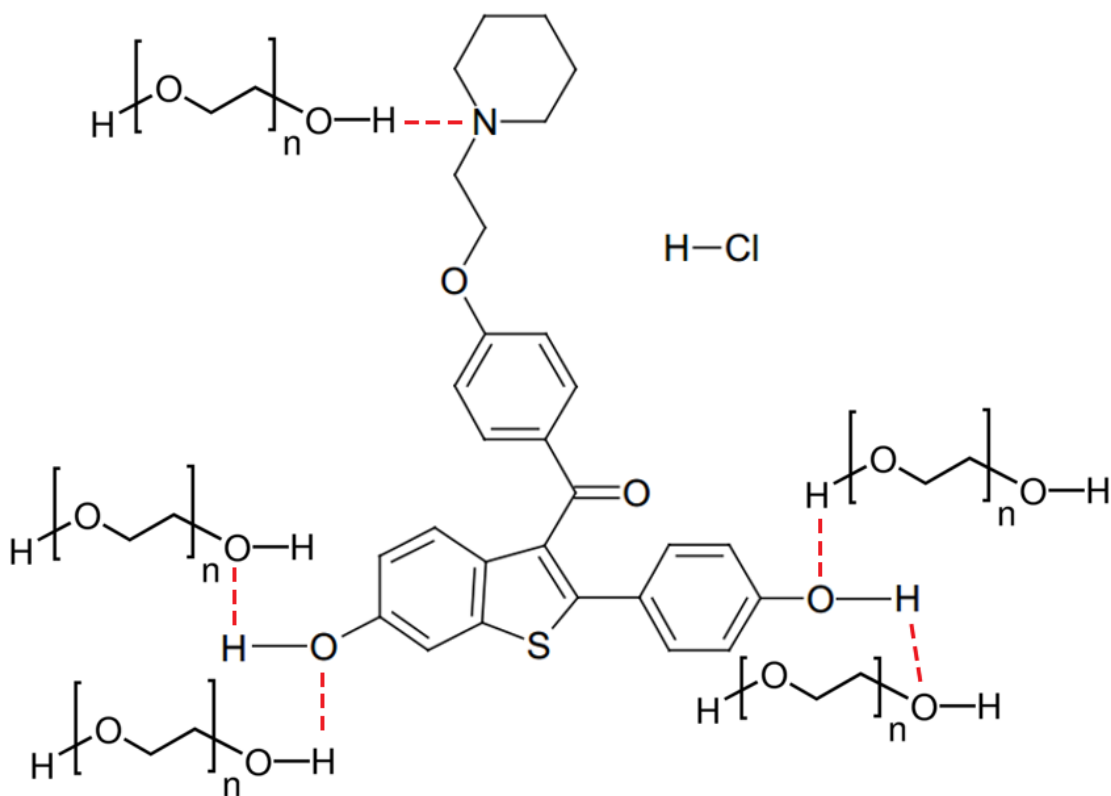


**Figure 15.** Possible hydrogen bondings (- - -) formed between amine and phenolic-OH groups of Ral and hydroxyl groups of PEG during conjugate reaction.

### 2.2.3. Characterization of Ral-PEG Conjugate

#### 2.2.3.1. Fourier Transform Infrared Spectroscopy

In order to analyze the chemical interaction between Ral and PEG after conjugation, fourier transform infrared spectroscopy (FT-IR) was performed for the samples of Ral, PEG and Ral-PEG with FT-IR spectrophotometer of PerkinElmer L1050002 series (PerkinElmer, Inc., UK) at BIOMATEN, Center of Excellence in Biomaterials and

Tissue Engineering, METU. FT-IR was carried out with spectrum 100/100N software programme in transmission mode. The analysis was conducted within the range 400-4000  $\text{cm}^{-1}$ , with a resolution of 4  $\text{cm}^{-1}$ , and using a total of 50 scans per sample. Subsequent to mixing the samples with KBr, the spectra of all samples were corrected for background and atmosphere inside the FT-IR spectrophotometer.

### **2.2.3.2. X-Ray Diffraction Analysis**

X-ray diffraction (XRD) method was used to investigate the degree of crystallinity of Ral before and after conjugation. XRD patterns of Ral, PEG, physical mixture of Ral and PEG, and Ral-PEG were traced using Rigaku X-ray diffractometer (Ultima D/MAX 2200PC, Japan) at the X-Ray Analysis Laboratory, Department of Metallurgical and Materials Engineering, METU. Samples were subjected to  $\text{Cu-K}\alpha$  radiation at a voltage of 40 kV and a current of 30 mA. Diffraction patterns were obtained over the range of  $2\theta$  between  $5^\circ$  and  $50^\circ$  with a sampling interval of  $0.02^\circ$  and a scanning rate of  $1^\circ/\text{min}$ .

### **2.2.3.3. Morphological Analysis by Scanning Electron Microscopy**

Crystal morphology of Ral before and after PEG conjugation were examined qualitatively by scanning electron microscopy (SEM) (FEI Nova NanoSEM 430, equipped with NORAN System 6 X-ray Microanalysis System & Semafore Digitizer) at the SEM Laboratory, Department of Metallurgical and Materials Engineering, METU. Before analysis, particles were adhered onto a metal stub by a carbon band and coated with gold with a sputter coating device (Quorum Technologies, SC7640 High Resolution Sputter Coater).

#### **2.2.4. Preparation of Ral- and Ral-PEG Conjugate-Loaded PCL and PCL:PLGA (1:1) Microspheres**

After preliminary studies, the oil-in-oil-in-water ( $o_1/o_2/w$ ) double emulsion-solvent evaporation method was selected to be used for the preparation of the microspheres and the methods of Tripathi et al. (2010) and Park et al. (2009) were used with some changes. Subsequent to preparation of Ral-PEG (1:2) conjugate for the aim of increasing rate of Ral release from the microspheres, the following six types of microspheres (of which the first and second ones served as controls) were prepared with the optimized method (Ral-PEG is used instead of Ral-PEG (1:2) conjugate from this section forward):

- i) Unloaded (empty) PCL:PLGA (1:1) microspheres
- ii) Unloaded (empty) PCL microspheres
- iii) Ral-loaded PCL microspheres
- iv) Ral-loaded PCL:PLGA (1:1) microspheres
- v) Ral-PEG-loaded PCL microspheres
- vi) Ral-PEG-loaded PCL:PLGA (1:1) microspheres

Steps of the procedure for preparation of microspheres is shown in Figure 16. Shortly, internal oil phase ( $o_1$ ) was formed by dissolving Ral or Ral-PEG (6 or 18 mg) in MeOH (1.2 mL). PCL or a blend of PCL:PLGA (1:1) was dissolved in DCM (9 mL) to obtain 2% (w/v) polymer concentration, yielding external oil phase ( $o_2$ ). Ral or Ral-PEG solution was then poured into polymer solution dropwise and the mixture was sonicated for 1 min on ice by the sonicator (Sonorex, Bandelin, Germany). The obtained primary emulsion ( $o_1/o_2$ ) was then poured into 120 mL aqueous solution of PVA (2%, w/v) with pipette while stirring the aqueous phase at 15000 rpm with the homogenizer (T-25 Ultra-Turrax, IKA, Germany). Second emulsion was stirred with the homogenizer for 3 min. Then, to remove the organic solvent, the resulting double emulsion was gently

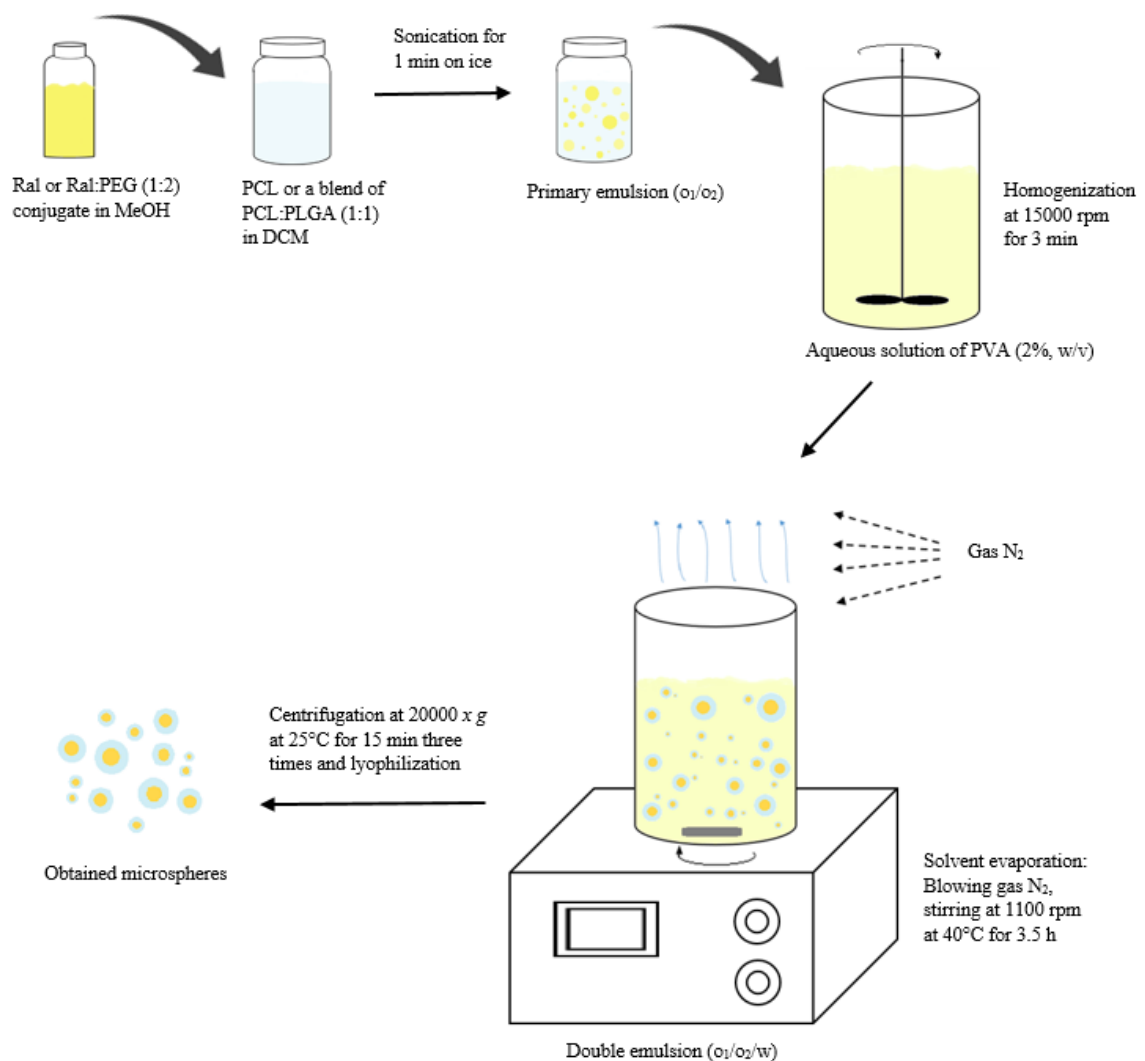


**Figure 16.** Procedure for preparation of microspheres.

stirred for 3.5 h at 1100 rpm under N<sub>2</sub> gas at 40°C with the magnetic stirrer (Schott, Mainz, Germany). Afterwards, the microsphere suspension was centrifuged at 20000g for 15 min at 25°C with a centrifuge (Sigma 3-30 K, Germany). Following removal of supernatant, the microspheres were washed twice with distilled water. The obtained

suspension was frozen at -20°C overnight and lyophilized by a freeze dryer (Labconco Co., USA). Obtained microspheres were stored at 4°C prior to use.

## **2.2.5. Characterization of Ral- and Ral-PEG-Loaded PCL and PCL:PLGA (1:1) Microspheres**

### **2.2.5.1. Morphological Analysis by SEM**

Morphology, surface topography and particle size distribution of the microspheres before and after release studies were investigated by SEM (FEI Nova NanoSEM 430, equipped with NORAN System 6 X-ray Microanalysis System & Semafore Digitizer) at the SEM Laboratory, Department of Metallurgical and Materials Engineering, METU. Before analysis, spheres were adhered onto a metal stub by a carbon band and coated with gold with a sputter coating device (Quorum Technologies, SC7640 High Resolution Sputter Coater).

### **2.2.5.2. Particle Size Analysis**

In order to perform particle size analyses, diameters of 1200 microspheres (for each group) on SEM micrographs were measured using Image J analysis software (NIH, USA). Particle size distribution was shown by a histogram with an equal number of bins between the maximum and minimum values and a cumulative arithmetic curve. In order to evaluate heterogeneity level of the distribution, polydispersity (PDI) value was calculated using the equation below (Torrado et al., 1989):

$$PDI = \frac{d(0.9) - d(0.1)}{d(0.5)}$$

d(0.9), d(0.5) and d(0.1) denote the diameters where 90%, 50% and 10% of the microspheres is smaller than the stated value, respectively. A low value of PDI refers to a narrow particle size distribution.

### **2.2.5.3. Determination of Ral Encapsulation Efficiency and Loading**

The spectrophotometric method described by Öcal et al. (2014) was followed with some modifications to determine Ral content in the microspheres. Briefly, microspheres were dissolved in DCM and then equal volume of MeOH was added to solubilize Ral. With a UV/VIS spectrophotometer (Hitachi U-2800A, Japan), the amount of Ral encapsulated in the microspheres was quantified by measuring optical density at 287 nm. The calibration curve was plotted with different concentrations of Ral (in the range of 5-25 µg/mL) in the solvent mixture DCM:MeOH (1:1). 287 nm was chosen as the wavelength for quantitation of Ral as PCL, PLGA and PEG in the extraction samples did not give interference with Ral optical measurements. Encapsulation efficiency (%) and loading (%) of the microspheres were calculated as follows:

$$\text{Encapsulation efficiency (\%)} = \frac{\text{Experimental Ral Content}}{\text{Theoretical Ral Content}} \times 100$$

$$\text{Loading (\%)} = \frac{\text{Experimental Ral Amount in the Microspheres}}{\text{Experimental Amount of the Microspheres}} \times 100$$

### **2.2.5.4. Ral Release Profiles of the Microspheres**

Release studies were performed in order to understand the effect of PEG conjugation to Ral and the effect of polymer composition on Ral release properties of microspheres. Release profiles of Ral-loaded PCL and Ral-loaded PCL:PLGA (9.1:1, w/w)

microspheres prepared by the solid-in-oil-in-water method (mentioned in Section 2.2.1.2) during the optimization studies as well as Ral-loaded PCL, Ral-loaded PCL:PLGA (1:1), Ral-PEG-loaded PCL and Ral-PEG-loaded PCL:PLGA (1:1) microspheres prepared by the optimized oil-in-oil-in-water method (mentioned in Section 2.2.4) were investigated. Except Ral-PEG-loaded PCL:PLGA (1:1) microspheres, 5 mg of microspheres from each group was incubated in 4 mL of phosphate buffer saline (PBS, pH 7.4). For Ral-PEG-loaded PCL:PLGA (1:1) microspheres, 10 mg of microspheres from each group was incubated in 4 mL PBS (pH 7.4). Microspheres belonging to all groups were incubated at 37°C in a shaking water bath (Nüve, ST 402, Turkey) for two months. At specific time points, total release media was centrifuged at 6000 rpm for 15 min and aliquots from supernatant were taken to determine the amount of Ral release with respect to time. After taking aliquots from supernatant, total release media was refreshed with fresh PBS except for the first time point at which half of the release media was refreshed. All release samples collected were mixed with MeOH at 1:1 ratio. The amount of Ral release was found either by high performance liquid chromatography (HPLC) or spectrophotometry.

#### **2.2.5.4.1. HPLC Analysis**

Ral release from Ral-loaded PCL and Ral-loaded PCL:PLGA (9.1:1, w/w) microspheres prepared by solid-in-oil-in-water method during the optimization studies with respect to time was analysed by HPLC and the method of Öcal et al. (2014) was used. Briefly, analytical chromatographic separation was carried out on a liquid chromatography system controlled by LCsolution software. It was equipped with an isocratic pump, an autosampler, a column thermostat and an UV detector (all the parts of the chromatograph are the products of Shimadzu, Japan). The mobile phase was delivered isocratically with a flow rate of 0.8 mL/min, the injection volume was 20 µL and the wavelength for UV detection was 287 nm. The total analysis time was 15 min and the column was thermostated at 25°C. The mobile phase was prepared by mixing MeOH

with distilled water (85:15, v/v), then filtered and degassed. Stock solution was prepared by dissolving Ral in MeOH at the concentration of 50 µg/mL. Using stock solution, standard solutions in the range of 0-20 µg/mL were prepared by appropriate dilution and mixing with PBS at 1:1 ratio. Using the calibration curve, Ral amount in the release samples (which were mixed with MeOH at 1:1 ratio) was found. All release data were expressed as cumulative (µg and %) release with respect to time.

#### **2.2.5.4.2. Spectrophotometric Analysis**

Ral release profiles of Ral-loaded PCL, Ral-loaded PCL:PLGA (1:1), Ral-PEG-loaded PCL and Ral-PEG-loaded PCL:PLGA (1:1) microspheres prepared by the optimized oil-in-oil-in-water method were investigated by spectrophotometric analysis. Briefly, the absorbances of release samples (which were mixed with MeOH at 1:1 ratio) were measured at 287 nm with the UV/VIS spectrophotometer (Hitachi U-2800A, Japan) and the amount of Ral release was determined using the calibration curve constructed with Ral in MeOH:PBS (1:1) in the range of 0-8 µg/mL. Release data were expressed as cumulative (µg and %) release with respect to time.

#### **2.2.6. Cell Culture Studies**

##### **2.2.6.1. Isolation and Proliferation of Adipose-Derived Mesenchymal Stem Cells**

Upon approval of the protocol by Afyon Kocatepe University Ethical Committee for Animal Experiments (Appendix A), female adipose-derived mesenchymal stem cells were isolated from Sprague-Dawley rats with the group of Assoc. Prof. Dr. Korhan Altunbaş at Afyon Kocatepe University, Veterinary Faculty, Histology and Embryology Department. The method of Meruane et al. (2012) was followed for enzymatic isolation

of adipose-derived mesenchymal stem cells. Briefly, adipose tissue was harvested and minced. Minced tissue was treated with collagenase and incubated at 37°C for about 1 h. After pipetting and filtering through mesh (with pore size: 70 µm), the cell suspension was centrifuged at 1800 rpm for 10 min. Isolated mesenchymal stem cells were cultured in growth medium ( $\alpha$ -MEM supplemented with 10% FBS, 80 U/mL penicillin and 80 µg/mL streptomycin) at 37°C under 5% CO<sub>2</sub> in a carbon dioxide incubator (SL SHEL LAB, USA). Medium was refreshed every third day and the cells were passaged with 0.1% Trypsin-EDTA solution in a 1:3 ratio. Phase contrast micrographs of the primer cells and the cells at 1<sup>st</sup> and 2<sup>nd</sup> passages were taken by an inverted microscope (Nikon ECLIPSE, TS 100, Japan) to examine the morphology of the cells at different passages. After proliferation to 3<sup>rd</sup> passage, mesenchymal stem cells were used for cell culture studies.

#### **2.2.6.2. Human Fetal Osteoblast Cell Line (hFOB)**

hFOB 1.19 cells purchased from ATCC® were cultivated in growth medium (DMEM/F-12 (1:1) supplemented with 10% FBS, 80 U/mL penicillin and 80 µg/mL streptomycin) at 37°C under 5% CO<sub>2</sub> in the carbon dioxide incubator (SL SHEL LAB, USA). The cells were passaged using 0.1% trypsin-EDTA in a 1:4 ratio. The morphology of these cells was also studied by phase contrast microscopy with the inverted microscope (Nikon ECLIPSE, TS 100, Japan). For cell culture studies, hFOB cells at passage 9 were used.

#### **2.2.6.3. Dose-Dependent Effects of Ral and Ral-PEG on Adipose-Derived Mesenchymal Stem Cells and hFOB Cells**

Cells at 3<sup>rd</sup> and 9<sup>th</sup> passages were used for adipose-derived mesenchymal stem cells and hFOB cells, respectively. Cells were seeded at an initial seeding density of 15000

cells/cm<sup>2</sup> in 24-well plates. After seeding, the cells were allowed to recover for 2 days. On the 2<sup>nd</sup> day, medium of the cells was removed and medium containing various doses of Ral and Ral-PEG was added to the wells. Both kinds of cells were cultivated in their corresponding growth medium during this study and the drug was replenished in every medium change. The cells cultivated in the medium including DMSO (solvent of Ral and Ral-PEG) were used as control for comparison. Specified doses of Ral and Ral-PEG, and duration of the treatment period were indicated for each analysis in the following sections.

#### **2.2.6.3.1. *In Vitro* Cytotoxicity Studies**

Dose-dependent effects of Ral and Ral-PEG on the viability of adipose-derived stem cells and hFOB cells were investigated with Prestoblue assay. The effects of different doses of Ral and Ral-PEG (0.1, 1 and 10  $\mu$ M) on viability of adipose-derived stem cells were tested after 3, 7 and 14 days of treatment. For hFOB cell line, the analysis was performed after 1, 4, 7 and 14 days of Ral and Ral-PEG treatment at the doses of 0.01, 0.1, 1 and 10  $\mu$ M.

Prestoblue assay provides to determine the extent of the metabolic activity of the cells. If the cell is alive, Prestoblue, an oxidation-reduction indicator, is reduced by the cell and the colour of the medium changes from blue to red. In this assay, briefly, cell medium including 10% Prestoblue was added to each well. After 6 hours of incubation at 37°C under 5% CO<sub>2</sub>, optical densities were measured at 570 nm and 600 nm with a microplate reader (BioTek  $\mu$ Quant, USA). The following calculation was performed to find the percentage difference in reduction between treatment and control groups according to the manufacturer's protocol and the resulting data were expressed as relative cell viability (% of control group):

$$\% \text{ Difference in reduction between treatment and control groups} = \frac{(O2 \times A1) - (O1 \times A2)}{(O2 \times P1) - (O1 \times P2)} \times 100$$

where:

O1 = molar extinction coefficient (E) of oxidized AlamarBlue® at 570 nm = 80586

O2 = E of oxidized AlamarBlue® at 600 nm = 117216

A1 = absorbance of treatment group at 570 nm

A2 = absorbance of treatment group at 600 nm

P1 = absorbance of control group at 570 nm

P2 = absorbance of control group at 600 nm

### **2.2.6.3.2. Alkaline Phosphatase (ALP) Activity Analysis**

In order to investigate the effects of different doses of Ral and Ral-PEG on osteogenic differentiation of hFOB cells, Ral and Ral-PEG at the doses of 0.01, 0.1, 1 and 10  $\mu$ M were added to the growth medium of the cells. After 7 days of treatment, ALP activity analysis was performed.

ALP, which is an intracellular enzyme, catalyzes the hydrolysis of *p*-nitrophenyl phosphate, producing an organic radical (*p*-nitrophenol) and inorganic phosphate (Figure 17). High level of ALP activity indicates improved osteogenic differentiation of the related cells.

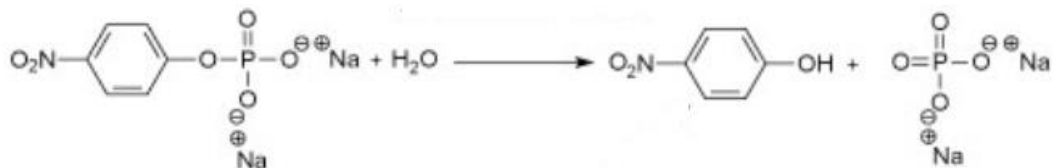


**Figure 17.** Hydrolysis of *p*-nitrophenyl phosphate into an organic radical (*p*-nitrophenol) and inorganic phosphate ([www.sigmaaldrich.com/life-science/metabolomics/enzyme-explorer/analytical-enzymes/alkaline-phosphatase.html](http://www.sigmaaldrich.com/life-science/metabolomics/enzyme-explorer/analytical-enzymes/alkaline-phosphatase.html)).

In this study, ALP assay kit was used to measure the ALP activity of the cells in each group. In this method, the cells were lysed with assay buffer and centrifugated at 13000  $\times$  g for 3 min. Then, *p*-nitrophenyl phosphate substrate was added to the supernatant and the mixture was incubated at 25°C for 60 min. After adding the stop solution to inhibit enzyme activity, the optical density of the resulting reaction solution was measured at 405 nm with the microplate reader (BioTek  $\mu$ Quant, USA). The obtained product (*p*-nitrophenol) amount was determined by the calibration curve plotted with different amounts of *p*-nitrophenol (0-20 nmol/well) produced by ALP enzyme belonging to the kit. For each sample, ALP activity was divided by the incubation time (60 min) and expressed as nmol/min.

#### **2.2.6.4. Effects of Ral- and Ral-PEG-Loaded Microspheres on Adipose-Derived Mesenchymal Stem Cells**

Microspheres of all types of groups (empty PCL:PLGA (1:1), empty PCL, Ral-loaded PCL, Ral-loaded PCL:PLGA (1:1), Ral-PEG-loaded PCL and Ral-PEG-loaded PCL:PLGA (1:1) microspheres) were sterilized with UV for 2 h (with 20 min on-20 min off intervals) and added into the growth and osteogenic differentiation (growth medium supplemented with 50  $\mu$ g/mL ascorbic acid, 10 mM  $\beta$ -glycerophosphate and  $10^{-8}$  M

dexamethasone) media to allow Ral and Ral-PEG release from the microspheres. Growth medium was used for cytotoxicity analyses whereas osteogenic differentiation medium was used for Alizarin red S analyses. Concentration of the microspheres in the corresponding cell culture medium was specified as 5 mg/4 mL, which was same with the concentration of Ral-PEG-loaded PCL:PLGA microspheres used for release studies in PBS (pH 7.4) at 37°C.

The female adipose-derived mesenchymal stem cells at 3<sup>rd</sup> passage were seeded at an initial seeding density of 15000 cells/cm<sup>2</sup> in 24-well plates. After 2 days, the medium of the cells was removed. Medium samples containing Ral and Ral-PEG released from the microspheres after 24 hours of incubation were added to the wells. Half of the medium in which the microspheres were incubated was given to the cells and the withdrawn volume was replaced with an equal volume of fresh cell culture medium to keep the total volume constant. Same procedure was followed after 2 and 5 days of incubation of microspheres in the related medium.

#### **2.2.6.4.1. *In Vitro* Cytotoxicity Studies**

Prestoblue assay was used to determine the effects of Ral- and Ral-PEG-loaded microspheres on the viability of female adipose-derived mesenchymal stem cells. Analysis was performed after 1, 4 and 7 days of cultivation of the cells in the medium containing Ral and Ral-PEG released from the microspheres. For this analysis, steps mentioned in Section 2.2.6.3.1 were followed. Untreated cells which were cultivated in the growth medium were used as control for comparison.

#### **2.2.6.4.2. Alizarin Red S Staining**

By Alizarin red S staining, mineralization of the matrix deposited by the female adipose-derived mesenchymal stem cells was evaluated on 7<sup>th</sup> day subsequent to

cultivation of the cells in the osteogenic differentiation medium containing Ral and Ral-PEG released from the microspheres. In brief, the cells were washed with PBS and fixed with 4% paraformaldehyde. After washing with distilled water, the cells were stained with Alizarin red S solution (pH 4.1) for 5 min at room temperature. The stained cells were washed with distilled water and phase contrast micrographs of the cells were taken by the inverted microscope (Nikon ECLIPSE, TS 100, Japan).

With the use of Image J analysis software (NIH, USA), degree of mineralization in each image was quantified by measuring intensity of the red colour of stain expressed as a percentage of image area. These data were used to make comparison between the mineralization levels of the cells cultured in the release media of the various microsphere groups. Empty PCL:PLGA (1:1) and empty PCL microsphere groups were served as controls.

### **2.2.7. Statistical Analysis**

All results were represented as mean  $\pm$  standard deviation (S.D.). Statistical analyses of the data were performed by non-parametric Mann-Whitney U test using SPSS Software version 11.5 (SPSS Inc., USA). Statistically significant difference was assigned at the level of  $p \leq 0.05$ .



## CHAPTER 3

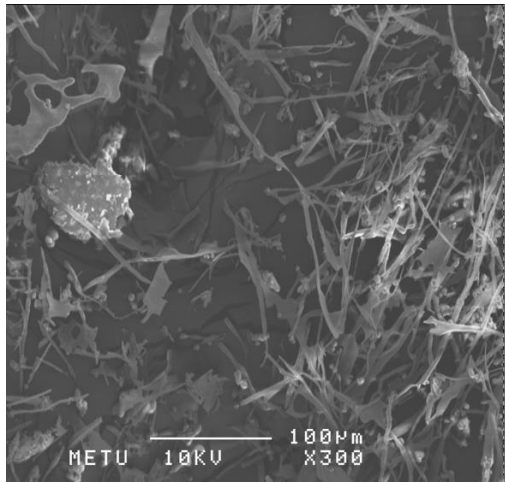
### RESULTS AND DISCUSSION

#### 3.1. Optimization Studies for the Preparation of Ral-Loaded Microspheres

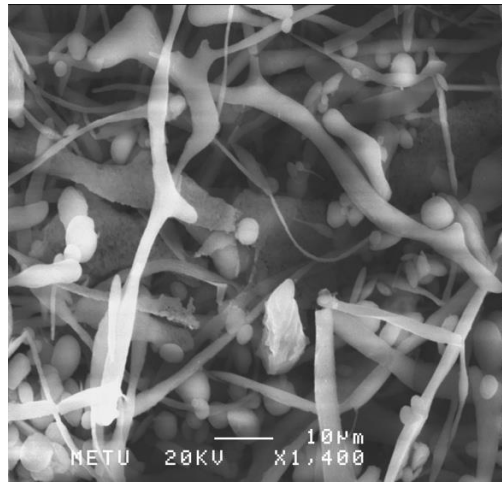
In order to obtain Ral-loaded polymer microspheres that will provide desired physical characteristics for *in vivo* applications besides enabling long-term controlled delivery of Ral at effective doses, optimization studies were carried out initially. To achieve this purpose, various methods (co-precipitation, solid-in-oil-in-water and oil-in-oil-in-water) were tried and many parameters were modified to optimize preparation method of Ral-loaded microspheres. During these studies, results such as particles not being in the form of spheres, or spheres having large size distribution or with low Ral loading were considered as unsuccessful. These outcomes are presented with the representative images in this section.

##### 3.1.1. Co-precipitation Method

Co-precipitation method mostly yielded fibrillar structures as observed by SEM analysis. Ral-loaded PCL microspheres were rare but present as embedded in the fibrils (Figure 18). In this trial, mixture was stirred overnight to evaporate acetone. Similar results were obtained when PLGA was used as the polymer (Figure 19).

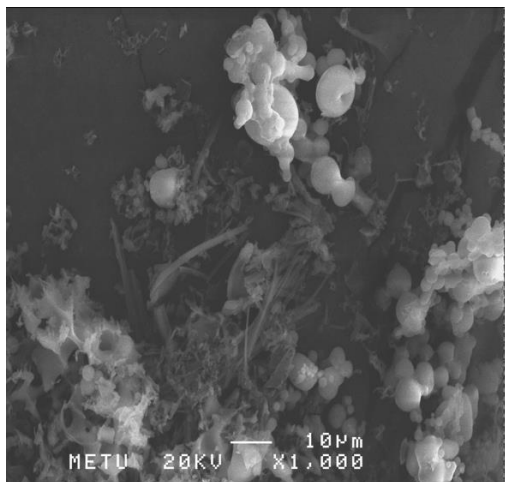


a)

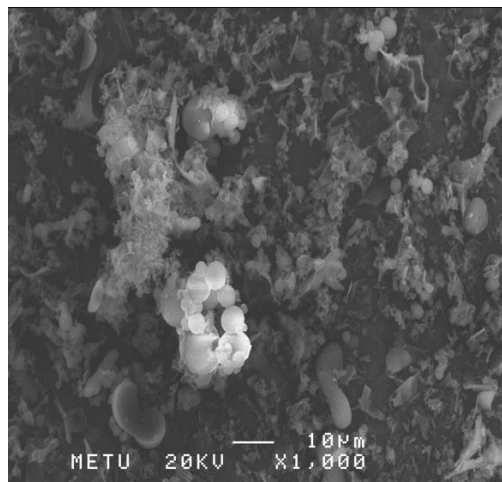


b)

**Figure 18.** SEM micrographs of Ral-loaded PCL microstructures obtained by co-precipitation method (stirring rate: 800 rpm) (a) 300X and b) 1400X).



a)



b)

**Figure 19.** SEM micrographs of Ral-loaded PLGA microstructures obtained by co-precipitation method (stirring rate: 800 rpm) (a) 1000X and b) 1000X).

In the next trial, in order to understand whether Ral has effect on the formation of spherical forms or not, the same method was used to prepare empty PLGA microspheres. Here, acetone was evaporated in 4 h by increasing the surface area of the beaker and stirring the solvent in the beaker at 1100 rpm continuously throughout the experiment. However, most of the resulting microstructures were observed to be not in the shape of spheres suggesting that co-precipitation was not a suitable method for the polymers chosen for this study (Figure 20).

During the co-precipitation trials, it was also observed that when stirring rate for the solvent in the beaker was increased to 8000 rpm, instead of spherical particles, larger sized foamy structures having micro pores were obtained (Figure 21). Although this form is not suitable for the purpose of the study as a drug delivery system, it might be suggested for development of micro porous scaffolds for tissue engineering applications.

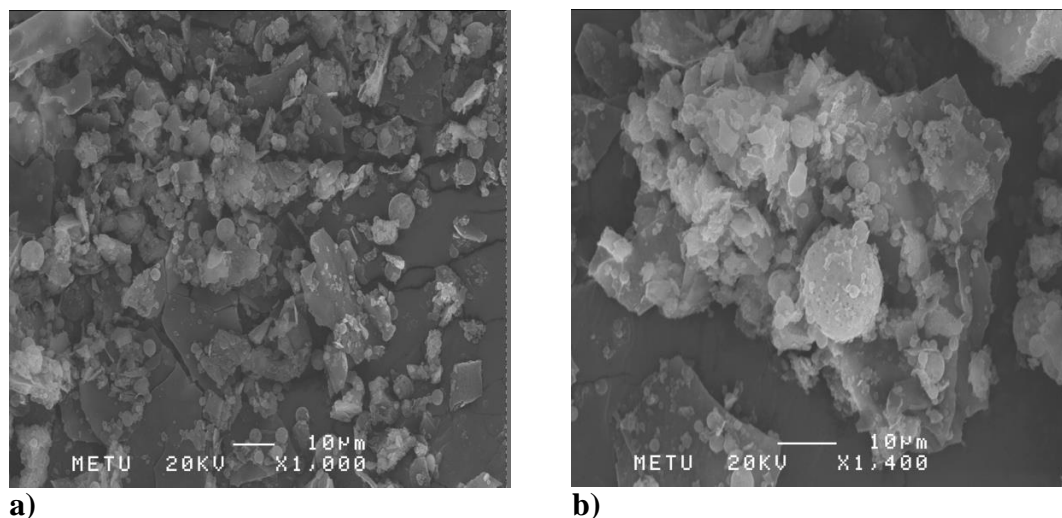


**Figure 20.** SEM micrographs of empty PLGA microstructures obtained by co-precipitation method (stirring rate: 1100 rpm) (a) 1000X and b) 1400X).

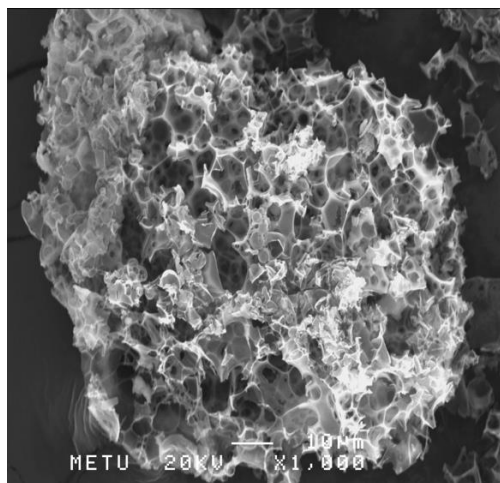


**Figure 21.** SEM micrograph of empty PLGA microstructures obtained by co-precipitation method (stirring rate: 8000 rpm) (1000X).

### **3.1.2. Solid-in-Oil-in-Water Method**

By modification of the solid-in-oil-in-water method (in which PVA solution at the concentration of 2% was used and the stirring rate of the homogenizer was set at 14000 rpm) as mentioned in Section 2.2.1.2, Ral-loaded PCL microspheres could be obtained and most of the microspheres had spherical shape and smooth surfaces (Figure 22). However, the particle size distribution of the microspheres was not narrow.

Therefore, the stirring rate of the homogenizer was further increased and set to 18000 rpm for the next trial. Most of the microspheres prepared by this modified method were observed to have spherical shape and smooth surfaces (Figure 23 a & b). However, the size distribution of the microspheres was still not narrow. Additionally, there were some irregular-shaped particles on which Ral-loaded microspheres were attached (Figure 23

c). It is thought that these particles could be PCL residuals which did not form microspheres.

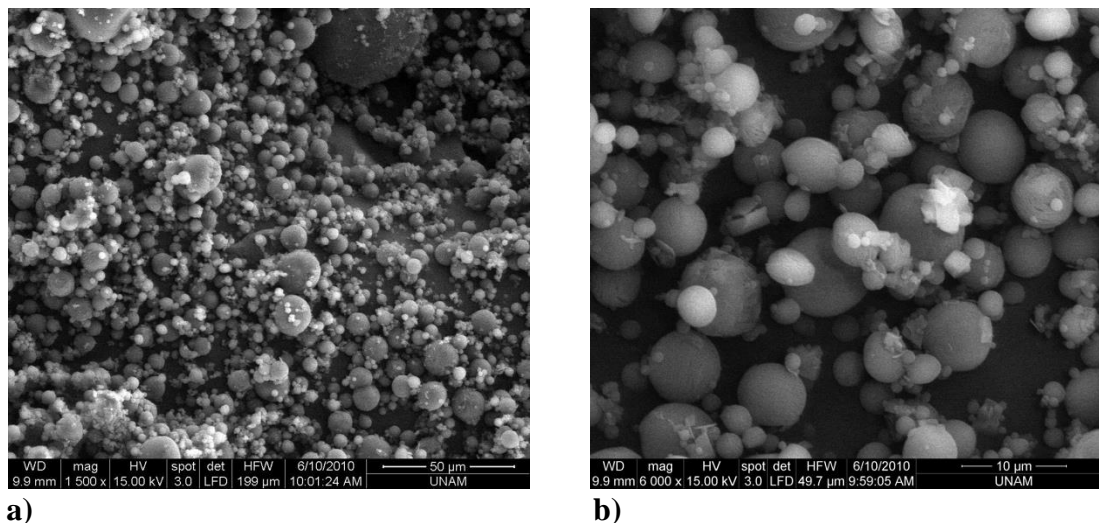
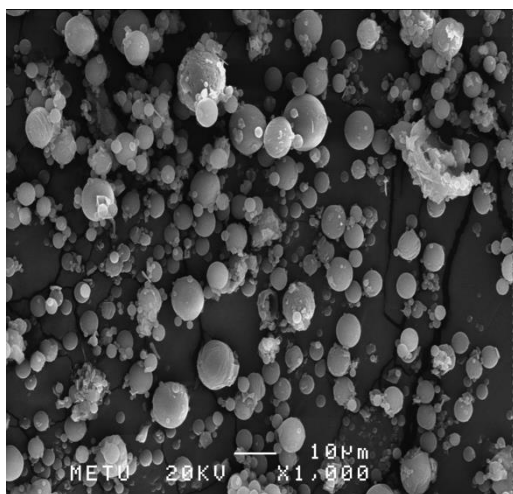
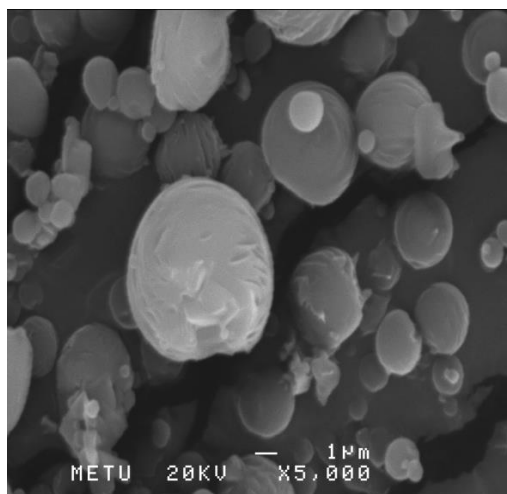


**Figure 22.** SEM micrographs of Ral-loaded PCL microspheres obtained by solid-in-oil-in-water method (PVA concentration: 2% and stirring rate: 14000 rpm) (a) 1500X and b) 6000X).

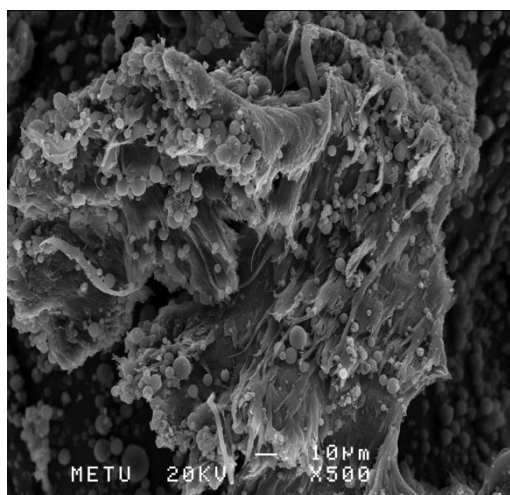
In order to find Ral amount encapsulated in these microspheres, a calibration curve was plotted with different concentrations of Ral (in the range of 5-25  $\mu\text{g/mL}$ ) prepared in the solvent mixture DCM:MeOH (1:1) (Figure 61 in Appendix C). Using this calibration curve, encapsulation efficiency (%) of Ral-loaded PCL microspheres was found as  $55.09 \pm 4.32$  and loading (%) of the same microspheres with a theoretical loading (%) of 9.09 was found as  $9.08 \pm 0.71$ .



a)



b)



c)

**Figure 23.** SEM micrographs of Ral-loaded PCL microspheres obtained by solid-in-oil-in-water method (PVA concentration: 2% and stirring rate: 18000 rpm). At c), the microspheres attached onto polymer structures are shown (a) 1000X, b) 5000X and c) 500X).

Ral release profile of these PCL microspheres was examined by HPLC. A representative chromatogram is shown in Figure 58 in Appendix B. By the calibration curve constructed with different concentrations of Ral (0-20  $\mu\text{g/mL}$ ) in MeOH:PBS (1:1) (Figure 59 in Appendix B), amount of Ral release was calculated. Data are presented as cumulative release amount of Ral ( $\mu\text{g}$  and %) with respect to time as shown in Figure 24 a & b, respectively. It can be seen that only 2.9% of Ral was released after 60 days, although it corresponds to cumulative amount of 14  $\mu\text{g}$ . The possible reason behind this result is thought to be the hydrophobic natures of both Ral and PCL. Ral is known as a water-insoluble drug belonging to class II of BDDCS. Second reason might be the high crystalline form of Ral. Similarly, Bikiaris et al. (2009) reported that diffusion of Ral crystals through the polyester based nanoparticles is remarkably difficult.

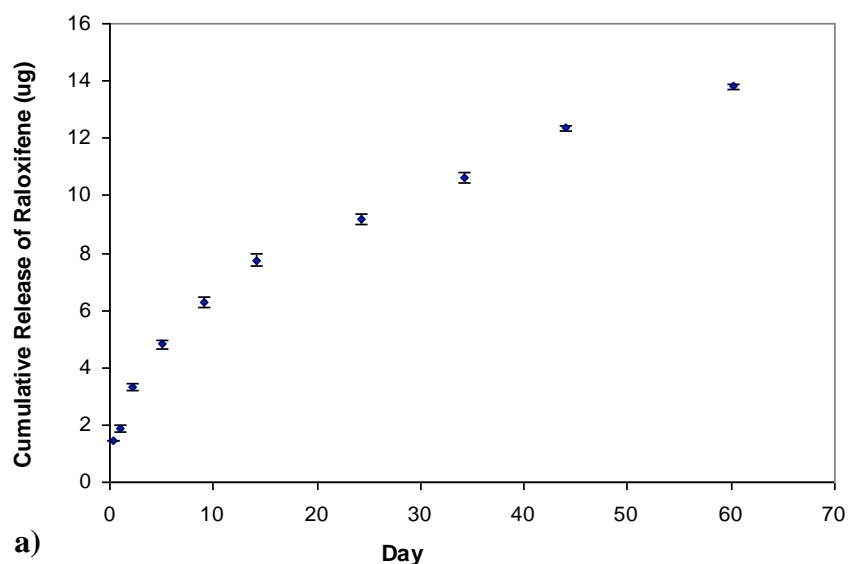


**Figure 24.** Ral release profile (a)  $\mu\text{g}$ ) of PCL microspheres (obtained by solid-in-oil-in-water method, PVA concentration: 2% and stirring rate: 18000 rpm) incubated in PBS (0.1 M, pH 7.4) at 37°C for 60 days (n=4).

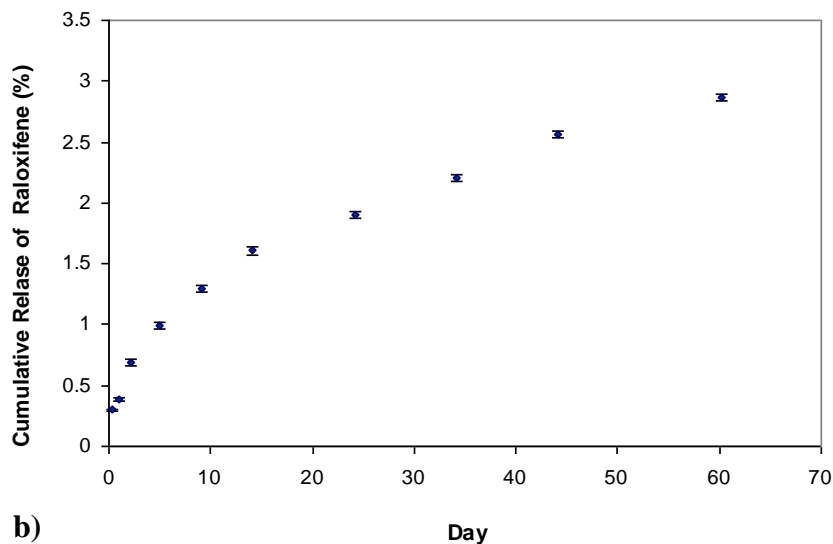


**Figure 24. (continued)** Ral release profile (b) %) of PCL microspheres (obtained by solid-in-oil-in-water method, PVA concentration: 2% and stirring rate: 18000 rpm) incubated in PBS (0.1 M, pH 7.4) at 37°C for 60 days (n=4).

After release study, it was observed that most of the microspheres still had spherical shape and smooth surfaces indicating that PCL did not degrade so much in this period as expected (Figure 25 a & b).

In this study, to benefit from the advantages of both PCL and PLGA, blends of these two polymers with various ratios were also used for microsphere preparation as mentioned in Section 1.3.2. SEM analysis of Ral-loaded PCL:PLGA (9.1:1, w/w) microspheres prepared by solid-in-oil-in-water method showed that most of the microspheres had spherical shape and smooth surfaces (Figure 26 a & b). However, the size distribution of the microspheres was not narrow. Moreover, polymer fragments were also observed indicating that not all polymer material could be turned into microspheres. During the preparation of these microspheres, the organic phase was

added dropwise into foamed PVA aqueous solution while not stirring as indicated in Section 2.2.1.2. Just before stirring the mixture with the homogenizer, it was observed that some droplets remained on the foam at the top of the solvent. Therefore, this method might have obstructed homogeneous distribution of Ral in the polymer mixture, thus yielding low values of encapsulation efficiency (% , 16.50) and loading (% , 4.14) with theoretical loading (%) of 8.67.

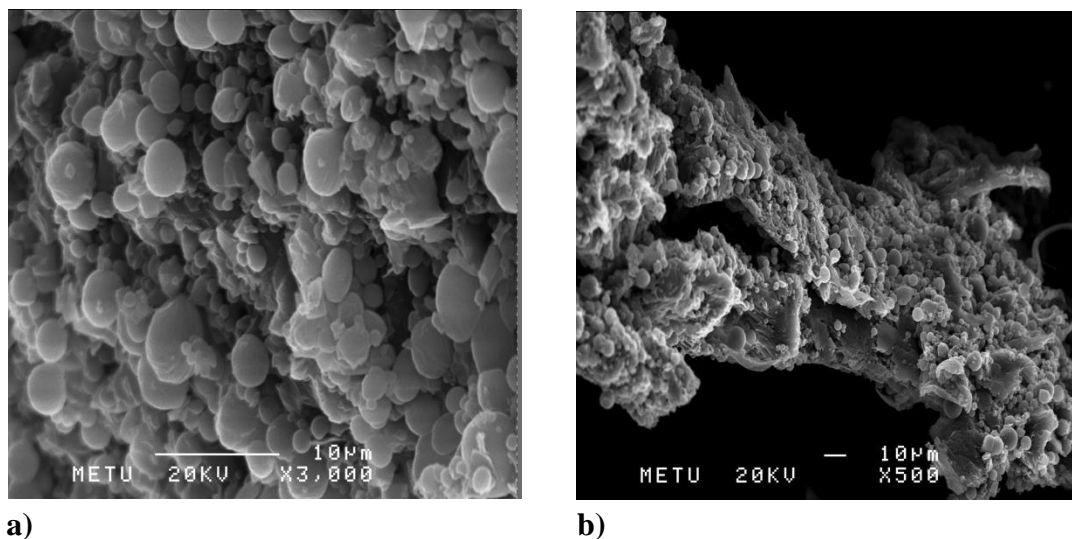


**Figure 25.** SEM micrographs of Ral-loaded PCL microspheres (obtained by solid-in-oil-in-water method, PVA concentration: 2% and stirring rate: 18000 rpm) after 60 days of release in PBS (0.1 M, pH 7.4) at 37°C (a) 3000X and b) 500X).

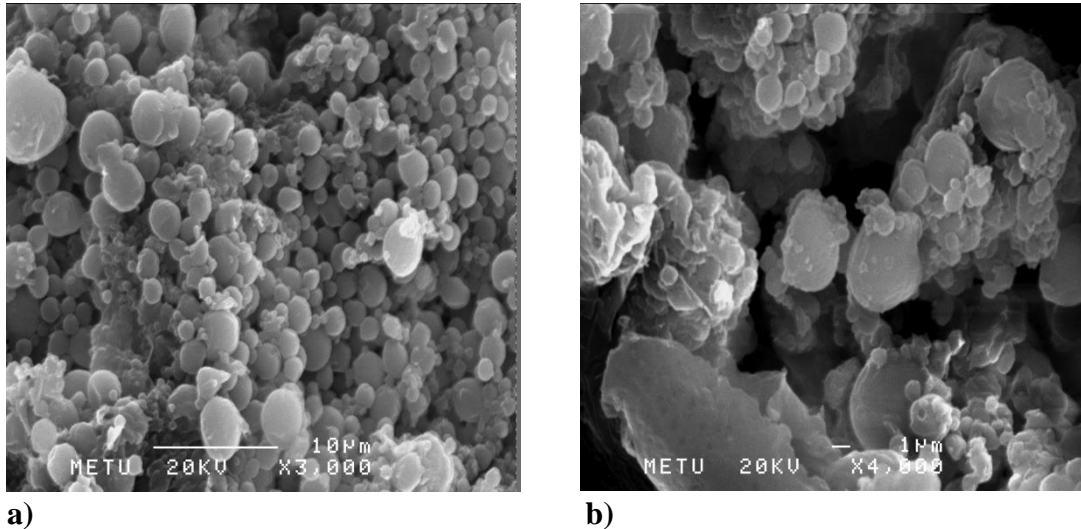
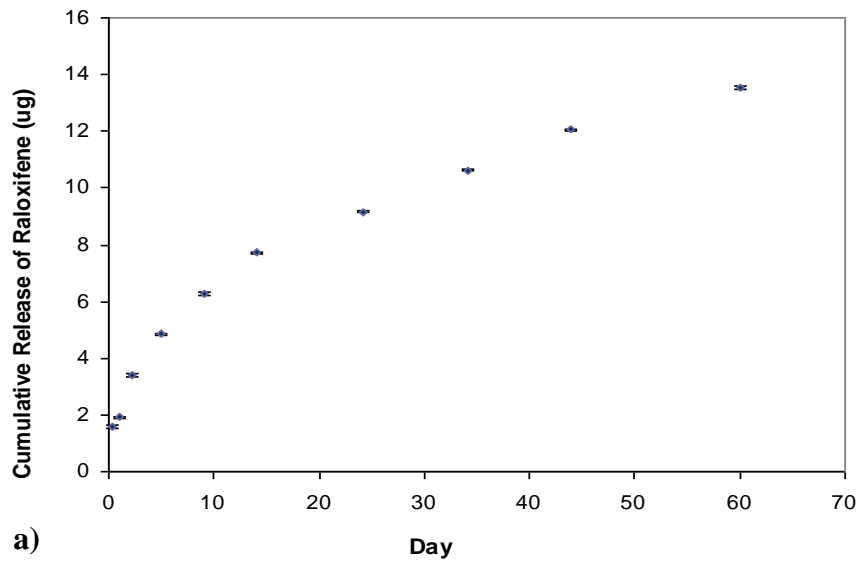
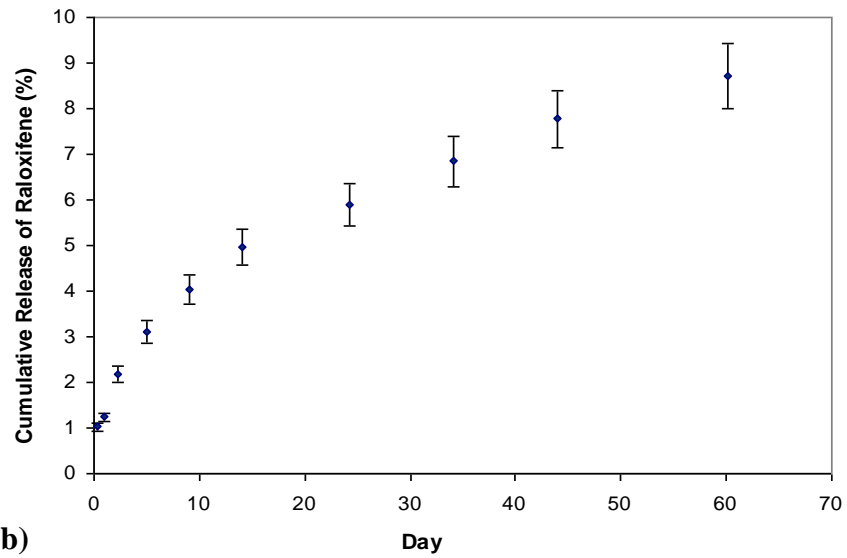


**Figure 26.** SEM micrographs of Ral-loaded PCL:PLGA (9.1:1, w/w) microspheres obtained by solid-in-oil-in-water method (a) 3000X and b) 4000X).

Ral release profile of PCL:PLGA (9.1:1, w/w) microspheres was also investigated by HPLC and Ral amount was found using the calibration curve constructed with different concentrations of Ral (0-20  $\mu\text{g/mL}$ ) in MeOH:PBS (1:1) (Figure 59 in Appendix B). Release data are presented as cumulative release amount of Ral ( $\mu\text{g}$  and %) with respect to time as shown in Figure 27 a & b, respectively. In Figure 27 b, it can be seen that only 8.7% of Ral was released after 60 days. The important point here is that cumulative release (%) increased from 2.9 to 8.7 after using PLGA in addition to PCL even at the ratio of 9.1:1 (PCL:PLGA). As it is known, PLGA degrades faster than PCL. Hence, it might have enabled more Ral to be released from the microspheres. However, cumulative release was still below 10% after 60 days of incubation. This low Ral release amount was supported by SEM analysis (Figure 28) as there was not an observable change in the morphology of the microspheres after release.



a)



b)

**Figure 27.** Ral release profiles (a)  $\mu\text{g}$  and b) %) of PCL:PLGA (9.1:1, w/w) microspheres (obtained by solid-in-oil-in-water method) incubated in PBS (0.1 M, pH 7.4) at 37°C for 60 days (n=3).

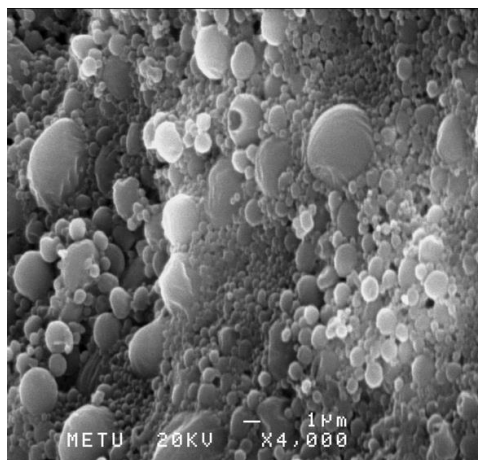


**Figure 28.** SEM micrograph of Ral-loaded PCL:PLGA (9.1:1, w/w) microspheres (obtained by solid-in-oil-in-water method) after 60 days of release in PBS (0.1 M, pH 7.4) at 37°C (4000X).

Encapsulation efficiency (%) and loading (%) results for Ral-loaded PCL:PLGA (10:4) microspheres prepared by various modifications of the solid-in-oil-in-water method are demonstrated in Table 5.

By solid-in-oil-in-water technique, it was recognized that Ral did not dissolve mostly in DCM, thus, in the organic phase. This indicates that Ral could not be distributed homogeneously in the polymer mixture by this method. Even in some cases, Ral particles floating on the surface of organic phase were observed during the microencapsulation process. This might have caused low encapsulation efficiency results. Moreover, Wischke & Schwendeman (2008) reported that a low drug particle size is necessary to obtain high encapsulation of the drug crystals for solid-in-oil-in-water method. In other words, they mentioned that the size of drug crystals intended to be encapsulated should be lower than size of the polymer microspheres/particles to

achieve high encapsulation efficiency. In our study, sizes of Ral crystals from two different stock batches which were used for microsphere preparation were analysed by SEM. It was observed that sizes of many Ral crystals in the first batch (Figure 29 a) were higher than approximately 25  $\mu\text{m}$  whereas sizes of most of Ral crystals in the second batch (Figure 29 b) were higher than 100  $\mu\text{m}$ . Therefore, this variation observed for crystal sizes of Ral belonging to different batches might have been reflected to the variation obtained for encapsulation efficiency values. For example, considering Table 5, encapsulation efficiency (%) for group A) was found as  $28.99 \pm 0.63$  whereas the one for group B) was found as  $54.12 \pm 5.77$ . Furthermore, slight solubility and thus, nonhomogeneous distribution of Ral in the organic phase might have accounted for the irregular-shaped structures which were arised during the formation of microspheres and later seen in SEM micrographs.

**Table 5.** Encapsulation efficiency (%), loading (%) and theoretical loading (%) values of Ral-loaded PCL:PLGA (10:4) microspheres belonging to the groups A) - D) in Table 3.

<b>Group</b>	<b>Encapsulation efficiency (%)</b>	<b>Loading (%)</b>	<b>Theoretical loading (%)</b>
A)	$28.99 \pm 0.63$	$9.66 \pm 0.21$	10
B)	$54.12 \pm 5.77$	$8.59 \pm 0.92$	10
C)	53.99	8.41	10
D)	$53.71 \pm 0.56$	$7.88 \pm 0.08$	9

n=2 for all groups except for group C) where n=1.

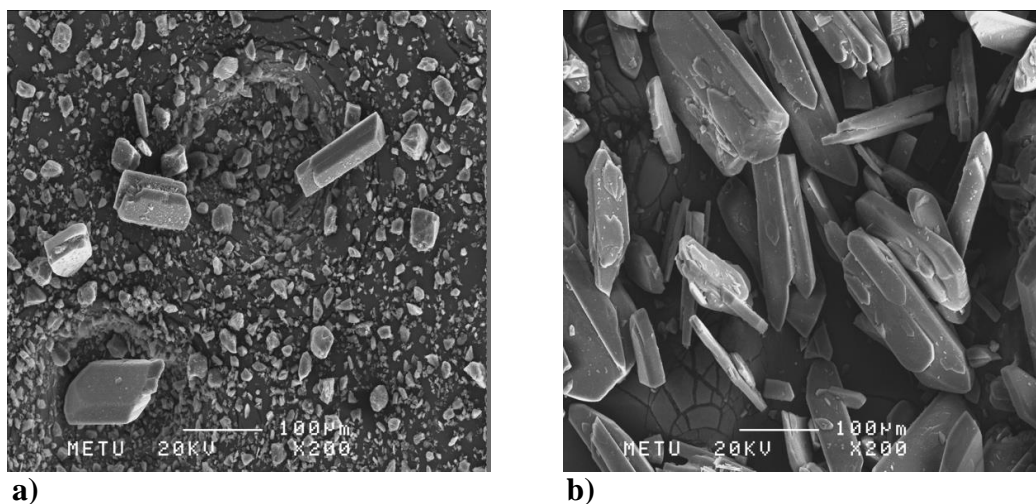


**Figure 29.** SEM micrographs of Ral from two different stock batches as obtained from the producer a) Batch 1 (200X) and b) Batch 2 (200X).

### 3.1.3. Oil-in-Oil-in-Water Method

Oil-in-oil-in-water ( $o_1/o_2/w$ ) double emulsion-solvent evaporation method was the third method of choice for the preparation of Ral-loaded microspheres. Wischke & Schwendeman (2008) reported that this method provides appropriate drug dispersion in the organic phase, resulting in homogeneous drug dispersion within the polymer matrix and thus, high encapsulation efficiency. In connection with this phenomenon, it is expected that homogeneous Ral dispersion in the organic phase would provide to form microparticles which are more uniform and mostly spherical in shape. After all optimization studies, oil-in-oil-in-water ( $o_1/o_2/w$ ) double emulsion-solvent evaporation method with the specified parameters mentioned in Section 2.2.4 was chosen for microsphere preparation and used for further analyses. Results of characterization studies related with the microspheres prepared by this method are given in Section 3.3.

## 3.2. Characterization of Ral-PEG

### 3.2.1. FT-IR Analysis

In order to identify possible chemical interactions formed between Ral and PEG during preparation of Ral-PEG, FT-IR analysis was performed and FT-IR spectra of PEG, Ral-PEG and Ral are demonstrated in Figure 30 a, b & c, respectively. The FT-IR spectrum of PEG (Figure 30 a) displayed characteristic absorption bands at around  $1100\text{ cm}^{-1}$  and  $3441.18\text{ cm}^{-1}$  owing to primary alcohol and aliphatic-OH groups, respectively. The spectrum of Ral (Figure 30 c) showed characteristic absorption bands at  $3201.02\text{ cm}^{-1}$  for functional N-H bond and  $3141.44\text{ cm}^{-1}$  for functional phenolic-OH group, besides other characteristic absorption bands at  $2958.21\text{ cm}^{-1}$  for aromatic C-H stretching,  $1642.00\text{ cm}^{-1}$  for C=O stretching,  $1595.88\text{ cm}^{-1}$  for C=C stretching,  $1464.09\text{ cm}^{-1}$  for S-benzothiofuran,  $1258.77\text{ cm}^{-1}$  for C-O stretching,  $905.00\text{ cm}^{-1}$  for benzene ring and  $806.06\text{ cm}^{-1}$  for thiophene C-H bond.

In the study of Bandela & Anupama (2009), Ral-PEG was prepared at a ratio of 1:3.5 (Ral:PEG) ( $M_w$  of PEG:  $35000\text{ g/mol}$ ) and it was mentioned that a new absorption band at  $3448\text{ cm}^{-1}$  was observed in the FT-IR spectrum of the conjugate. Similarly, in another study (Talukder et al., (poster presentation)), Ral-PEG was prepared at a ratio of 1:1 (Ral:PEG) ( $M_w$  of PEG:  $8000\text{ g/mol}$ ) and it was mentioned that a new absorption peak was seen at  $3240\text{ cm}^{-1}$  in the spectrum of the conjugate. In these both researches, these findings were attributed to hydrogen bonding formed by attachment of hydroxyl group of PEG to amine group of Ral and proposed as the confirmation of conjugate formation between Ral and PEG. In this study, considering the spectrum of Ral-PEG (Figure 30 b), it was seen that all characteristic peaks belonging to Ral and PEG were preserved and no new peak was formed. Additionally, a slight shift in the peak at  $3441.18\text{ cm}^{-1}$  due to aliphatic-OH group of PEG to lower frequency ( $3423.67\text{ cm}^{-1}$ ) was observed after the

conjugation reaction. Moreover, upon conjugation reaction, decrease was observed in the intensity of absorption bands at  $3201.02\text{ cm}^{-1}$  and  $3141.44\text{ cm}^{-1}$  belonging to the functional N–H bond and functional phenolic–OH group of Ral, respectively. Decrease was also observed in the intensity of absorption bands at around  $1100\text{ cm}^{-1}$  and  $3441.18\text{ cm}^{-1}$  due to primary alcohol and aliphatic–OH groups of PEG, respectively. These results might be ascribed to hydrogen bonding formed by interacting the amine and phenolic–OH groups of Ral with the hydroxyl groups of PEG, indicating the possibility of conjugate formation between Ral and PEG.

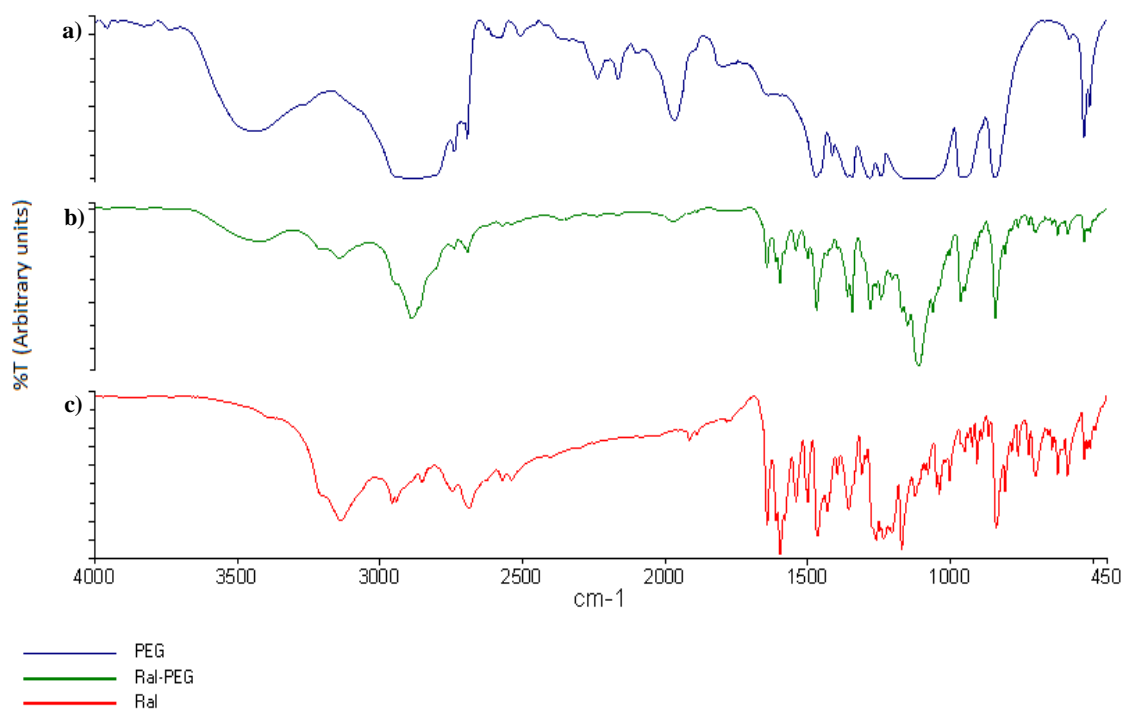


**Figure 30.** FT-IR spectra of a) PEG, b) Ral-PEG and c) Ral.

### 3.2.2. XRD Analysis

XRD analysis was conducted to examine whether crystallinity change in Ral occurred after conjugation to PEG. Diffractogram of Ral (Figure 31) exhibited distinct peaks at angles of 13.44, 14.42, 15.74, 19.06, 21.30, 22.60, 24.00, 24.38, 25.88, 27.96 and 28.14, showing highly crystalline nature of Ral. XRD pattern of PEG (Figure 32) displayed remarkably lower number of peaks at  $2\theta$  of 19.18, 23.30, 26.24, 26.94 and 27.86, exhibiting amorphous form of PEG. In the pattern of the physical mixture of Ral and PEG (Figure 33 a), characteristic peaks of Ral at angles of 14.58, 15.72, 21.28, 25.86 and 27.82 as well as the ones belonging to PEG at angles of 19.22, 23.40, 26.28, 27.08 and 28.10 can be clearly seen. Additionally, all intensities of the peaks were observed to be reduced and little shifts of the peak positions were seen.

In the study of Bandela & Anupama (2009) who prepared Ral-PEG at a ratio of 1:3.5 (Ral:PEG), significant reduction in Ral peaks was observed in the XRD spectrum of the conjugate and this finding was attributed to the complete change of crystalline nature of Ral into amorphous form after conjugation. Moreover, in the study of Talukder et al. (poster presentation), XRD pattern of Ral-PEG prepared at a ratio of 1:1 (Ral:PEG) demonstrated some shifts in the peak positions and remarkable reduction in the intensities of Ral peaks upon conjugation. By the authors, this observation was related with loss of Ral crystallinity after conjugation.

In this study, the pattern of Ral-PEG (Figure 33 b) demonstrated that characteristic peaks of Ral observed in the pattern of physical mixture of Ral and PEG – namely the peaks at  $2\theta$  of 14.58, 15.72, 21.28, 25.86 and 27.82 – almost disappeared upon conjugation. The other prominent peaks were almost completely related with PEG as it can be seen in the pattern of PEG (Figure 32) and physical mixture of Ral and PEG (Figure 33 a). Therefore, it might be deduced that the crystalline nature of Ral was converted to amorphous state upon conjugation to PEG.

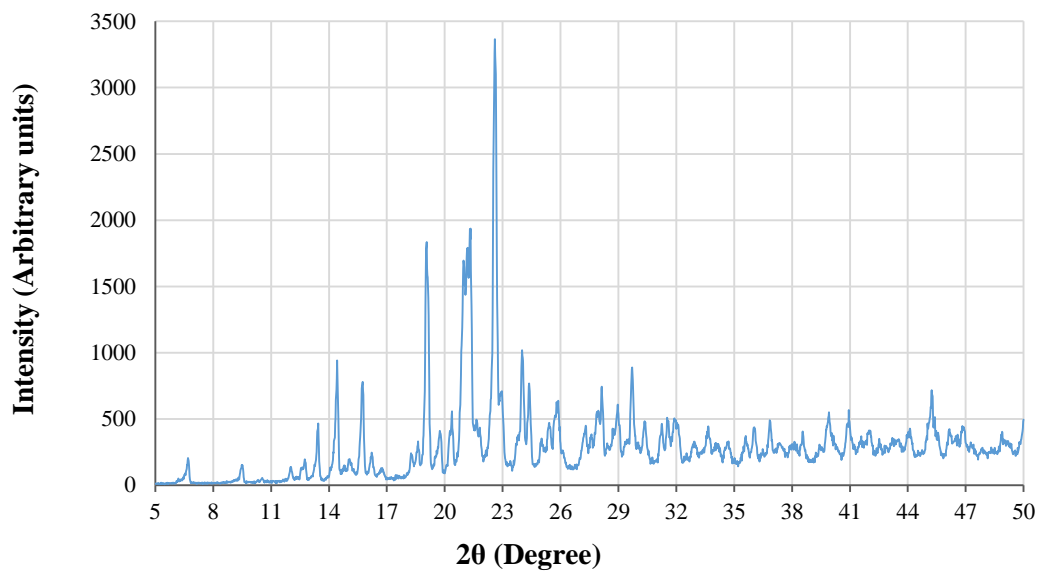


**Figure 31.** XRD diffractogram of Ral.

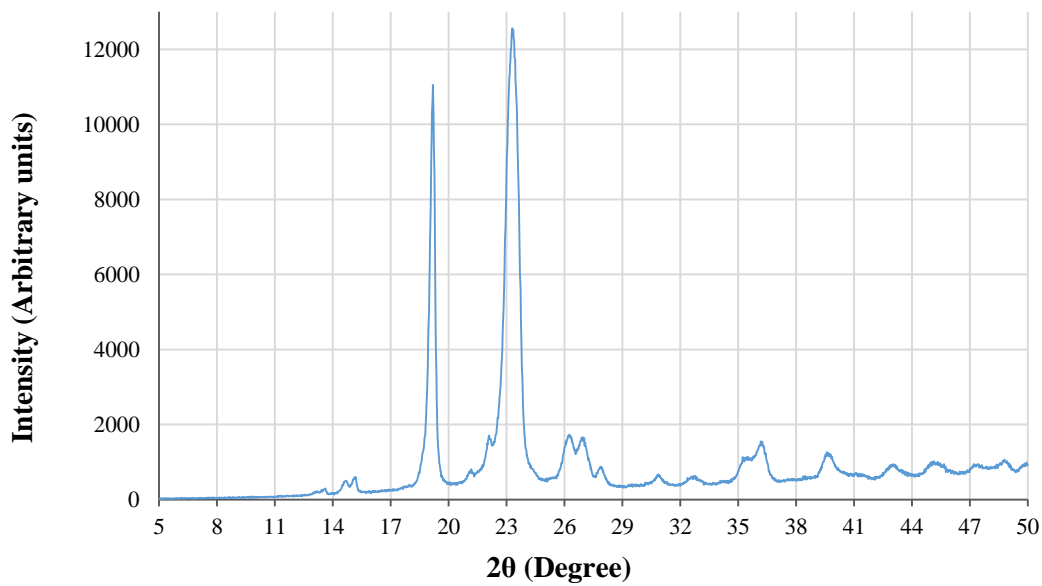


**Figure 32.** XRD diffractogram of PEG.

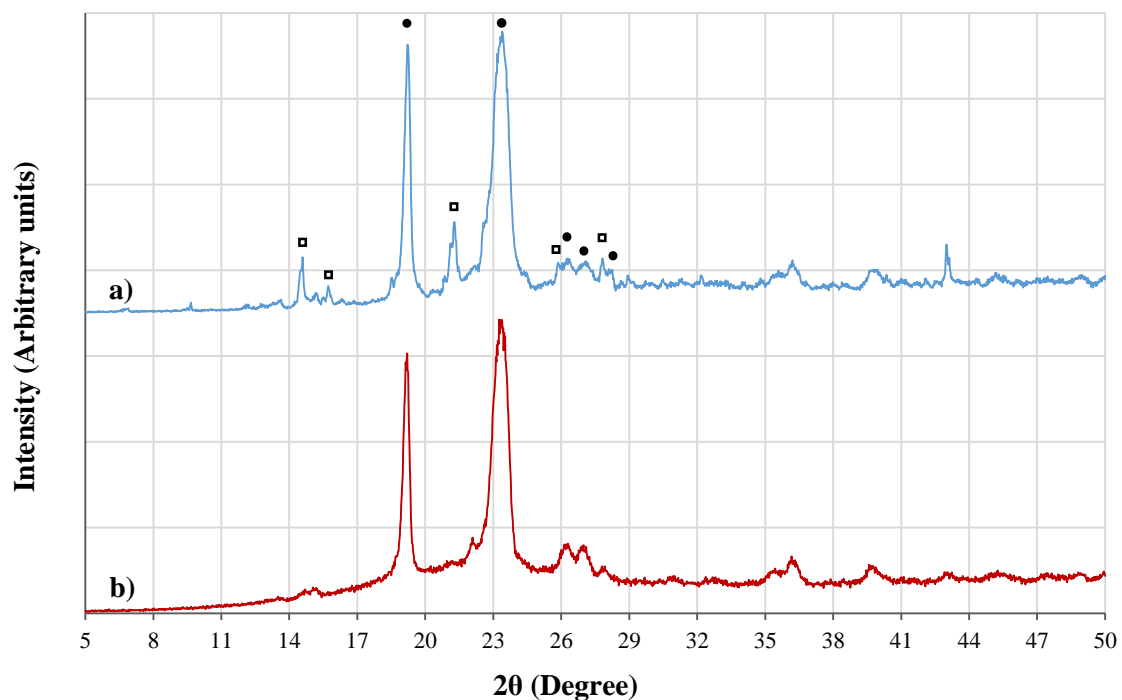


**Figure 33.** XRD diffractograms of a) the physical mixture of Ral and PEG and b) Ral-PEG.  $\square$  refers to the peaks of Ral and  $\bullet$  refers to the peaks of PEG.

### 3.2.3. Morphological Analysis by SEM

SEM analysis was performed to morphologically investigate the possible change in crystalline nature of Ral upon conjugation to PEG. Before PEG conjugation, it was observed that Ral powders were composed of separate and irregular-shaped particles with sharp edges indicating highly crystalline nature of Ral as seen in Figures 29 b & 34 (Garg et al, 2009; Tran et al, 2013).



**Figure 34.** SEM micrograph of Ral powders before conjugation reaction with PEG (30X).

On the other hand, Ral-PEG was appeared as bulk mass and two different types of morphology which could be expected for a physical mixture of two components were not observed (Figure 35 a & b). Thus, these outcomes suggested that Ral might be interacted with PEG having amorphous nature, resulting in loss of crystalline form of Ral (Garg et al., 2009; Tran et al., 2013). It should be noted that this analysis is not complete since SEM images of PEG and physical mixture of Ral and PEG are missing. However, even these findings supported XRD results demonstrating conversion of crystalline nature of Ral to amorphous form after conjugation.

Considering the outcomes of FT-IR, XRD and SEM analyses, it can be mentioned that it is probable to prepare Ral-PEG with the parameters specified in this study.

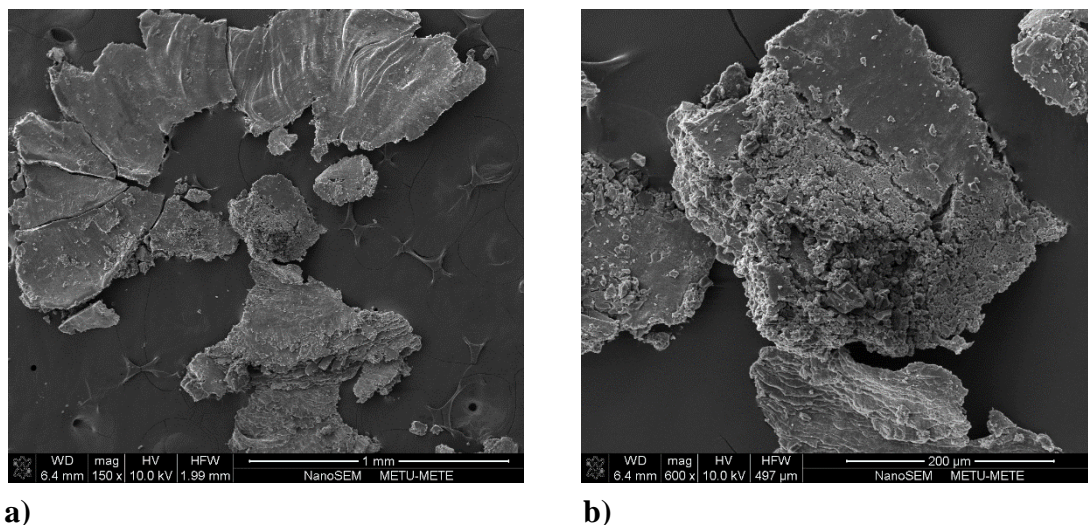


**Figure 35.** SEM micrographs of Ral-PEG (a) 150X and b) 600X).

### **3.3. Characterization of Ral- and Ral-PEG-Loaded PCL and PCL:PLGA (1:1) Microspheres**

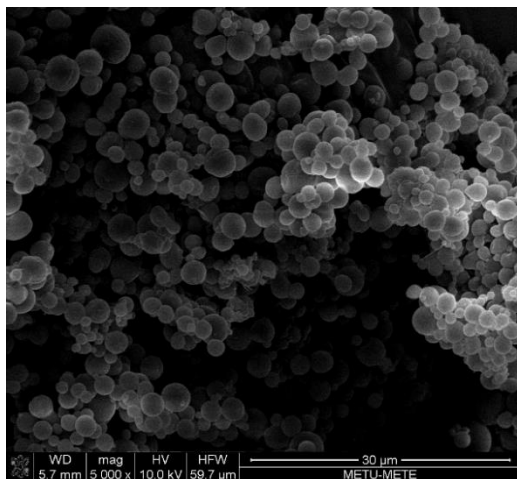
In this section, characterization results of PCL and PCL:PLGA (1:1) microspheres loaded with Ral and Ral-PEG (used to increase the rate of Ral release from the microspheres) and prepared by the optimized method, the oil-in-oil-in-water ( $o_1/o_2/w$ ) double emulsion-solvent evaporation method, with the parameters mentioned in Section 2.2.4 were presented and discussed.

#### **3.3.1. Morphological Analysis by SEM**

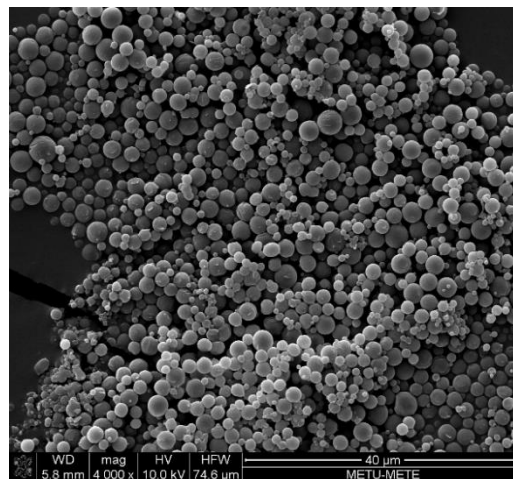
SEM analysis was performed in order to examine the morphology, surface topography and particle size distribution of the microspheres. SEM micrographs of empty PCL, Ral-loaded PCL, Ral-loaded PCL:PLGA (1:1), Ral-PEG-loaded PCL and Ral-PEG-loaded

PCL:PLGA (1:1) microspheres are shown in Figures 36, 37, 38, 39 & 40, respectively. It was observed that most of the microspheres had spherical shape and smooth surfaces. Additionally, in comparison to the morphology and particle size distribution results of the microspheres prepared by the solid-in-oil-in-water method during the optimization studies (shown in Section 3.1.2), these microspheres were observed to be mostly lack of irregular-shaped particles and have more uniform particle size distribution. Thus, these results suggest that the optimized oil-in-oil-in-water method is more favourable with respect to the solid-in-oil-in-water method in terms of morphology and particle size distribution of the microspheres for this study. In order to analyse surface topography of the microspheres in more details, SEM images obtained at higher magnification relative to those in Figures 36-40 were necessary. However, during SEM analyses, increasing of magnification caused the microspheres to get charged resulting in melting and hence structure deterioration. Thus, images with higher magnifications could not be obtained. Nevertheless, even considering these SEM micrographs, it is possible to indicate that the microspheres were mostly devoid of visible pores on their surfaces.

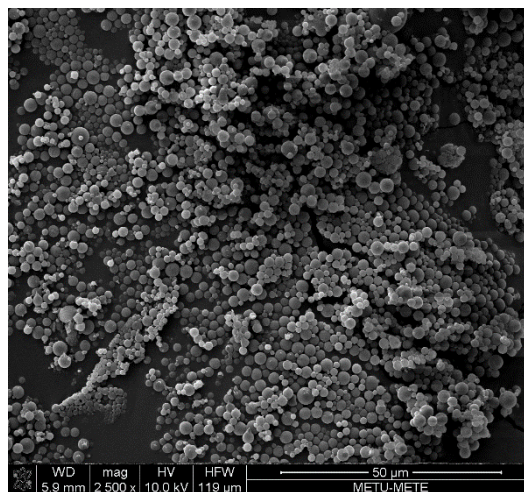
Moreover, it was observed that microsphere aggregation for Ral-PEG-loaded PCL microspheres (Figure 39) was higher in comparison to the other microsphere groups and mean particle size of Ral-PEG-loaded PCL:PLGA (1:1) microspheres (Figure 40) appeared to be the highest one. On the other hand, subsequent to comparison with empty PCL microspheres (Figure 36), it was revealed that both Ral and Ral-PEG loading did not influence the shape and surface topography of the microspheres (Figures 37 & 39). Similarly, Hariharan et al. (2006) reported that estradiol loading did not alter the surface topography and shape of PLGA nanoparticles.



a)

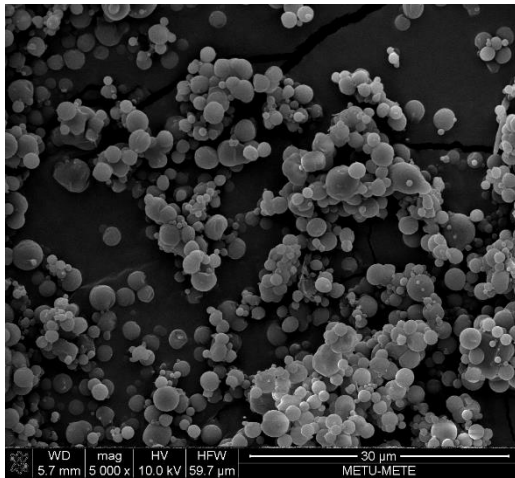


b)

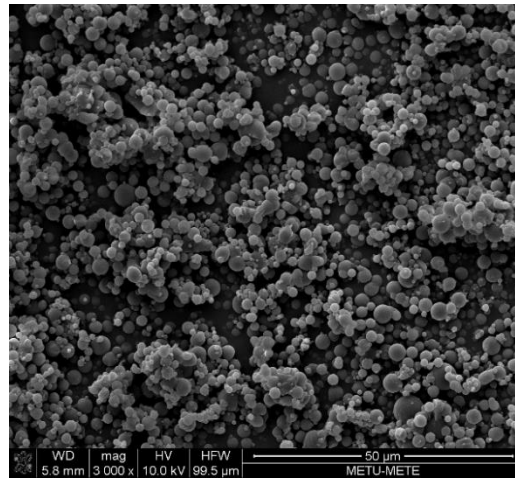


c)

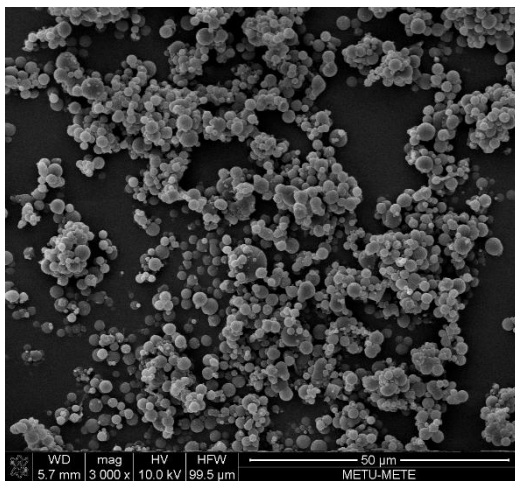
**Figure 36.** SEM micrographs of empty PCL microspheres prepared by the optimized oil-in-oil-in-water method (a) 5000X, b) 4000X and c) 2500X).



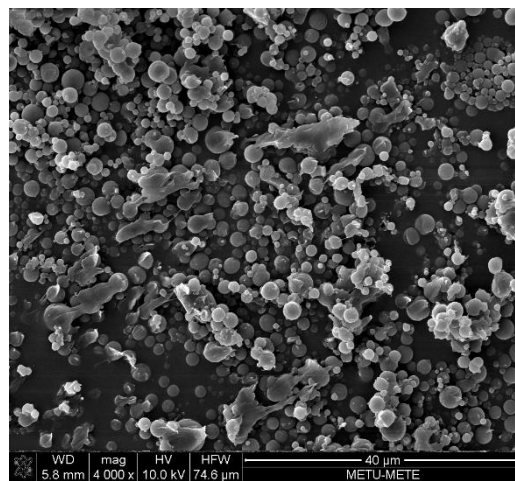
a)



b)

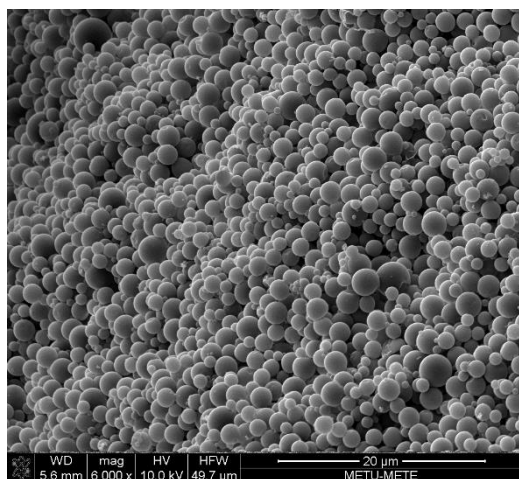


c)

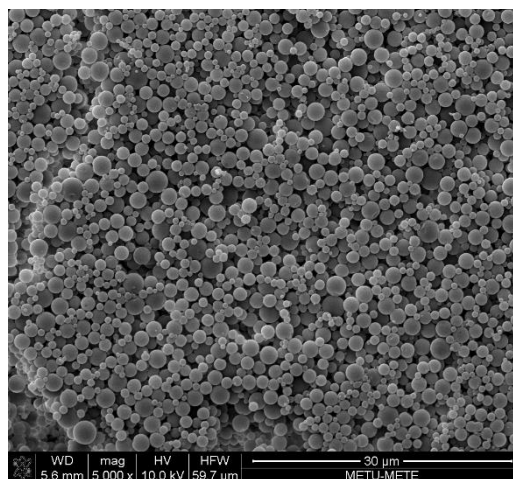


d)

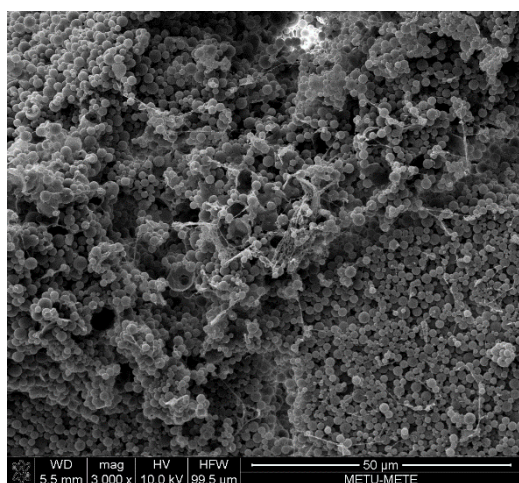
**Figure 37.** SEM micrographs of Ral-loaded PCL microspheres prepared by the optimized oil-in-oil-in-water method (a) 5000X, b) 3000X, c) 3000X and d) 4000X).



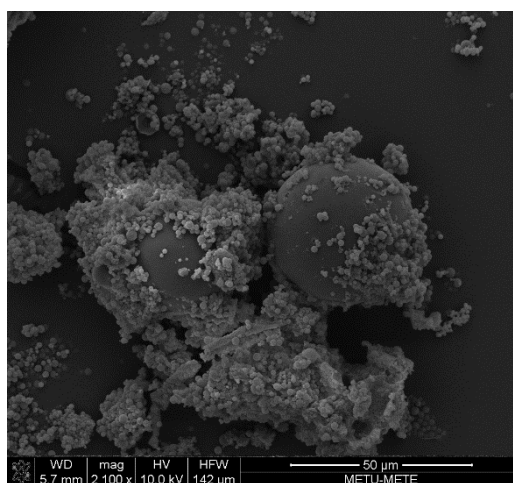
a)



b)

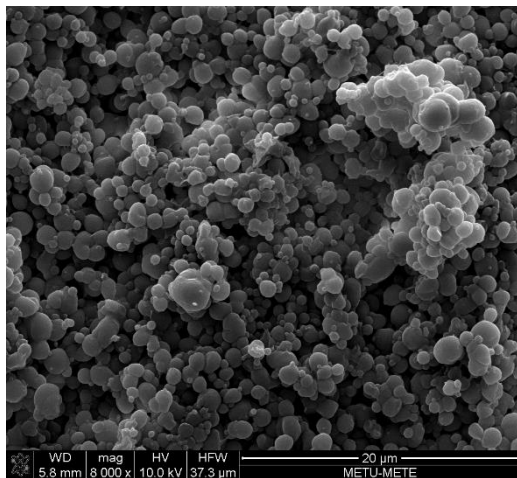


c)

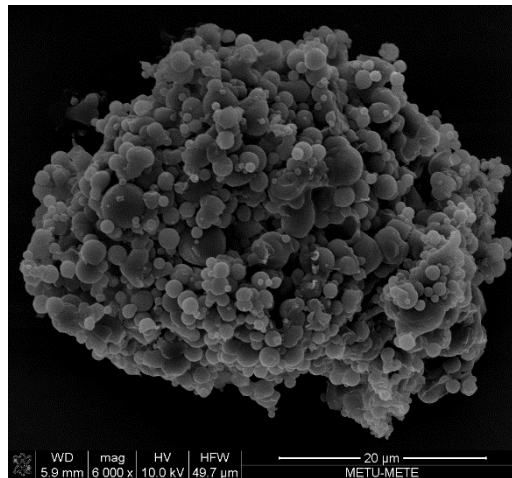


d)

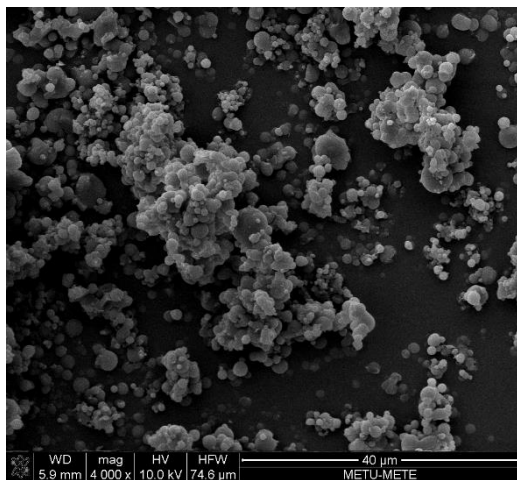
**Figure 38.** SEM micrographs of Ral-loaded PCL:PLGA (1:1) microspheres prepared by the optimized oil-in-oil-in-water method (a) 6000X, b) 5000X, c) 3000X and d) 2100X).



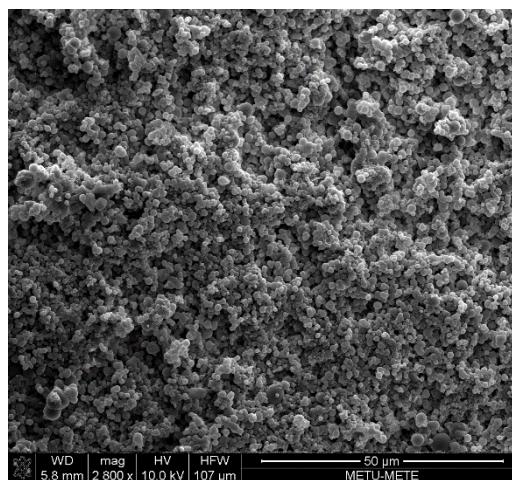
a)



b)

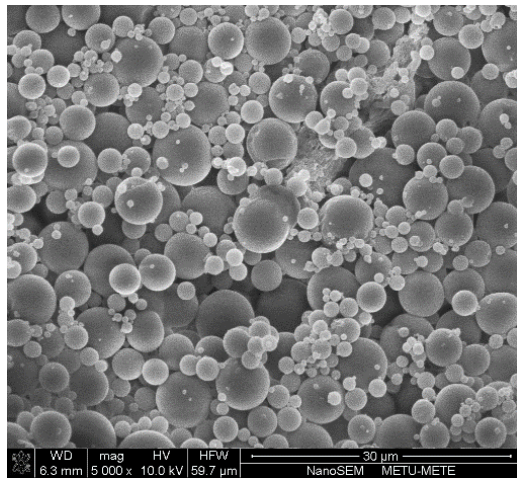


c)

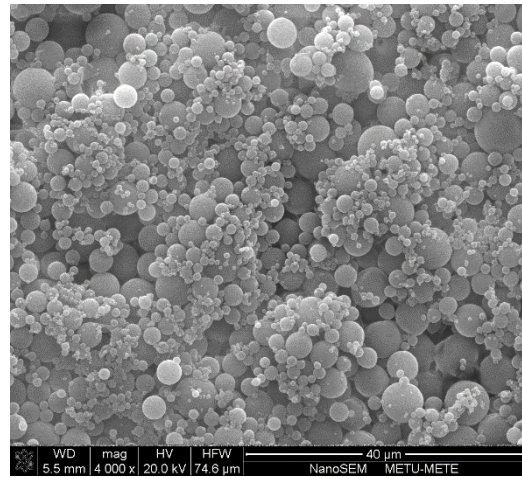


d)

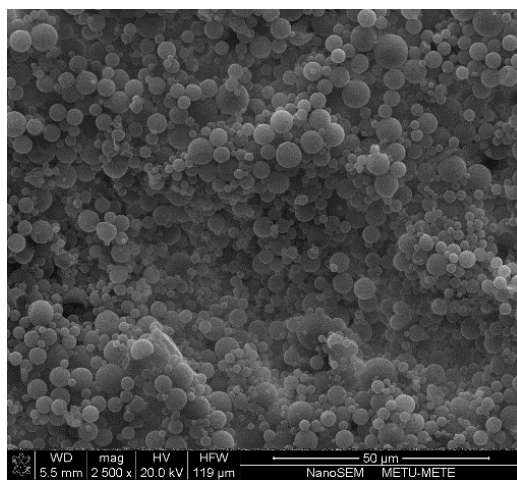
**Figure 39.** SEM micrographs of Ral-PEG-loaded PCL microspheres prepared by the optimized oil-in-oil-in-water method (a) 8000X, b) 6000X, c) 4000X and d) 2800X).



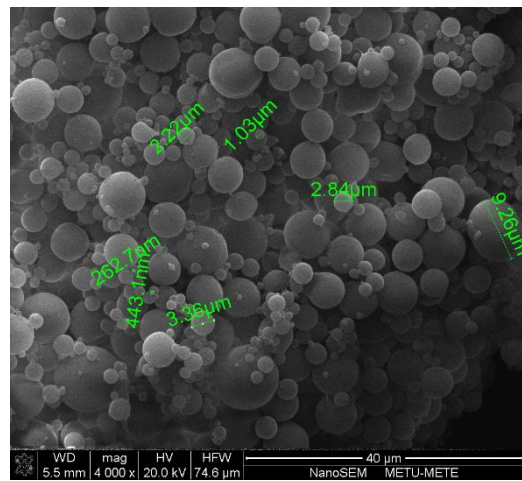
a)



b)

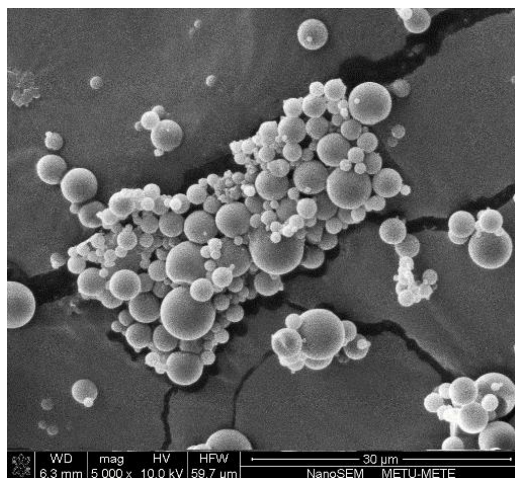


c)



d)

**Figure 40.** SEM micrographs of Ral-PEG-loaded PCL:PLGA (1:1) microspheres prepared by the optimized oil-in-oil-in-water method (a) 5000X, b) 4000X, c) 2500X and d) 4000X).



e)

**Figure 40. (continued)** SEM micrograph of Ral-PEG-loaded PCL:PLGA (1:1) microspheres prepared by the optimized oil-in-oil-in-water method (e) 5000X).

### 3.3.2. Particle Size Analysis

As seen in Table 6, there is no significant difference in particle size values among all microsphere groups. Although not significantly different, mean particle size ( $\mu\text{m}$ ,  $2.16 \pm 1.80$ ) of Ral-PEG-loaded PCL:PLGA (1:1) microspheres was found to be the highest relative to the other groups. It can be indicated that this outcome is in correlation with the SEM micrographs (Figures 36-40). In addition, it was observed that empty PCL and Ral-PEG-loaded PCL microspheres had the lowest PDI values of 1.33 and 1.11, respectively, indicating that these two groups had the narrowest size distributions. Furthermore, lowest mean particle size value was observed for Ral-PEG-loaded PCL microsphere group ( $\mu\text{m}$ ,  $1.08 \pm 0.50$ ).

**Table 6.** Particle size distribution of all microsphere groups.

Groups	Particle size ( $\mu\text{m}$ )				
	Average	d(0.1)	d(0.5)	d(0.9)	PDI
Empty PCL microspheres	1.66 $\pm$ 0.80	0.69	1.54	2.75	1.33
Ral-loaded PCL microspheres	1.58 $\pm$ 0.92	0.54	1.43	2.79	1.57
Ral-loaded PCL:PLGA (1:1) microspheres	1.21 $\pm$ 0.67	0.37	1.17	2.13	1.50
Ral-PEG-loaded PCL microspheres	1.08 $\pm$ 0.50	0.55	1.01	1.67	1.11
Ral-PEG-loaded PCL:PLGA (1:1) microspheres	2.16 $\pm$ 1.80	0.50	1.55	5.04	2.93

Data are expressed as mean  $\pm$  S.D., n=1200.

d(0.9), d(0.5) and d(0.1) denote the diameters where 90%, 50% and 10% of the microspheres is smaller than the stated value, respectively.

PDI refers to polydispersity index.

Ral to PEG ratio is 1:2.

In addition, a histogram and a cumulative arithmetic curve were plotted for each group to present the particle size distribution of the microspheres (Figures 41-43). Histograms

of particle sizes showed that when single polymer (PCL) was used a unimodal distribution was observed (Figures 41, 42 a & 43 a) and the one resembling to Gaussian distribution was observed especially for Ral-PEG-loaded PCL microspheres (Figure 43 a). However, when two polymers were used together, distribution was either bimodal as for Ral-loaded PCL:PLGA (1:1) microspheres (Figure 42 b) or more skewed as for Ral-PEG-loaded PCL:PLGA (1:1) microspheres (Figure 43 b).

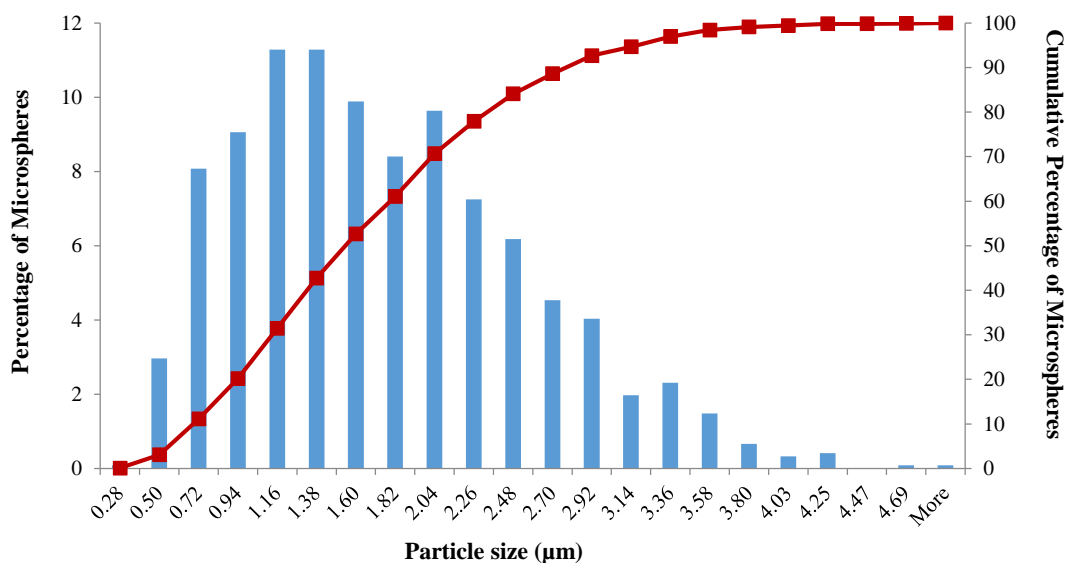
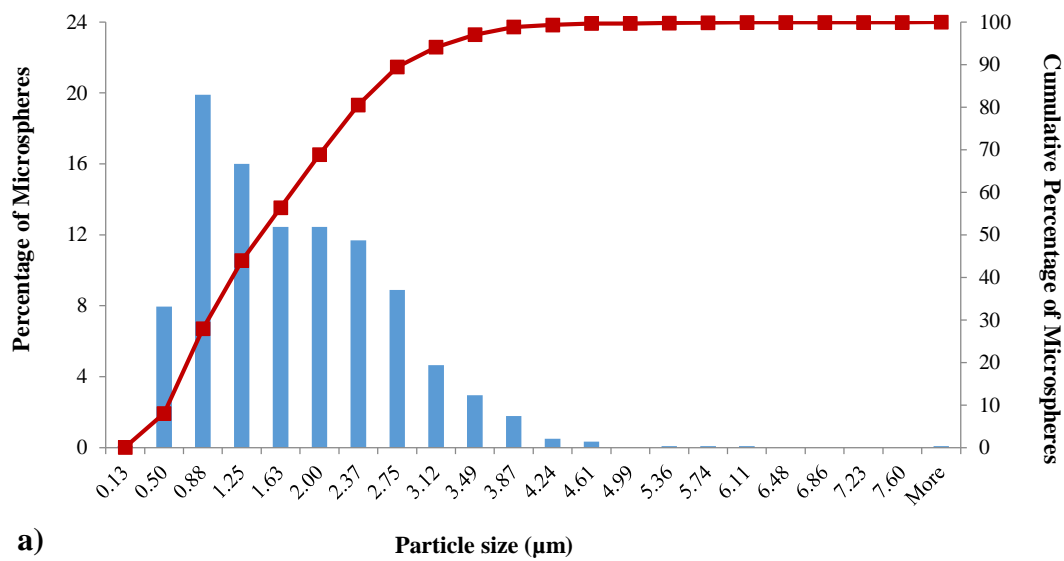
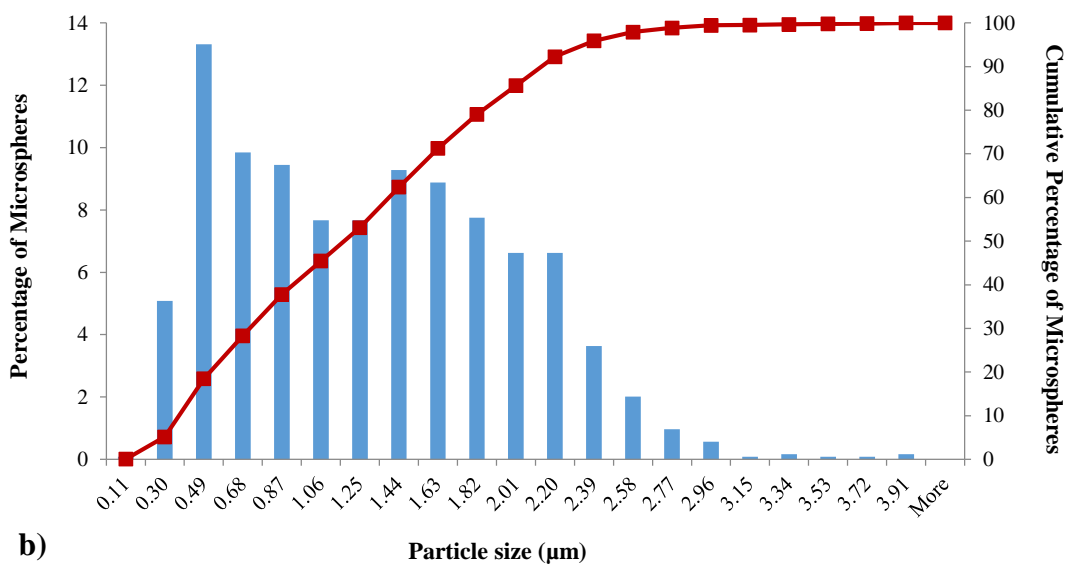


**Figure 41.** Particle size distribution of empty PCL microspheres (prepared by the optimized oil-in-oil-in-water method) presented as a histogram and a cumulative arithmetic curve.

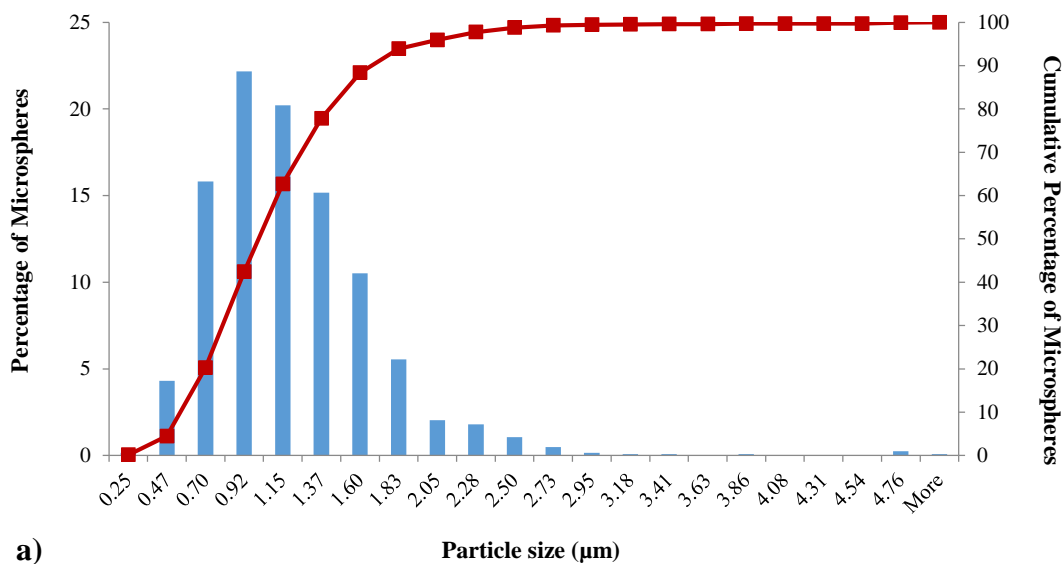


a)

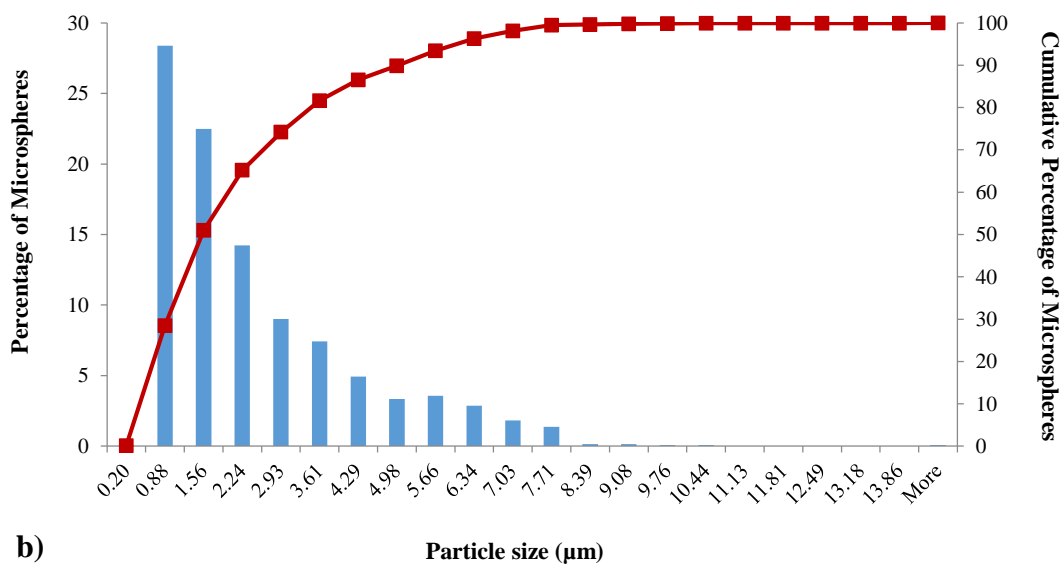


b)

**Figure 42.** Particle size distribution of a) Ral-loaded PCL and b) Ral-loaded PCL:PLGA (1:1) microspheres (prepared by the optimized oil-in-oil-in-water method) presented as a histogram and a cumulative arithmetic curve.



a)



b)

**Figure 43.** Particle size distribution of a) Ral-PEG-loaded PCL and b) Ral-PEG-loaded PCL:PLGA (1:1) microspheres (prepared by the optimized oil-in-oil-in-water method) presented as a histogram and a cumulative arithmetic curve.

### 3.3.3. Ral Encapsulation Efficiency and Loading

Ral amount encapsulated in Ral-loaded PCL, Ral-loaded PCL:PLGA (1:1), Ral-PEG-loaded PCL and Ral-PEG-loaded PCL:PLGA (1:1) microspheres prepared by the optimized oil-in-oil-in-water method was found by the calibration curve plotted with different concentrations of Ral (5-25  $\mu\text{g/mL}$ ) in DCM:MeOH (1:1) (Figure 61 in Appendix C). The encapsulation efficiency and loading results of the groups are given in Table 7. Ral-loaded PCL microsphere group had the highest encapsulation efficiency (% ,  $70.73 \pm 4.98$ ), though difference among groups was not significant. This result is an expected outcome since Ral is a highly hydrophobic drug (solubility in water is  $627.4 \pm 132.0 \mu\text{g.mL}^{-1}$ ) (Teeter & Meyerhoff, 2002) whereas PEG possesses high aqueous solubility. Moreover, although both PCL and PLGA have hydrophobic nature, PCL is more hydrophobic than PLGA (Murillo et al., 2002; Singh et al., 2006). Consequently, relative to PEG, Ral is more prone to remain in PCL matrix rather than passing into the external water phase during preparation of microspheres, and more amount of Ral is expected to be in touch with PCL (100%) in comparison to the blend of PCL:PLGA (1:1). Similarly, in the study of Hiremath & Devi (2010), it was stated that tamoxifen-loaded PCL microspheres had rather high (60-67%) encapsulation efficiency values and high lipophilicity nature of tamoxifen was pointed for this result. On the other hand, the highest loading value (% ,  $4.36 \pm 0.70$ ) was observed for Ral-PEG-loaded PCL microspheres. In addition, microspheres composed of only one kind of polymer – namely Ral-loaded PCL and Ral-PEG-loaded PCL microspheres – had higher loading values relative to their corresponding theoretical loadings whereas in the other groups (microspheres composed of two kinds of polymers), they showed lower loading values relative to their corresponding theoretical loadings. Taking into account that Ral-loaded PCL:PLGA (1:1) and Ral-PEG-loaded PCL:PLGA (1:1) microspheres did not have low encapsulation efficiency values, the only possible reason for this outcome might be less partitioning of hydrophobic Ral molecules within the polymer core during formation of

microspheres. This might be due to decreased homogeneity of the organic phase where two polymers with different dissolution properties are found.

**Table 7.** Encapsulation efficiency (%), loading (%) and theoretical loading (%) values of Ral- and Ral-PEG-loaded microspheres prepared by the optimized oil-in-oil-in-water method (n=3).

<b>Groups</b>	<b>Encapsulation efficiency (%)</b>	<b>Loading (%)</b>	<b>Theoretical loading (%)</b>
Ral-loaded PCL microspheres	70.73 ± 4.98	3.88 ± 0.27	3.26
Ral-loaded PCL:PLGA (1:1) microspheres	60.39 ± 8.58	2.79 ± 0.40	3.27
Ral-PEG-loaded PCL microspheres	59.69 ± 9.61	4.36 ± 0.70	3.28
Ral-PEG-loaded PCL:PLGA (1:1) microspheres	63.58 ± 3.79	2.99 ± 0.18	3.11

### 3.3.4. Ral Release Profiles of the Microspheres

In order to find Ral amount released from Ral-loaded PCL, Ral-loaded PCL:PLGA (1:1), Ral-PEG-loaded PCL and Ral-PEG-loaded PCL:PLGA (1:1) microspheres prepared by the optimized oil-in-oil-in-water method, a calibration curve was plotted with different concentrations of Ral (0-20 µg/mL) in MeOH:PBS (1:1) by

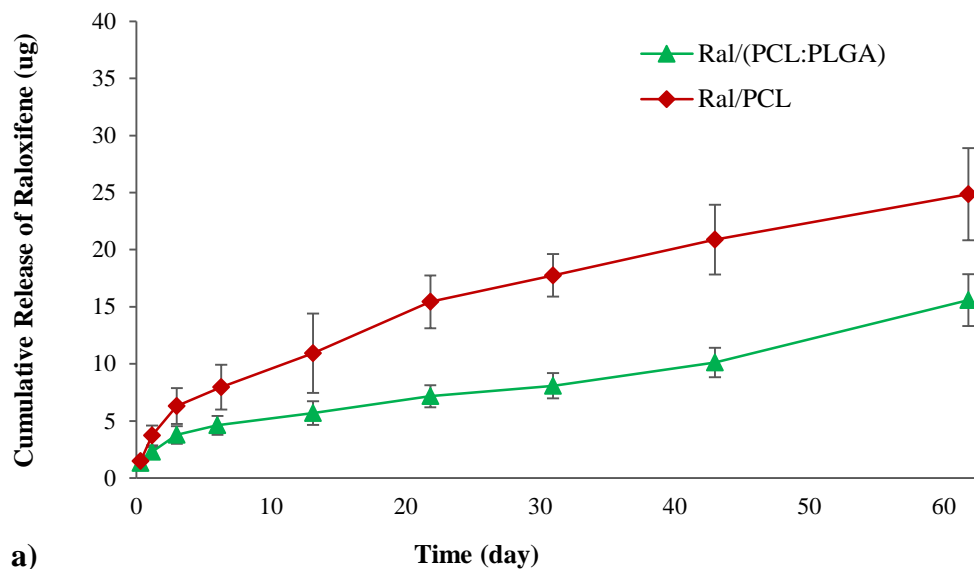
spectrophotometry (Figure 60 in Appendix B). Ral release profiles of all microsphere groups shown in Figures 44 & 45 can be characterized by moderate burst effect of Ral, being higher for Ral-PEG-loaded PCL:PLGA (1:1) microspheres. Burst effect is thought to be arised from release of Ral adsorbed on or close to the surfaces of the microspheres. It was followed by slower and sustained Ral release for all groups. However, on 43<sup>rd</sup> day, release rates increased for PLGA containing microsphere groups – namely Ral-loaded PCL:PLGA (1:1) and Ral-PEG-loaded PCL:PLGA(1:1) microspheres. It is known that a drug is released from biodegradable polymeric drug delivery systems in three stages (Ramtoola et al., 1992; Fitzgerald & Corrigan, 1996): a) burst phase owing to drug dissolution or diffusion then b) lag phase and lastly c) controlled release of drug directed by polymer degradation. Considering the release profiles of Ral-loaded PCL:PLGA (1:1) and Ral-PEG-loaded PCL:PLGA (1:1) microspheres, three stages mentioned above can be seen and it can be said that third stage at which Ral release rates increased depending on degradation behaviors of PLGA and PCL for both groups. In addition, PCL is known as a biodegradable polymer of which degradation is much slower in comparison to other degradable polymers (Jeong et al., 2003). Therefore, it can be mentioned that third stage is mainly controlled by degradation behaviour of PLGA. According to Lewis (1990), Agrawal et al. (1992) and Proikakis et al. (2006), during hydrolytic degradation of polylactide/glycolide family, sharp decrease in polymer mass and a high increase in rate of drug release takes place when a critical molecular weight is reached. Thus, it can be concluded that the corresponding critical molecular weight might have been reached during degradation of PLGA on just 43<sup>rd</sup> day and depending on this, amounts of Ral release might have increased from this point forward. However, since PCL degradation is very slow, these changes might have not occurred and therefore release rate might have not altered for only PCL containing microsphere groups – namely Ral-loaded PCL and Ral-PEG-loaded PCL microspheres.

At the end of two months, cumulative amounts of Ral release from Ral-loaded PCL:PLGA (1:1) and Ral-loaded PCL microspheres were found as  $15.59 \mu\text{g} \pm 2.27$  and

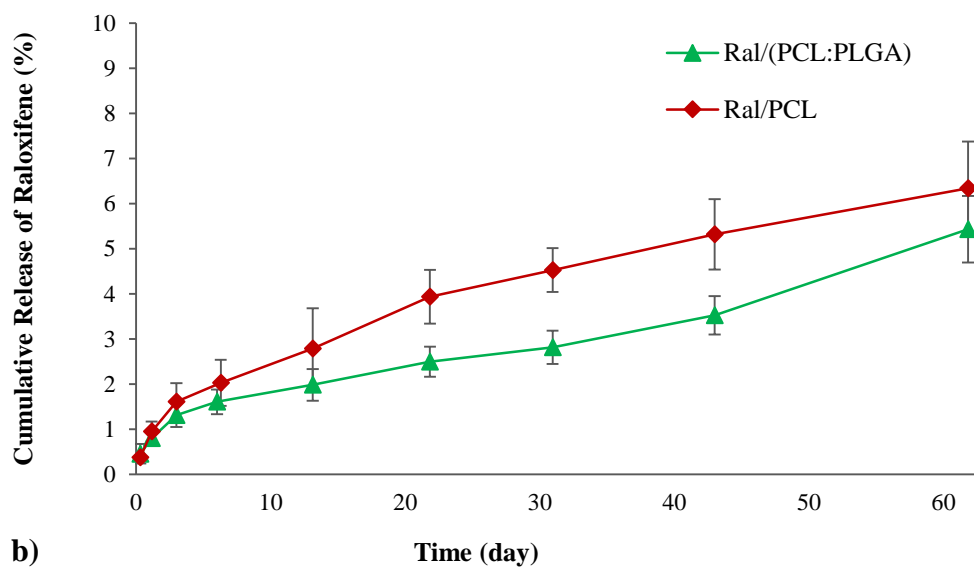
24.86  $\mu\text{g} \pm 4.03$ , respectively (Figure 44 a). As mentioned above, PCL degradation is much slower than that of PLGA. Therefore, it was expected that existence of PLGA would further increase Ral release amount for Ral-loaded PCL:PLGA (1:1) microspheres. Despite this expectation, Ral-loaded PCL microspheres showed higher amounts of drug release due to higher drug encapsulation efficiency and loading values than those of Ral-loaded PCL:PLGA (1:1) microspheres. These results suggest that the loading has a more pronounced effect on release amounts than addition of a less hydrophobic polymer, PLGA, to the polymer phase for Ral containing microsphere groups. On the other hand, these remarkable differences were not reflected to cumulative percent release values of these two groups because release results were not significantly different (5.43%  $\pm 0.74$  and 6.34%  $\pm 1.03$  for Ral-loaded PCL:PLGA (1:1) and Ral-loaded PCL microspheres, respectively) (Figure 44 b). The reason for this outcome is that Ral-loaded PCL microspheres had the higher drug encapsulation efficiency and loading results in comparison to those of Ral-loaded PCL:PLGA (1:1) microspheres.

Cumulative amounts of Ral release were obtained as 40.21  $\mu\text{g} \pm 13.16$  and 16.92  $\mu\text{g} \pm 2.25$  for Ral-PEG-loaded PCL:PLGA (1:1) and Ral-PEG-loaded PCL microspheres, respectively (Figure 45 a), whereas cumulative percent release values were found as 26.92%  $\pm 8.81$  and 3.78%  $\pm 0.52$  for the same groups (Figure 45 b). Among all groups, Ral-PEG-loaded PCL:PLGA (1:1) microsphere group had the maximum Ral release rate value. This result can be explained by several factors. By Klose et al. (2008), it has been stated that hydrophilic drugs, especially if they are loaded in high amounts, provide water penetration into drug-loaded polymeric systems and generate highly porous polymer structures by drug exit. Hence, polymer degradation rate increases. Additionally, in a study of Zacchigna et al. (2014), it was reported that ursolic acid having high hydrophobic nature was conjugated PEG and extremely increased water solubility was achieved. According to Bandela & Anupama (2009), PEG molecules increase the hydrodynamic radius of the corresponding conjugated drug and provide the

drug to have increased water solubility. That is water solubility of the drug is enhanced by wettability offered by PEG. Moreover, Garg et al. (2009) and Hancock & Parks (2000) have mentioned that amorphous forms of materials are notably more soluble than their crystalline counterparts. Thus, dissolution rate is enhanced (Ahuja et al., 2007; Friedrich et al., 2005). In our study, it was found that crystalline nature of Ral was converted to amorphous form after conjugation to PEG, as demonstrated by FT-IR, XRD and SEM results. In this manner, PEG conjugation to Ral in this study might have increased the degradation rate of the polymers, PCL and PLGA, as well as it might have increased solubility of Ral by enhancing wettability of Ral and changing crystalline nature of Ral to amorphous form. Totally, all these results might have accelerated both Ral dissolution and diffusion from the system, therefore providing increase in Ral release rate. In addition, presence of a less hydrophobic polymer component, PLGA, in the polymer matrix might have facilitated Ral exit from PCL:PLGA (1:1) microspheres, contributing in high Ral release rate. On the other hand, Ral-PEG-loaded PCL microspheres had low values of Ral release rate. This result might be attributed to high hydrophobic nature of PCL resisting to water penetration into the microspheres despite of existence of Ral-PEG in the system.

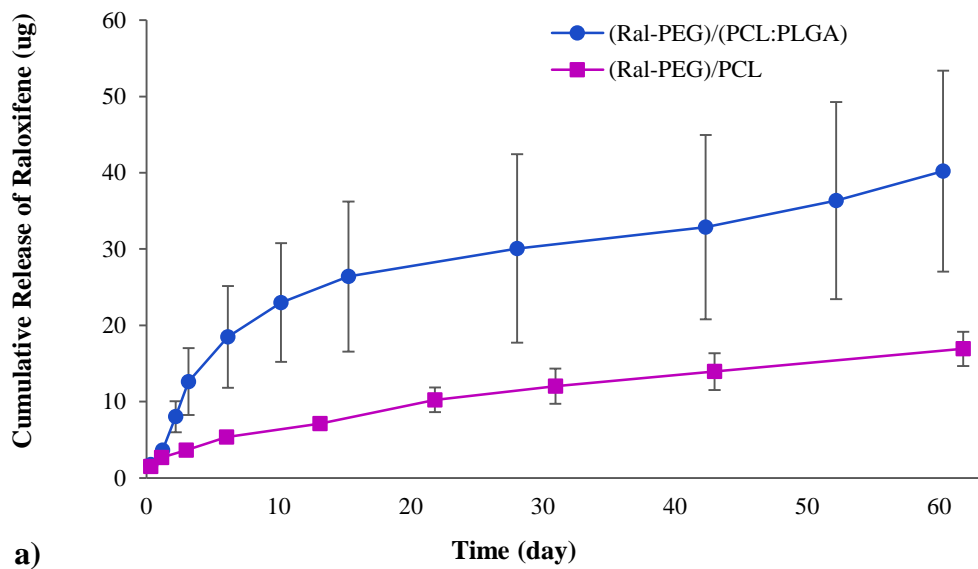


a)

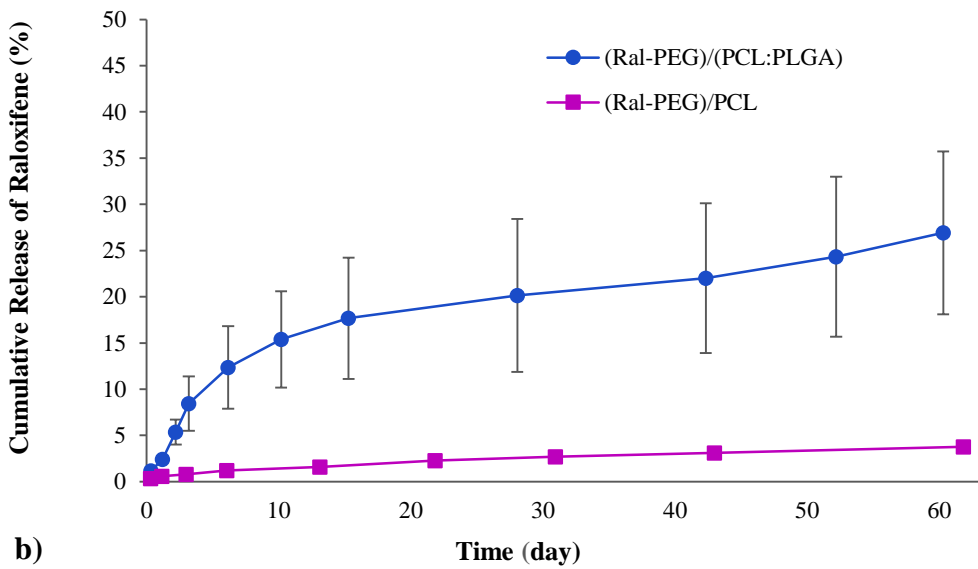


b)

**Figure 44.** Ral release profiles (a)  $\mu\text{g}$  and b) %) of Ral-loaded PCL:PLGA (1:1) and Ral-loaded PCL microspheres (prepared by the optimized oil-in-oil-in-water method) incubated in PBS (0.1 M, pH 7.4) at  $37^\circ\text{C}$  for 60 days (n=3).



a)

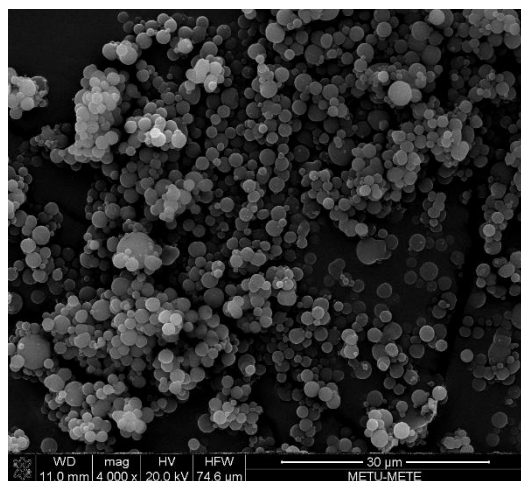


b)

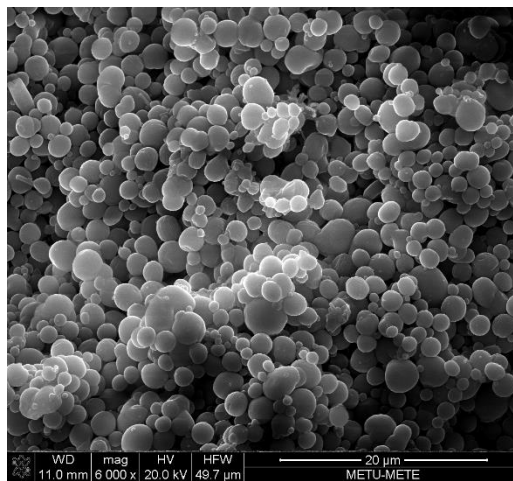
**Figure 45.** Ral release profiles (a)  $\mu\text{g}$  and b) %) of Ral-PEG-loaded PCL:PLGA (1:1) and Ral-PEG-loaded PCL microspheres (prepared by the optimized oil-in-oil-in-water method) incubated in PBS (0.1 M, pH 7.4) at  $37^\circ\text{C}$  for 60 days ( $n=3$ ) (Ral to PEG ratio is 1:2).

### **3.3.5. Morphological Analysis of the Microspheres after Release**

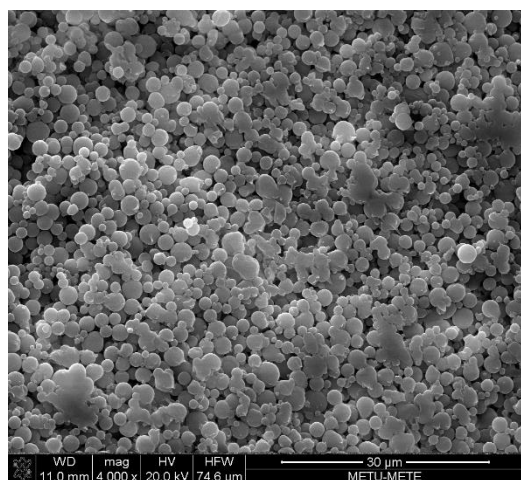
SEM analysis was performed to investigate the morphology of the microspheres after 60 days of release. Related SEM micrographs of Ral-loaded PCL, Ral-loaded PCL:PLGA (1:1), Ral-PEG-loaded PCL and Ral-PEG-loaded PCL:PLGA (1:1) microspheres (prepared by the optimized oil-in-oil-in-water method) are shown in Figures 46, 47, 48 and 49, respectively. After 60 days of release, the minimum change of spherical shape of the microspheres was observed for Ral-loaded PCL group (Figure 46). This result is expected because of very slow degradation behavior of PCL and high hydrophobic and crystalline nature of Ral leading majority of Ral to remain in PCL matrix. For the other groups, in many sites, it was observed that the peripheries of microspheres became indistinct producing views as if microspheres fused to each other. Additionally, in some images, a thin coating was observed among the microspheres. These outcomes might be ascribed to relatively fast degradation of PLGA and/or increased water solubility of Ral provided by enhanced wettability as well as amorphous form of Ral upon conjugation reaction with PEG. Moreover, these outcomes might have been originated from relatively increased degradation rates of PCL and PLGA, provided by enhanced wettability of Ral. On the other hand, as mentioned in Section 3.3.4., critical molecular weight of PLGA might have been reached upon degradation on 43<sup>rd</sup> day of release period. From this point forward, oligomers might have started to diffuse out from PLGA. Along with this phenomenon, easy transfer of Ral or Ral-PEG from the microspheres into the dispersant aqueous medium might have been occurred during release period. Because of these possibilities, extra mass of material might have caused deterioration of spherical shape of the microspheres, observed after drying process.



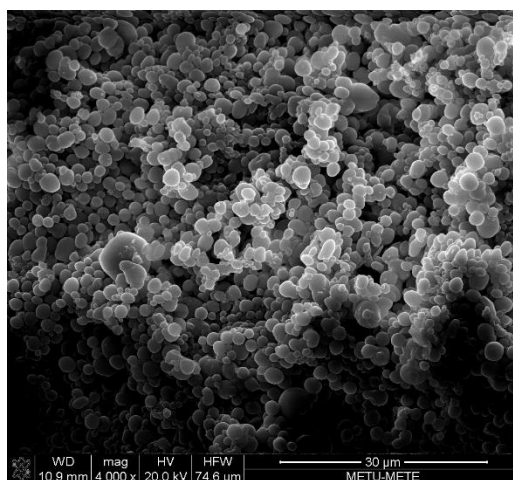
a)



b)

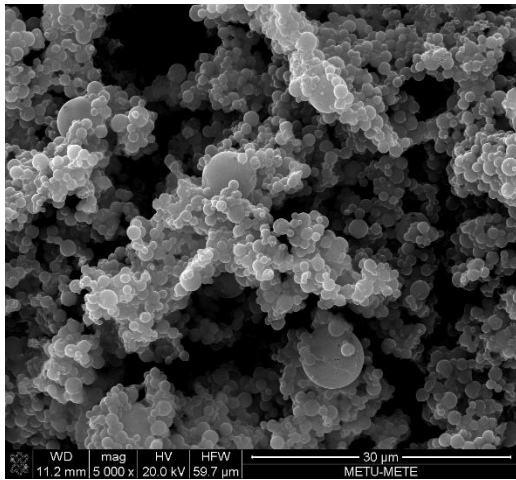


c)

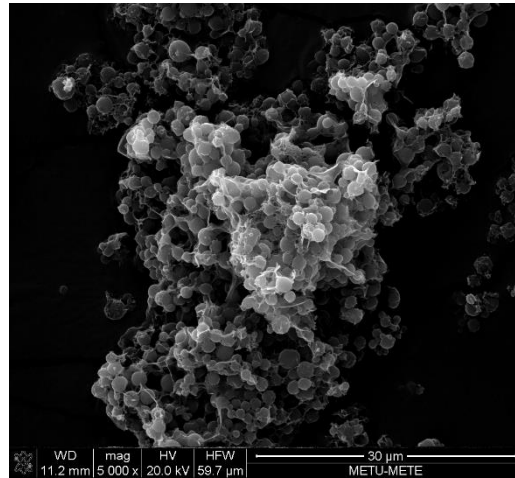


d)

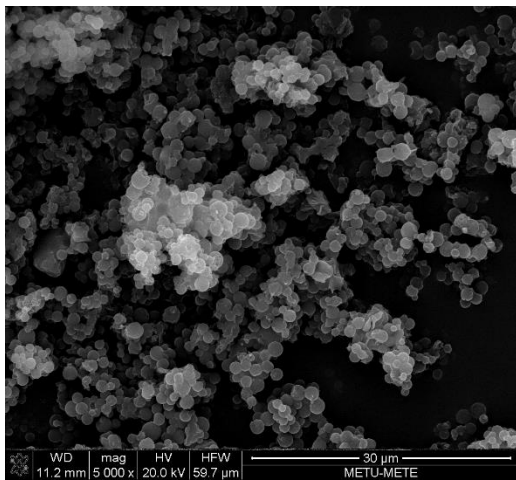
**Figure 46.** SEM micrographs of Ral-loaded PCL microspheres (prepared by the optimized oil-in-oil-in-water method) after 60 days of release in PBS (0.1 M, pH 7.4) at 37°C (a) 4000X, b) 6000X, c) 4000X and d) 4000X).



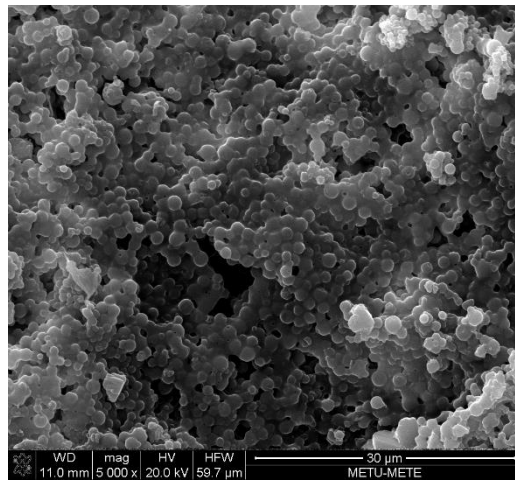
a)



b)

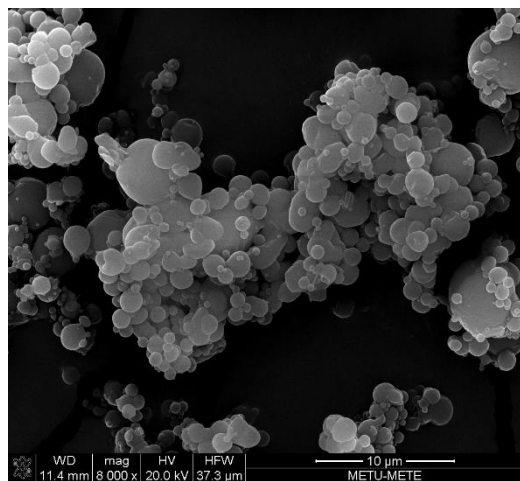


c)

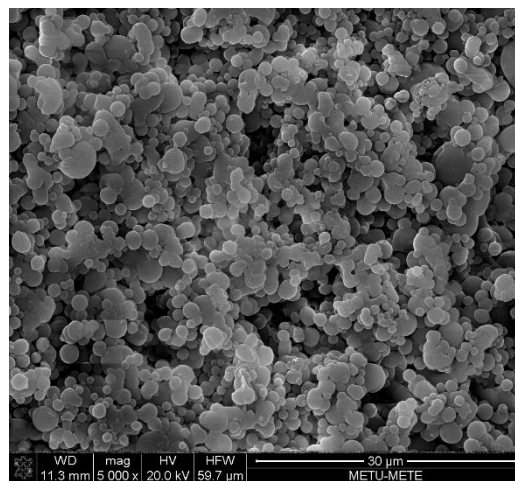


d)

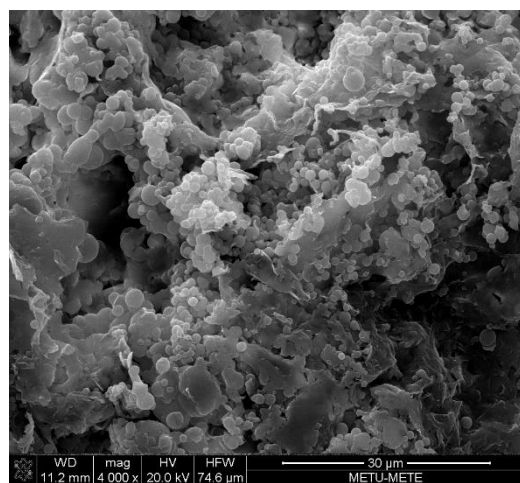
**Figure 47.** SEM micrographs of Ral-loaded PCL:PLGA: (1:1) microspheres (prepared by the optimized oil-in-oil-in-water method) after 60 days of release in PBS (0.1 M, pH 7.4) at 37°C (a) 5000X, b) 5000X, c) 5000X and d) 5000X).



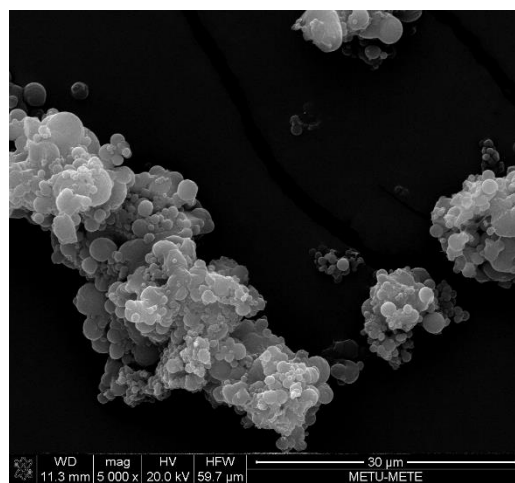
a)



b)



c)



d)

**Figure 48.** SEM micrographs of Ral-PEG-loaded PCL microspheres (prepared by the optimized oil-in-oil-in-water method) after 60 days of release in PBS (0.1 M, pH 7.4) at 37°C (a) 8000X, b) 5000X, c) 4000X and d) 5000X (Ral to PEG ratio is 1:2).

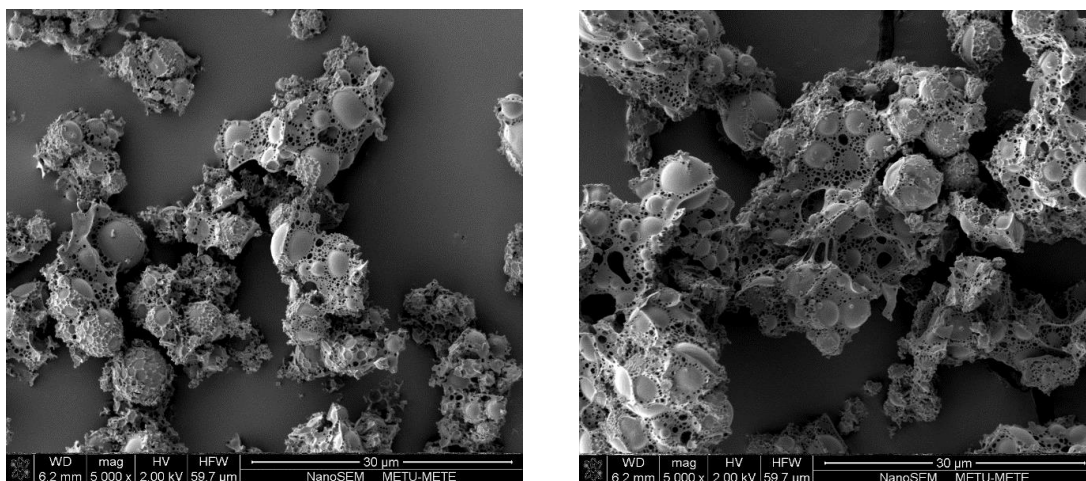


**Figure 49.** SEM micrographs of Ral-PEG-loaded PCL:PLGA (1:1) microspheres (prepared by the optimized oil-in-oil-in-water method) after 60 days of release in PBS (0.1 M, pH 7.4) at 37°C (a) 5000X and b) 5000X (Ral to PEG ratio is 1:2).

### 3.4. Cell Culture Studies

Adipose-derived mesenchymal stem cells were isolated from Sprague-Dawley rats and cultured in growth medium ( $\alpha$ -MEM supplemented with 10% FBS, 80 U/mL penicillin and 80  $\mu$ g/mL streptomycin) at 37°C under 5% CO<sub>2</sub> in a carbon dioxide incubator. Phase contrast micrographs of primer cells (Figure 50 a & b) and the cells at 1<sup>st</sup> (Figure 50 c & d) and 2<sup>nd</sup> passages (Figure 50 e & f) are presented below. The cells were observed to get a partly more fibroblastic appearance with each passage. After proliferation to 3<sup>rd</sup> passage, they were used for cell culture studies.

hFOB cells were cultivated in growth medium (DMEM/F-12 (1:1) supplemented with 10% FBS, 80 U/mL penicillin and 80  $\mu$ g/mL streptomycin) at 37°C under 5% CO<sub>2</sub> in

the carbon dioxide incubator. Phase contrast micrographs of hFOB cells at 9<sup>th</sup> passage are shown in Figure 51.

When the morphology of two kinds of cells were compared, more polygonal shape was observed for hFOB cells.

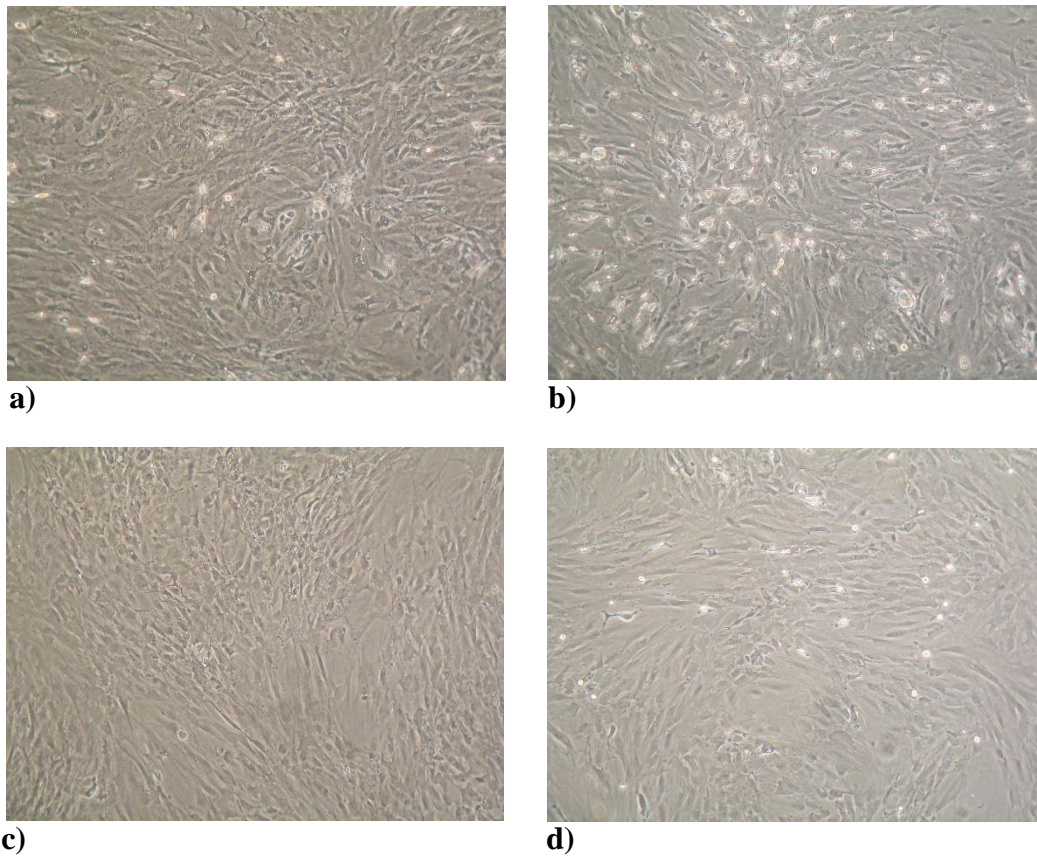
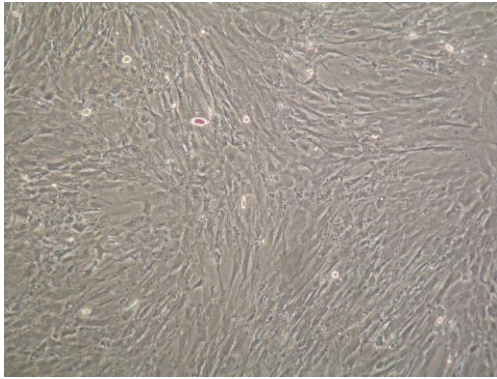
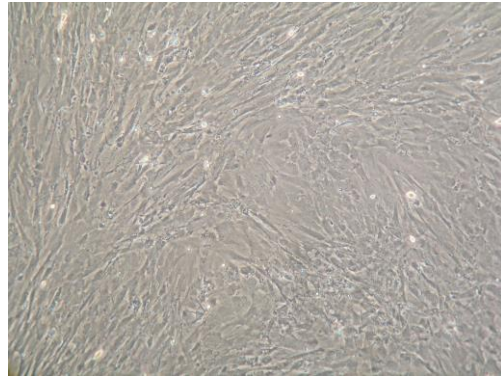


**Figure 50.** Phase contrast micrographs of adipose-derived mesenchymal stem cells isolated from Sprague-Dawley rats (10X) (a) and b) primer, c) and d) 1<sup>st</sup> passage).



e)



f)

**Figure 50. (continued)** Phase contrast micrographs of adipose-derived mesenchymal stem cells isolated from Sprague-Dawley rats (10X) (e) and f) 2<sup>nd</sup> passage).

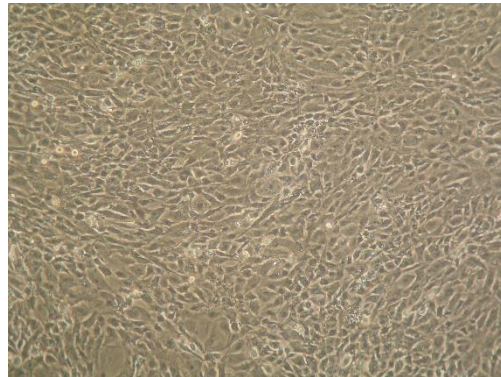
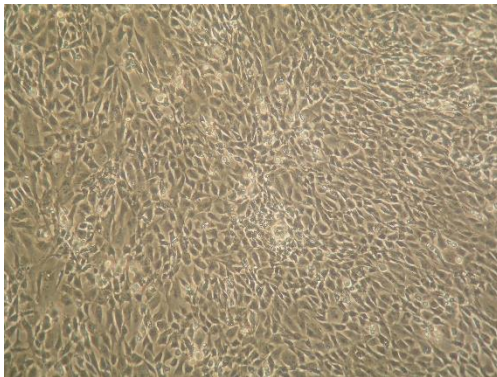


**Figure 51.** Phase contrast micrographs of hFOB cells (10X) (9<sup>th</sup> passage).

### **3.4.1. Dose-Dependent Effects of Ral and Ral-PEG on Adipose-Derived Mesenchymal Stem Cells and hFOB Cells**

#### **3.4.1.1. *In Vitro* Cytotoxicity Studies**

Effects of Ral and Ral-PEG (at different doses mentioned in Section 2.2.6.3.1) on cell viability of adipose-derived stem cells (3<sup>rd</sup> passage) and hFOB cells (9<sup>th</sup> passage) were investigated by Prestoblue assay. Results shown in Figure 52 showed that Ral and Ral-PEG at the doses of 0.1  $\mu\text{M}$  did not have any toxic effect on adipose-derived stem cells cultivated in growth medium, having values higher than 80% relative cell viability at all time points of the experiment. On the other hand, especially on days 7 and 14, both Ral and Ral-PEG at the doses of 1 and 10  $\mu\text{M}$  caused to decrease the cell viability of adipose-derived stem cells sharply. Cell viabilities of the cells treated with of 1 and 10  $\mu\text{M}$  Ral and Ral-PEG were found to be statistically lower than those of the cells treated with 0.1  $\mu\text{M}$  Ral and Ral-PEG on days 7 and 14. Similar significant decreases were observed on day 3 except for the viability of the cells treated with 1  $\mu\text{M}$  Ral. This dose of Ral resulted in cell viability almost same with that of the cells treated with 0.1  $\mu\text{M}$  Ral. Additionally, the viabilities of the cells treated with 1 and 10  $\mu\text{M}$  Ral-PEG were found to be significantly lower than those of 0.1  $\mu\text{M}$  Ral- and Ral-PEG-treated cells. However, relative cell viability values of these groups were higher than 80%.

Effects of Ral and Ral-PEG treatment at the doses of 0.01, 0.1, 1 and 10  $\mu\text{M}$  on cell viability of hFOB cells are shown in Figure 53. It can be seen that all cell viability results were higher than 85% during 14 days although there were statistically significant differences in the relative cell viabilities between 0.1  $\mu\text{M}$  Ral-treated cells and the cells treated with 1 and 10  $\mu\text{M}$  Ral as well as 10  $\mu\text{M}$  Ral-PEG on day 14. Similarly, statistically significant differences were also observed between 0.1  $\mu\text{M}$  Ral-PEG-treated cells and 10  $\mu\text{M}$  Ral- and Ral-PEG-treated cells despite of the cell viability results

higher than 85%. Based on these data, it can be mentioned that both Ral and Ral-PEG at at the doses of 0.01, 0.1, 1 and 10  $\mu\text{M}$  do not have any toxic effects on hFOB cells for a period of 14 days. Similarly, Taranta et al. (2002) reported that Ral at the doses in the range of 0.1 –  $10^{-8}$   $\mu\text{M}$  induced an increase in proliferation of osteoblasts obtained from calvariae of female neonatal mice.

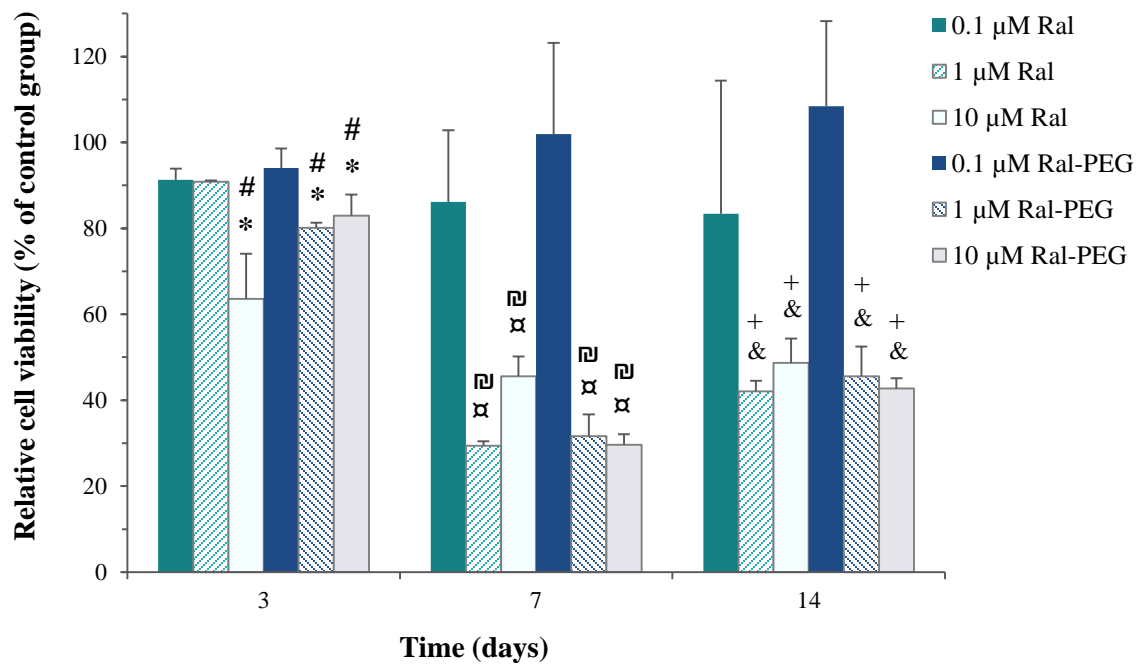


**Figure 52.** Relative cell viabilities of adipose-derived mesenchymal stem cells presented as percentages of cell viability of the control group. The cells were cultivated in growth medium and data were obtained after 3, 7 and 14 days of Ral and Ral-PEG treatment at the doses of 0.1, 1 and 10  $\mu\text{M}$ . \*, ρ and & represent statistically significant differences relative to 0.1  $\mu\text{M}$  Ral-treated cells at day 3, 7 and 14, respectively. #, ρ and + represent statistically significant differences relative to 0.1  $\mu\text{M}$  Ral-PEG-treated cells at day 3, 7 and 14, respectively.

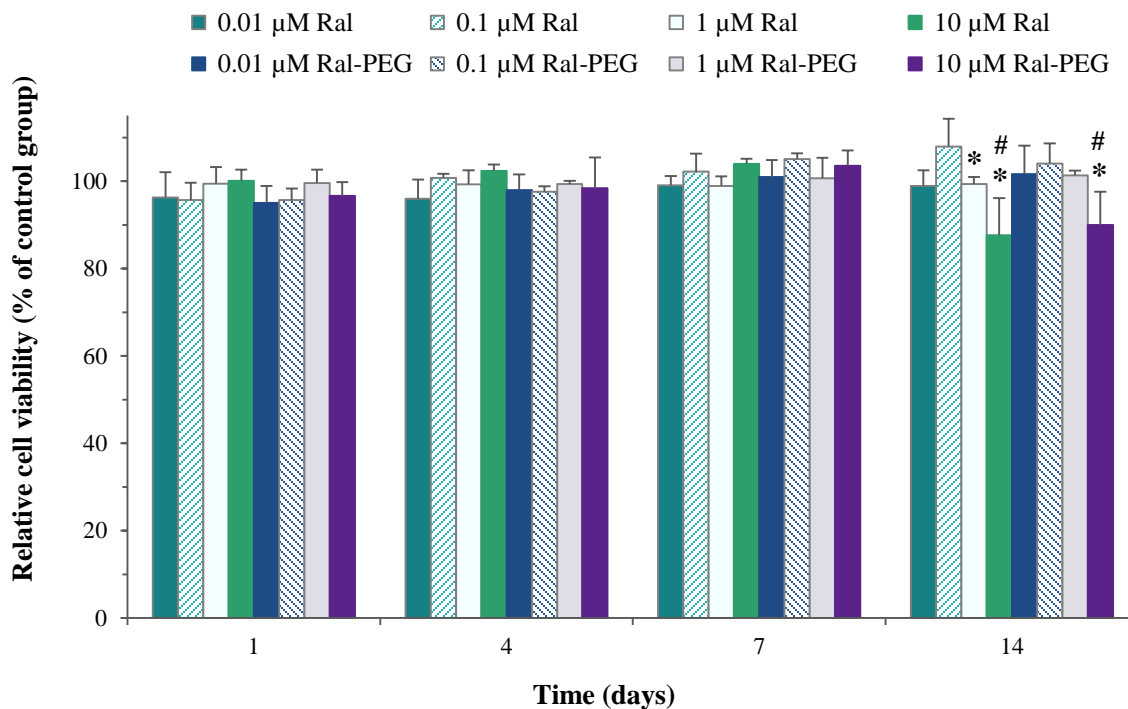


**Figure 53.** Relative cell viabilities of hFOB cells presented as percentages of cell viability of the control group. The cells were cultivated in growth medium and data were obtained after 1, 4, 7 and 14 days of Ral and Ral-PEG treatment at the doses of 0.01, 0.1, 1 and 10  $\mu\text{M}$ . \* and # represent statistically significant differences relative to 0.1  $\mu\text{M}$  Ral- and 0.1  $\mu\text{M}$  Ral-PEG-treated cells at day 14, respectively.

### 3.4.1.2. ALP Activity Analysis

Effects of different doses of Ral and Ral-PEG (0.01, 0.1, 1 and 10  $\mu\text{M}$ ) on ALP activity (nmol/min) of hFOB cells were analysed after 7 days of treatment. In order to find the ALP activity of the cells, a calibration curve was plotted with different amounts of *p*-nitrophenol product (0-20 nmol/well) produced by ALP enzyme belonging to the kit. The corresponding calibration curve is shown in Figure 62 in Appendix D. Results

showed that any Ral dose did not have a pronounced affect on ALP activity of hFOB cells in comparison to to the control group (Figure 54). Ral-PEG doses and especially 0.01  $\mu\text{M}$  Ral-PEG resulted with a slight numerical increase in ALP activity of the cells. However, any statistically significant difference relative to the control group was not found for all doses of Ral-PEG. On the other hand, all doses of Ral-PEG yielded significantly higher ALP activities of the cells in comparison to those of 0.1  $\mu\text{M}$  Ral-treated cells on day 7.

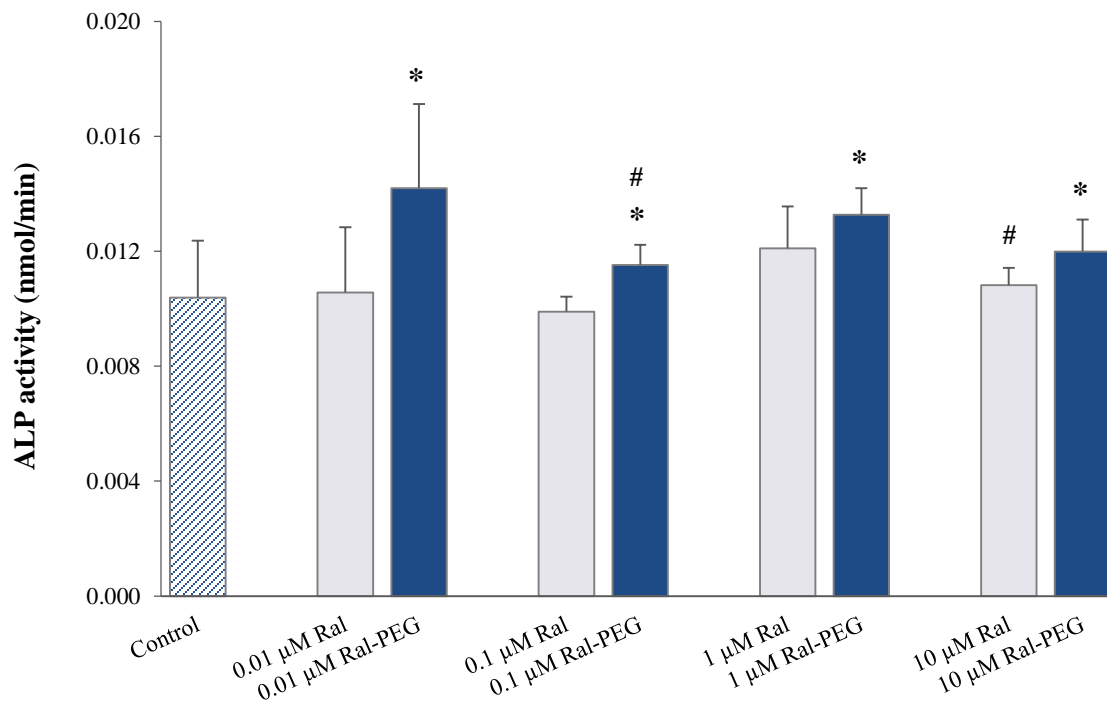


**Figure 54.** ALP activity (nmol/min) results of hFOB cells after 7 days of Ral and Ral-PEG treatment at the doses of 0.01, 0.1, 1 and 10  $\mu\text{M}$ . \* and # represent statistically significant differences relative to 0.1  $\mu\text{M}$  Ral- and 1  $\mu\text{M}$  Ral-PEG-treated cells, respectively.

Moreover, ALP activity of the cells treated with 1  $\mu\text{M}$  Ral-PEG was found to be significantly higher than those of 0.1  $\mu\text{M}$  Ral-PEG- and 10  $\mu\text{M}$  Ral-treated cells. In the study of Taranta et al. (2002), it was indicated that Ral stimulated osteoblast activity *in vitro* and it was demonstrated that collagen I mRNA expression was upregulated in osteoblasts exposed to Ral (0.1 and  $10^{-4}$   $\mu\text{M}$ ) for 24 h. However, in the same study, no stimulatory effect of Ral was observed on ALP activity of the osteoblasts similar to the ALP results found in our study.

### **3.4.2. Effects of Ral- and Ral-PEG-Loaded Microspheres on Adipose Derived Mesenchymal Stem Cells**

#### **3.4.2.1. *In Vitro* Cytotoxicity Studies**

Cell viabilities upon 1, 4 and 7 days of cultivation of female adipose-derived mesenchymal stem cells (3<sup>rd</sup> passage) in the growth medium containing Ral and Ral-PEG released from the microspheres (Ral-loaded PCL, Ral-loaded PCL:PLGA (1:1), Ral-PEG-loaded PCL and Ral-PEG-loaded PCL:PLGA (1:1) microspheres) were analysed by Prestoblu assay. Empty PCL:PLGA (1:1) and PCL microspheres were used as controls. As seen in Figure 55, relative cell viability of the adipose-derived stem cells cultivated in the release medium of PCL:PLGA microspheres was found to be significantly higher than those of the cells cultivated in the release media of all the other microsphere groups at day 1. Additionally, Ral-PEG-loaded PCL and Ral-PEG-loaded PCL:PLGA microspheres yielded relative cell viabilities significantly higher than that of the cells cultivated in the release medium of Ral-loaded PCL microspheres at days 1 and 4. On the other hand, the relative cell viability of the cells cultivated in the release medium of Ral-PEG-loaded PCL microspheres was observed to be significantly higher than that of the cells cultivated in the release medium of PCL microspheres at day 4. In spite of these results, all relative cell viability values were found to be higher than 90%.

Thus, it can be concluded that content of the release mediums in which the adipose-derived stem cells were cultured for a period of 7 days had no cytotoxic effects, showing biocompatibility of the microspheres prepared.

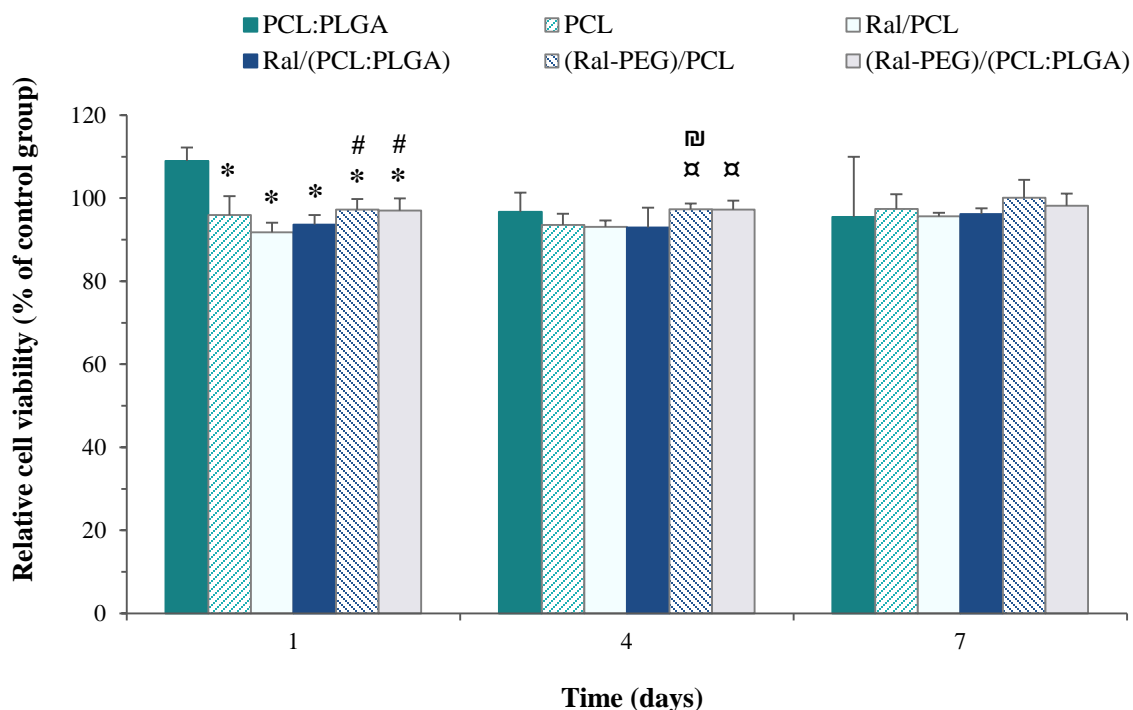


**Figure 55.** Relative cell viabilities of female adipose-derived mesenchymal stem cells presented as percentages of cell viability of the control group. Data were obtained after 1, 4 and 7 days of incubations of the cells in release media of various microsphere groups. \* refers to statistically significant difference relative to the cells cultivated in release medium of empty PCL:PLGA (1:1) microsphere group at day 1. # and α refer to statistically significant differences relative to the cells cultivated in release medium of Ral-loaded PCL microsphere group at days 1 and 4, respectively. ▣ refers to statistically significant difference relative to the cells cultivated in release medium of empty PCL microsphere group at day 4.

### 3.4.2.2. Alizarin Red S Staining

Subsequent to cultivation of female adipose-derived mesenchymal stem cells (3<sup>rd</sup> passage) in the osteogenic differentiation medium containing Ral and Ral-PEG released from the microspheres (Ral-loaded PCL, Ral-loaded PCL:PLGA (1:1), Ral-PEG-loaded PCL and Ral-PEG-loaded PCL:PLGA (1:1) microspheres) for 7 days, mineralization of matrix deposited by the cells was evaluated by Alizarin red S staining as one of the methods for functional evaluation of Ral-loaded microspheres on treatment of osteoporosis *in vitro*. Empty PCL:PLGA (1:1) and PCL microspheres were used as controls.

After Alizarin red S staining, phase contrast micrographs of the stained cells belonging to each microsphere group were taken (n=3). Top, middle and bottom zones of each replicate were photographed. As seen in representative images in Figure 56, all cells were stained with Alizarin red S. However, more intensive color of the stain and higher amounts of mineralized nodule-like formations were observed for the cells cultivated in the release medium of Ral-PEG-loaded PCL:PLGA (1:1) microspheres, indicating that the osteogenic differentiation of these cells might have been more enhanced during 7 days in comparison to other cells.

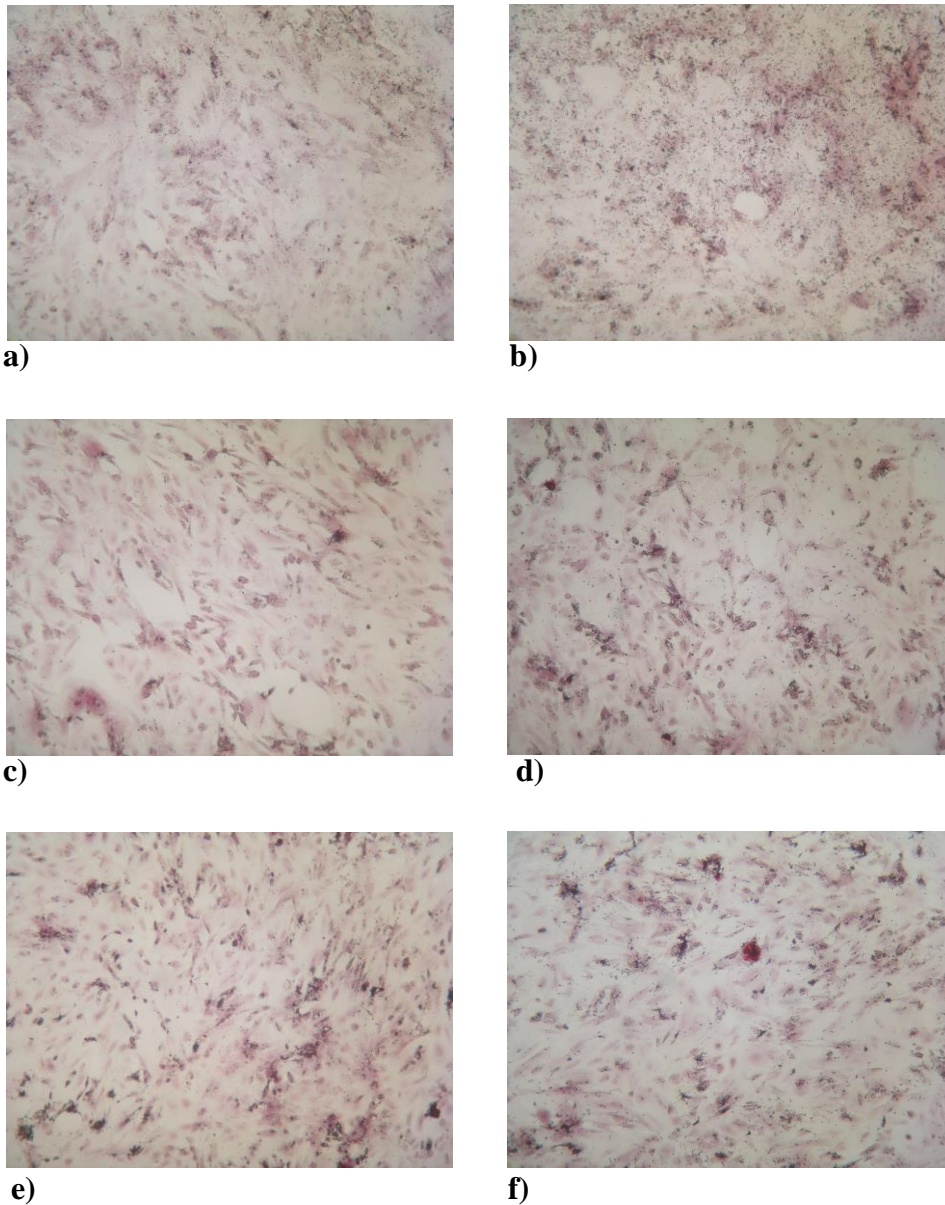


**Figure 56.** Phase contrast micrographs of the female adipose-derived mesenchymal stem cells stained with Alizarin red S after 7 days of cultivation in the release medium of various microsphere groups (a) and b) Empty PCL:PLGA (1:1) microspheres, c) and d) Empty PCL microspheres, e) and f) Ral-loaded PCL microspheres).

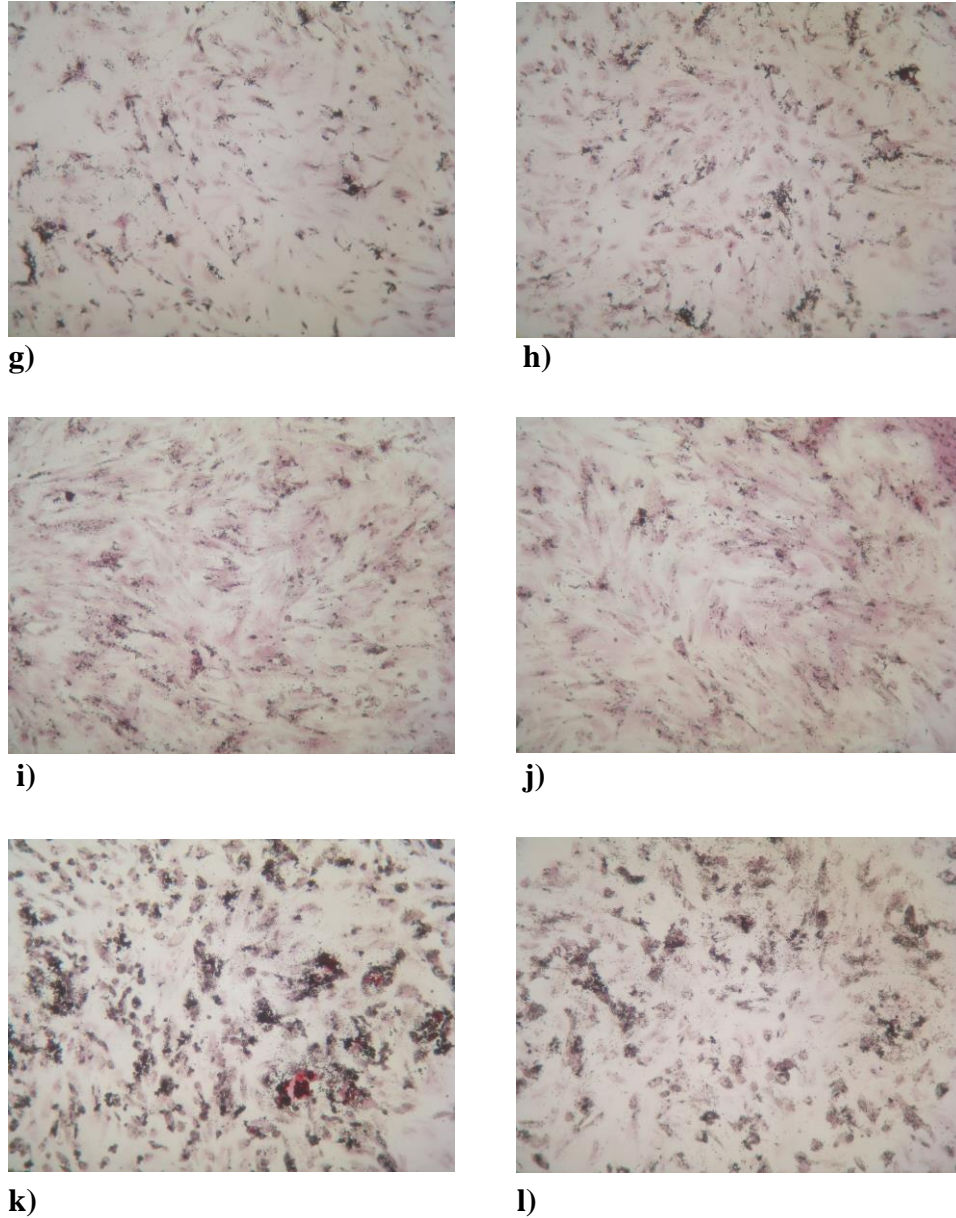


**Figure 56. (continued)** Phase contrast micrographs of the female adipose-derived mesenchymal stem cells stained with Alizarin red S after 7 days of cultivation in the release medium of various microsphere groups (g) and h) Ral-PEG-loaded PCL microspheres, i) and j) Ral-loaded PCL:PLGA (1:1) microspheres, k) and l) Ral-PEG-loaded PCL:PLGA (1:1) microspheres).

By Image J analysis software (NIH, USA), intensity of stain colour in each image was measured and expressed as a percentage of image area. Numerical values belonging to top, middle and bottom zones of each replicate were averaged and the resulting number was designated as mineral content of the corresponding replicate (n=3). Average mineral value of three replicates belonging to each microsphere group was used to make comparison between the groups. As it is seen in Figure 57, mineral content of the cells cultivated in the release medium of Ral-PEG-loaded PCL:PLGA (1:1) microspheres was found to be significantly higher than the cells cultivated in the release media of all the other microsphere groups. These results might be attributed to high amount of Ral release from Ral-PEG-loaded PCL:PLGA (1:1) microspheres. As it demonstrated in Section 3.3.4, cumulative percent release value of Ral for Ral-PEG-loaded PCL:PLGA (1:1) microspheres was found to be  $26.92\% \pm 8.81$  whereas maximum cumulative percent release value of Ral among the other microsphere groups was found to be only  $6.34\% \pm 1.03$  belonging to Ral-loaded PCL microspheres. Moreover, considering that Ral-PEG (1:2)-loaded PCL:PLGA (1:1) microspheres prepared with the parameters mentioned in this study were found to be non-toxic, it can be mentioned that this formulation of Ral delivery system has the potential of presenting therapeutic effects for osteoporosis, providing safe environment for the cells.

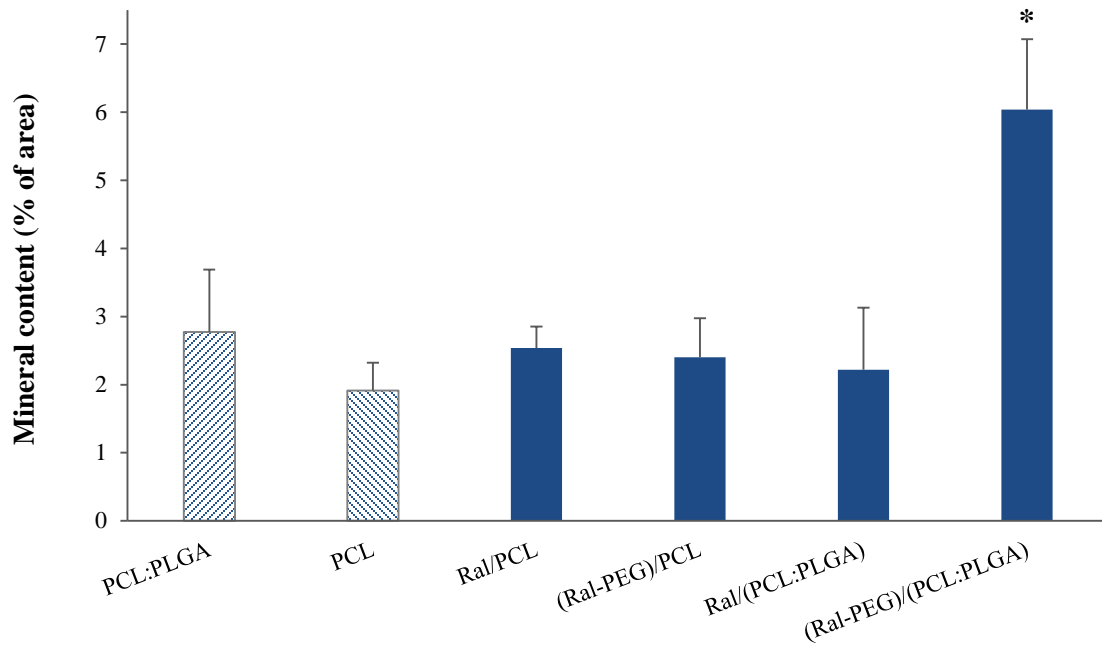


**Figure 57.** Mineral content of female adipose-derived mesenchymal stem cells incubated in the release media of various microsphere groups for 7 days. \* refers to statistically significant differences between the cells cultivated in release medium of Ral-PEG-loaded PCL:PLGA (1:1) microsphere group and the cells cultivated in release media of the other microsphere groups.



## CHAPTER 4

### CONCLUSIONS

Osteoporosis is a significant public health issue, as one of the most prevalent diseases in elderly people. It is characterized by a decrease in bone strength and bone mass, accompanied by an increase in fragility of bones and risk of fractures. Many therapeutic agents, most of which are administered systemically, have been used for treatment of osteoporosis in clinics. Ral is one of these drugs, having poor bioavailability. In order to maintain the therapeutic level, this drug has to be administered in high dosage forms and at frequent intervals. Hence, this route causes the patients to be at high risk of side effects which influence all the body. Possible side effects of Ral are venous thromboembolism, pulmonary embolism, hot flushes and leg cramps (Goodman and Gilman's, 2001; Maximov et al., 2013). Moreover, the treatment method costs highly and the patients have to put up with the tiresome therapy period. Therefore, alternative new treatment strategies are needed. As an alternative, controlled drug delivery systems have been investigated recently. By controlled Ral delivery systems, in comparison to free drug formulations, side effects and administration frequency of Ral, and total amount of Ral sufficient for therapy can be lowered as well as Ral treatment efficacy can be enhanced.

In this study, Ral and Ral-PEG were successfully encapsulated into microspheres comprising PCL and PCL:PLGA (1:1) blend. *In situ* and *in vitro* evaluation and comparison of these formulations were documented for the first time in literature.

Microspheres were prepared by the optimized method, the oil-in-oil-in-water ( $O_1/O_2/W$ ) double emulsion-solvent evaporation method. By SEM examinations, it was observed that most of the microspheres had spherical shape and smooth surfaces, and particle sizes of the microspheres were about 1.5  $\mu\text{m}$ . This size may not be appropriate for intravenous delivery of the microspheres. Thus, for *in vivo* studies, it can be suggested that the parameters of the microsphere preparation method should be modified in order to reduce the particle size of the microspheres to nano scale. The other option might be implantation of the microspheres within a scaffold to a bone defect site, originated from osteoporosis. Owing to high hydrophobic natures of both Ral and PCL, Ral-loaded PCL microspheres possessed the maximum encapsulation efficiency (%). Ral is a highly hydrophobic and crystalline drug, resulting with very slight solubility in water and thus, rate of Ral release from the microspheres is very low. In order to overcome this issue, conjugation reaction between Ral and PEG was performed and it was observed that crystalline nature of Ral was converted to amorphous form, which was clearly seen especially by XRD results. Additionally, since PEG is a highly hydrophilic polymer, it is expected that wettability of Ral is increased by conjugation to PEG. Both of these factors provide to increase water-solubility of Ral. It also is known that a hydrophilic drug, which is Ral-PEG in this study, provides water penetration into drug-loaded polymeric systems and generates highly porous polymer structures by drug exit, leading to increased degradation rate of polymers, which are PCL and PLGA in our study (Klose et al., 2008). In other words, enhanced wettability of Ral increases degradation rates of PCL and PLGA by allowing more water penetration into the polymer matrix. In parallel with these finding, expectation and literature knowledge, total amount of Ral released from Ral-PEG-loaded PCL:PLGA (1:1) microspheres was found to be significantly higher than those from other microsphere groups. *In vitro* cytotoxicity studies performed using adipose-derived mesenchymal stem cells demonstrated that none of the microspheres were cytotoxic. Alizarin red S assay was used to evaluate the effects of Ral release from the microspheres on osteogenic differentiation of female

adipose-derived mesenchymal stem cells and it was found that Ral release from Ral-PEG-loaded PCL:PLGA (1:1) microspheres resulted with significantly higher mineralization of the cells in comparison to other microsphere groups. This outcome can be ascribed to significantly higher total amount of Ral released from Ral-PEG-loaded PCL:PLGA (1:1) microspheres relative to other groups. By this finding, it can be deduced that higher rate of Ral release provided higher stimulatory effect on osteogenic differentiation without any toxic effect, referring to enhanced efficacy.

Moreover, dose studies of Ral and Ral-PEG revealed that Ral and Ral-PEG especially at the doses of 0.1  $\mu\text{M}$  were non-toxic for adipose-derived mesenchymal stem cells whereas the other Ral and Ral-PEG doses (1 and 10  $\mu\text{M}$ ) resulted with reduced cell viability. On the other hand, Ral and Ral-PEG at doses of 0.01, 0.1, 1 and 10  $\mu\text{M}$  were non-toxic for hFOB cells. Furthermore, dose-dependent effects Ral and Ral-PEG on ALP activity of hFOB cells were evaluated. It was found that Ral and Ral-PEG at doses of 0.01, 0.1, 1 and 10  $\mu\text{M}$  did not have remarkable stimulatory effects on ALP activity of the cells. In this manner, as Ral effects may vary for different types of cells and for different determinants of osteogenic activity of the cells, the administration route, release rate and amount of drug encapsulated in the carrier should be considered in details during designing a Ral delivery system.

As an advantage of Ral-PEG (1:2)-loaded PCL:PLGA (1:1) microsphere formulation, it can be mentioned that this group provided increased Ral release rate and therefore enhanced mineralization of the stem cells compared to the other formulations in this study. It can be stated that Ral-PEG (1:2)-loaded PCL:PLGA (1:1) microsphere formulation holds promise for osteoporosis therapy as an effective controlled and sustained drug delivery system. Moreover, for forthcoming studies, PEG conjugation to Ral presents the possibility of adjusting release rate of Ral by changing PEG ratio in the conjugate and thus reaching the optimum composition of the microspheres. However,

these positive outcomes obtained in this study should be supported by more analyses for functional evaluation of the system, and further *in vivo* studies should be performed for conclusive results.

## REFERENCES

- Agrawal, C.M., Haas, K.F., Leopold, D.A. & Clark, H.G. Evaluation of poly(L-lactic acid) as a material for intravascular polymeric stents. *Biomaterials*. 1992; 13(3): 176-182.
- Ahuja, N., Katare, O.P. & Singh, B. Studies on dissolution enhancement and mathematical modeling of drug release of poorly water-soluble drug using water soluble carriers. *European journal of pharmaceutics and biopharmaceutics*. 2007; 65: 26–38.
- Anon. HRT: what are women (and their doctors) to do? *Lancet*. 2004; 364: 2069–2070.
- Arias, J.L., López-Viota, M., Sáez-Fernández, E. & Ruiz, M.A. Formulation and physicochemical characterization of poly(epsilon-caprolactone) nanoparticles loaded with ftorafur and diclofenac sodium. *Colloids and Surfaces B: Biointerfaces*. 2010; 75(1): 204-208.
- Attama, A.A. & Mpamaugo, V.E. Pharmacodynamics of piroxicam from self-emulsifying lipospheres formulated with homolipids extracted from *Capra hircus*. *Drug delivery*. 2006; 13: 133–137.
- Babanejad, N., Nikjeh, M.M.A., Amini, M. & Dorkoosh, F.A. A nanoparticulate raloxifene delivery system based on biodegradable carboxylated polyurethane: Design, optimization, characterization, and in vitro evaluation. *Journal of Applied Polymer Science*. 2014; 131(1).
- Bandela, J.J. & Anupama, C.H. Advanced PEGylation for the Development of Raloxifene Hydrochloride, BCS Class II Drug. *Journal of Young Pharmacists*. 2009; 1(4): 295–300.

- Baron, R. & Rawadi, G. Targeting the Wnt/beta-catenin pathway to regulate bone formation in the adult skeleton. *Endocrinology*. 2007; 148(6): 2635–2643.
- Barrett-Connor, E. The economic and human costs of osteoporotic fracture. *The American Journal of Medicine*. 1995; 98(suppl 2A): 3S–8S.
- Bekker, P.J., Holloway, D.L., Rasmussen, A.S., et al. A single-dose placebo-controlled study of AMG 162, a fully human monoclonal antibody to RANKL, in postmenopausal women. *Journal of bone and mineral research*. 2004; 19: 1059–1066.
- Berrodin, T.J., Chang, K.C.N., Komm, B.S., Freedman, L.P. & Nagpal, S. Differential biochemical and cellular actions of Premarin estrogens: Distinct pharmacology of bazedoxifene-conjugated estrogens combination. *Molecular endocrinology*. 2009; 23(1): 74–85.
- Bhandari, K.H., Newa, M., Uludag, H. & Doschak, M.R. Synthesis, characterization and in vitro evaluation of a bone targeting delivery system for salmon calcitonin. *International journal of pharmaceutics*. 2010; 394(1-2): 26–34.
- Bigham-Sadegh, A. & Oryan, A. Basic concepts regarding fracture healing and the current options and future directions in managing bone fractures. *International wound journal*. 2014.
- Bikiaris, D., Karavelidis, V. & Karavas, E. Novel biodegradable polyesters. Synthesis and application as drug carriers for the preparation of raloxifene HCl loaded nanoparticles. *Molecules*. 2009; 14(7): 2410–2430.
- Black, D.M., Cummings, S.R., Karpf, D.B., et al. for the Fracture Intervention Trial Research Group. Randomised trial of effect of alendronate on risk of fracture in women with existing vertebral fractures. *Lancet*. 1996; 348: 1535–1541.

- Black, D.M., Delmas, P.D., Eastell, R., et al. Once-yearly zoledronic acid for treatment of postmenopausal osteoporosis. *The New England journal of medicine*. 2007; 356: 1809–1822.
- Brown, J.P., Prince, R.L., Deal, C., et al. Comparison of the effect of denosumab and alendronate on BMD and biochemical markers of bone turnover in postmenopausal women with low bone mass: a randomized, blinded, phase 3 trial. *Journal of bone and mineral research*. 2009; 24: 153–161.
- Brzozowski, A.M., Pike, A.C., Dauter, Z., et al. Molecular basis of agonism and antagonism in the oestrogen receptor. *Nature*. 1997; 389(6652): 753–758.
- Buckwalter, J.A., Glimcher, M.J., Cooper, R.R. & Recker, R. Bone biology. *The Journal of Bone and Joint Surgery*. 1995; 77: 1256–1275.
- Burra, M., Jukanti, R., Janga, K.Y., Sunkavalli, S., Velpula, A., Ampati, S. & Jayaveera, K.N. Enhanced intestinal absorption and bioavailability of raloxifene hydrochloride via lyophilized solid lipid nanoparticles. *Advanced Powder Technology*. 2013; 24(1): 393–402.
- Cao, X. & Schoichet, M.S. Delivering neuroactive molecules from biodegradable microspheres for application in central nervous system disorders. *Biomaterials*. 1999; 20(4): 329–339.
- Chaumeil, J.C. Micronization: A method of improving the bioavailability of poorly soluble drugs. *Methods and findings in experimental and clinical pharmacology*. 1998; 20: 211–215.
- Chesnut, C.H. 3<sup>rd</sup>, Majumdar, S., Newitt, D.C., et al. Effects of salmon calcitonin on trabecular microarchitecture as determined by magnetic resonance imaging: results from the QUEST study. *Journal of bone and mineral research*. 2005; 20(9): 1548–1561.

- Chesnut, C.H. 3<sup>rd</sup>, Skag, A., Christiansen, C., et al. Effects of oral ibandronate administered daily or intermittently on fracture risk in postmenopausal osteoporosis. *Journal of bone and mineral research*. 2004; 19: 1241–1249.
- Chirra, H.D. & Desai, T.A. Emerging microtechnologies for the development of oral drug delivery devices. *Advanced drug delivery reviews*. 2012; 64(14): 1569–1578.
- Chlebowski, R.T., Wactawski-Wende, J., Ritenbaugh, C., et al. Women's Health Initiative Investigators. Estrogen plus progestin and colorectal cancer in postmenopausal women. *The New England Journal of Medicine*. 2004; 350: 991–1004.
- Cho, C.H. & Nuttall, M.E. Therapeutic potential of oestrogen receptor ligands in development for osteoporosis. *Expert opinion on emerging drugs*. 2001; 6(1): 137–154.
- Cho, J.C., Khang, G., Choi, H.S., et al. Preparation of biodegradable PLGA microspheres for sustained local anesthesia and their in vitro release behavior. *Polymer*. 2000; 24(5): 728–735.
- Christiansen, C., Chesnut, C.H. 3<sup>rd</sup>, Adachi, J.D., et al. Safety of bazedoxifene in a randomized, double-blind, placebo- and active-controlled phase 3 study of postmenopausal women with osteoporosis. *BMC musculoskeletal disorders*. 2010; 11: 130.
- Cohen, S., Yoshioka, T., Lucarelli, M., et al. Controlled delivery systems for proteins based on poly(lactic/glycolic acid) microspheres. *Pharmaceutical research*. 1991; 8(6): 713–720.
- Cowin, S.C., Moss-Salentijn, L. & Moss, M.L. Candidates for the mechanosensory system in bone. *Journal of biomechanical engineering*. 1991; 113(2): 191–197.

- Cummings, S.R., Black, D.M., Nevitt, M.C., Browner, W., Cauley, J., et al. Bone density at various sites for prediction of hip fractures. The Study of Osteoporotic Fractures Research Group. *Lancet*. 1993; 341: 72–75.
- Cummings, S.R., Black, D.M., Nevitt, M.C., et al. Appendicular bone density and age predict hip fracture in women: The study of Osteoporotic Fractures Research Group. *JAMA*. 1990; 263: 665–668.
- Cummings, S.R., Black, D.M., Thompson, D.E., et al. Effect of alendronate on risk of fracture in women with low bone density but without vertebral fractures: results from the Fracture Intervention Trial. *JAMA*. 1998; 280: 2077–2082.
- Cummings, S.R., Eckert, S., Krueger, K.A., et al. The effect of raloxifene on risk of breast cancer in postmenopausal women: results from the MORE randomized trial. Multiple Outcomes of Raloxifene Evaluation. *JAMA*. 1999; 281: 2189–2197.
- Cummings, S.R., Ensrud, K., Delmas, P.D., et al. Lasofoxifene in postmenopausal women with osteoporosis. *The New England journal of medicine*. 2010; 362: 686–696.
- Cummings, S.R., San Martin, J., McClung, M.R., et al. for the FREEDOM Trial. Denosumab for prevention of fractures in postmenopausal women with osteoporosis. *The New England journal of medicine*. 2009; 361: 756–765.
- Currey, J. The mechanical properties of materials and the structure of bone. In: *The mechanical adaptations of bones*. 1984; Princeton: Princeton University Press, p. 3–37.
- Darby, A.J. & Meunier, P.J. Mean wall thickness and formation periods of trabecular bone packets in idiopathic osteoporosis. *Calcified tissue international*. 1981; 33: 199–204.

- Davies, C., Godwin, J., Gray, R., et al. Relevance of breast cancer hormone receptors and other factors to the efficacy of adjuvant tamoxifen: patient-level meta-analysis of randomised trials. *Lancet*. 2011; 378: 771–784.
- Delmas, P.D., Bjarnason, N.H., Mitlak, B.H., et al. Effects of raloxifene on bone mineral density, serum cholesterol concentrations, and uterine endometrium in postmenopausal women. *The New England journal of medicine*. 1997; 337: 1641–1647.
- Delmas, P.D., Ensrud, K.E., Adachi, J.D., et al. for the HORIZON Pivotal Fracture Trial. Efficacy of raloxifene on vertebral fracture risk reduction in postmenopausal women with osteoporosis: four-year results from a randomized clinical trial. *The Journal of clinical endocrinology and metabolism*. 2002; 87: 3609–3617.
- Deshmane, V., Krishnamurthy, S., Melemed, A.S., Peterson, P. & Buzdar, A.U. Phase III double-blind trial of arzoxifene compared with tamoxifen for locally advanced or metastatic breast cancer. *Journal of clinical oncology*. 2007; 25: 4967–4973.
- Doblaré, M., García, J.M. & Gómez, M.J. Modelling bone tissue fracture and healing: A review. *Engineering Fracture Mechanics*. 2004; 71: 1809–1840.
- Elsheikh, M.A., Elnaggar, Y.S.R., Gohar, E.Y. & Abdallah, O.Y. Nanoemulsion liquid pre-concentrates for raloxifene hydrochloride: optimization and in vivo appraisal. *International journal of nanomedicine*. 2012; 7: 3787–802.
- Elva, C., Gallardo, A., Roman, J.S. & Cifuentes, A. Covalent polymer drug conjugates. *Molecules*. 2005; 10: 114–125.
- Ettinger, B., Black, D.M., Mitlak, B.H., et al. Reduction of vertebral fracture risk in postmenopausal women with osteoporosis treated with raloxifene: results from a 3-year randomized clinical trial. Multiple Outcomes of Raloxifene Evaluation (MORE) Investigators. *JAMA*. 1999; 282: 637–645.

- Fisher, B., Costantino, J.P., Redmond, C.K., Fisher, E.R., Wickerham, D.L. & Cronin, W.M. Endometrial cancer in tamoxifen-treated breast cancer patients: Findings from the National Surgical Adjuvant Breast and Bowel Project (NSABP) B-14. *Journal of the National Cancer Institute*. 1994; 86: 527–537.
- Fisher, B., Costantino, J.P., Wickerham, D.L., et al. Tamoxifen for prevention of breast cancer: Report of the National Surgical Adjuvant Breast and Bowel Project P-1 Study. *Journal of the National Cancer Institute*. 1998; 90: 1371–1388.
- Fitzgerald, J.F. & Corrigan, O.I. Investigation of the mechanisms governing the release of levamisole from poly-lactide-co-glycolide delivery systems. *Journal of Controlled Release*. 1996; 42(2): 125–132.
- Fleisch, H., Reszka, A., Rodan, G.A., et al. Bisphosphonates-mechanism of action. In: *Principles of Bone Biology*, Bilezikian, J.P., Raisz, L.G. & Rodan, G.A. (Editors), 2<sup>nd</sup> ed. 2002; Academic Press, San Diego, p. 1361–1385.
- Fouchereau-Peron, M., Moukhtar, M.S., Benson, A.A. & Milhaud, G. Characterization of specific receptors for calcitonin in porcine lung. *Proceedings of the National Academy of Sciences of the United States of America*. 1981; 78: 3973–3975.
- Friedrich, H., Nada, A. & Bodmeier, R. Solid state and dissolution rate characterization of co-ground mixtures of nifedipine and hydrophilic carriers. *Drug development and industrial pharmacy*. 2005; 31: 719–728.
- Frost, H.M. Bone dynamics in metabolic bone disease. *The Journal of bone and joint surgery*. 1966; 48: 1192–1203.

- Garg, A., Singh, S., Rao, V.U., Bindu, K. & Balasubramaniam, J. Solid state interaction of raloxifene HCl with different hydrophilic carriers during co-grinding and its effect on dissolution rate. *Drug development and industrial pharmacy*. 2009; 35(4): 455–470.
- Gennari, L. Lasofoxifene: A new type of selective estrogen receptor modulator for the treatment of osteoporosis. *Drugs of Today*. 2006; 42: 355–367.
- Gennari, L., Merlotti, D., De Paola, V. & Nuti, R. Lasofoxifene: Evidence of its therapeutic value in osteoporosis. *Core evidence*. 2009; 4: 113–29.
- Goodman and Gilman's. *The Pharmacological Basis of Therapeutics*. Hardman, J.G. & Limbird, L.E. (Editors), 10<sup>th</sup> ed. 2001; McGraw Hill: New York, NY, USA.
- Gorn, A.H., Lin, H.Y., Yamin, M., Auron, P.E., Flannery, M.R., Tapp, D.R., Manning, C.A., Lodish, H.F., Krane, S.M. & Goldring, S.R. Cloning, characterization and expression of a human calcitonin receptor from an ovarian carcinoma cell line. *The Journal of clinical investigation*. 1992; 90: 1726–1735.
- Greenspan, S.L., Bone, H.G., Ettinger, M.P., et al. for the Treatment of Osteoporosis with Parathyroid Hormone Study Group. Effect of recombinant human parathyroid hormone (1–84) on vertebral fracture and bone mineral density in postmenopausal women with osteoporosis: a randomized trial. *Annals of internal medicine*. 2007; 146: 326–339.
- Greenwald, R.B., Choe, Y.H., Mcguire, J. & Conover, C.D. Effective drug delivery by PEGylated drug conjugates. *Advanced Drug Delivery Reviews*. 2003; 55: 217–250.
- Grese, T.A., Sluka, J.P., Bryant, H.U., et al. Molecular determinants of tissue selectivity in estrogen receptor modulators. *Proceedings of the National Academy of Sciences of the United States of America*. 1997; 94(25): 14105–14110.

- Guénin, E., Monteil, M., Bouchemal, N., Prangé, T. & Lecouvey, M. Syntheses of phosphonic esters of alendronate, pamidronate and neridronate. *European Journal of Organic Chemistry*. 2007; 3380–3391.
- Hadji, P. The evolution of selective estrogen receptor modulators in osteoporosis therapy. *Climacteric*. 2012; 15(6): 513–523.
- Hancock, B.C. & Parks, M. What is true solubility advantage for amorphous pharmaceuticals? *Pharmaceutical research*. 2000; 17(4): 397–404.
- Hariharan, S., Bhardwaj, V., Bala, I., et al. Design of estradiol loaded PLGA nanoparticulate formulations: a potential oral delivery system for hormone therapy. *Pharmaceutical research*. 2006; 23(1): 184–195.
- Harris, S.T., Watts, N.B., Genant, H.K., et al. for the Vertebral Efficacy with Risedronate Therapy (VERT) Study Group. Effects of risedronate treatment on vertebral and nonvertebral fractures in women with postmenopausal osteoporosis: a randomized controlled trial. Vertebral Efficacy with Risedronate Therapy (VERT) Study Group. *JAMA*. 1999; 282: 1344–1352.
- Heaney, R.P. Why does bone mass decrease with age and menopause? In: *Proceedings of the 4<sup>th</sup> International Symposium on Osteoporosis and Consensus Development Conference*, Christiansen, C. (Editor). 1993; Hong Kong, p. 15.
- Hiremath, J.G. & Devi, V.K. Tamoxifen loaded poly ( $\epsilon$ -caprolactone) based injectable microspheres for breast cancer. *International Journal of Pharmacy & Pharmaceutical Sciences*. 2010; 2(4): 189–195.
- Ikegame, M., Ejiri, S. & Ozawa, H. Calcitonin-induced change in serum calcium levels and its relationship to osteoclast morphology and number of calcitonin receptors. *Bone*. 2004; 35(1): 27–33.

- Jeong, J.-C., Lee, J. & Cho, K. Effects of crystalline microstructure on drug release behavior of poly( $\epsilon$ -caprolactone) microspheres. *Journal of Controlled Release*. 2003; 92(3): 249–258.
- Kang, J. & Schwendeman, S.P. Pore closing and opening in biodegradable polymers and their effect on the controlled release of proteins. *Molecular pharmaceutics*. 2007; 4(1): 104–118.
- Karsdal, M.A., Martin, T.J., Bollerslev, J., et al. Are nonresorbing osteoclasts sources of bone anabolic activity? *Journal of bone and mineral research*. 2007; 22(4): 487–494.
- Keshavarz, A., Karimi-Sabet, J., Fattahi, A., Golzary, A., Rafiee-Tehrani, M. & Dorkoosh, F.A. Preparation and characterization of raloxifene nanoparticles using Rapid Expansion of Supercritical Solution (RESS). *Journal of Supercritical Fluids*. 2012; 63: 169–179.
- Khan, S., Batchelor, H., Hanson, P., Perrie, Y. & Mohammed, A.R. Physicochemical characterisation, drug polymer dissolution and in vitro evaluation of phenacetin and phenylbutazone solid dispersions with polyethylene glycol 8000. *Journal of pharmaceutical sciences*. 2011; 100(10): 4281–4294.
- Kleinman, D., Karas, M., Danilenko, M., Arbell, A., et al. Stimulation of endometrial cancer cell growth by tamoxifen is associated with increased insulin-like growth factor (IGF)-I induced tyrosine phosphorylation and reduction in IGF binding proteins. *Endocrinology*. 1996; 137(3): 1089–1095.
- Klose, D., Siepmann, F., Elkharraz, K. & Siepmann, J. PLGA-based drug delivery systems: Importance of the type of drug and device geometry. *International journal of pharmaceutics*. 2008; 354(1-2): 95–103.
- Lee, K.C., Park, M.O., Na, D.H., Youn, Y.S., Lee, S.D., Yoo, S.D., Lee, H.S. & DeLuca, P.P. Intranasal delivery of PEGylated salmon calcitonins: hypocalcemic effects in rats. *Calcified tissue international*. 2003; 73: 545–549.

- Lee, W.L., Chao, H.T., Cheng, M.H. & Wang, P.H. Rationale for using raloxifene to prevent both osteoporosis and breast cancer in postmenopausal women. *Maturitas*. 2008; 60: 92–107.
- Lewis, D.H. Controlled release of bioactive agents from lactide/glycolide polymers. In: *Biodegradable polymers as drug delivery systems*, Chasin, M. & Langer, R. (Editors). 1990; Marcel Dekker: New York, p. 1–43.
- Lim, V. & Clarke, B.L. New therapeutic targets for osteoporosis: beyond denosumab. *Maturitas*. 2012; 73(3): 269–272.
- Mahmood, S., Taher, M. & Mandal, U.K. Experimental design and optimization of raloxifene hydrochloride loaded nanotransfersomes for transdermal application. *International Journal of Nanomedicine*. 2014; 12(9): 4331–4346.
- Marks, S.C. Jr. & Odgren, P.R. Structure and development of the skeleton. In: *Principles of Bone Biology*, Bilezikian, J.P., Raisz, L.G. & Rodan, G.A. (Editors), 2<sup>nd</sup> ed. 2002; Academic Press, San Diego, p. 3–15.
- Maximov, P., Lee, T. & Jordan, V.C. The Discovery and Development of Selective Estrogen Receptor Modulators (SERMs) for Clinical Practice. *Current Clinical Pharmacology*. 2013; 8(2): 135–155.
- Mazess, R.B. On aging bone loss. *Clinical Orthopaedics & Related Research*. 1982; 165: 239–252.
- McClung, M.R., Geusens, P., Miller, P.D., et al. for the Hip Intervention Program Study Group. Effect of risedronate on the risk of hip fracture in elderly women. Hip Intervention Program Study Group. *The New England journal of medicine*. 2001; 344: 333–340.
- McDermott, M.T. & Kidd, G.S. The role of calcitonin in the development and treatment of osteoporosis. *Endocrine reviews*. 1987; 8: 377–390.

- McDonnell, D.P. The molecular pharmacology of estrogen receptor modulators: Implications for the treatment of breast cancer. *Clinical cancer research*. 2005; 11: 871s–877s.
- Melton, L.J. 3<sup>rd</sup>, Chrischilles, E.A., Cooper, C., Lane, A.W. & Riggs, B.L. Perspective. How many women have osteoporosis? *Journal of bone and mineral research*. 1992; 7(9): 1005–1010.
- Meruane, M.A., Rojas, M. & Marcelain, K. The use of Adipose Tissue-Derived Stem Cells within a dermal substitute improves skin regeneration by increasing neoangiogenesis and collagen synthesis. *Plastic and Reconstructive Surgery*. 2012; 130(1): 53–63.
- Meunier, P.J., Roux, C., Seeman, E., et al. The effects of strontium ranelate on the risk of vertebral fracture in women with postmenopausal osteoporosis. *The New England journal of medicine*. 2004; 350: 459–468.
- Miller, S.C. & Jee, W.S.S. Bone lining cells. In: *Bone*, Hall, B.K. (Editor). 1992; Boca Raton: CRC Press, p. 1–19.
- Mundy, G.R. Pathogenesis of osteoporosis and challenges for drug delivery. *Advanced drug delivery reviews*. 2000; 42(3): 165–173.
- Murillo, M., Gamazo, C., Goñi, M.M., Irache, J.M. & Blanco-Príeto, M.J. Development of microparticles prepared by spray-drying as a vaccine delivery system against brucellosis. *International journal of pharmaceutics*. 2002; 242(1-2): 341–344.
- Naot, D. & Cornish, J. The role of peptides and receptors of the calcitonin family in the regulation of bone metabolism. *Bone*. 2008; 43: 813–818.
- Neer, R.M., Arnaud, C.D., Zanchetta, J.R., et al. Effect of parathyroid hormone (1–34) on fractures and bone mineral density in postmenopausal women with osteoporosis. *The New England journal of medicine*. 2001; 344: 1434–1441.

- Nicholson, G.C., D'Santos, C.S., Evans, T., Moseley, J.M., Kemp, B.E., Michelangeli, V.P. & Martin, T.J. Human placental calcitonin receptors. *The Biochemical journal*. 1988; 250: 877–882.
- NIH Consensus Development Panel on Osteoporosis Prevention, Diagnosis, and Therapy. Osteoporosis prevention, diagnosis, and therapy. *JAMA*. 2001; 285: 785–795.
- Nilsson, S. & Koehler, K.F. Oestrogen receptors and selective oestrogen receptor modulators: Molecular and cellular pharmacology. *Basic and Clinical Pharmacology and Toxicology*. 2005; 96: 15–25.
- Öcal, Y., Kurum, B., Karahan, S., Tezcaner, A., Ozen, S. & Keskin, D. Characterization and evaluation of triamcinolone, raloxifene, and their dual-loaded microspheres as prospective local treatment system in rheumatic rat joints. *Journal of pharmaceutical sciences*. 2014; 103(8): 2396–2405.
- Park, J.H., Eom, S., Kim, D.S., Kim, W., Kim, Y.K., et al. Double-Layered PLGA Microspheres for Effective Controlled Release of Raloxifene-HCl: Preparation and Characterization. *Tissue Engineering and Regenerative Medicine*. 2009; 6(12): 1172–1178.
- Patel, S., Lyons, A.R. & Hosking, D.J. Drugs used in the treatment of metabolic bone diseases. *Drugs*. 1993; 46: 594–617.
- Patil, P.H., Belgamwar, V.S., Patil, P.R. & Surana, S.J. Solubility Enhancement of Raloxifene Using Inclusion Complexes and Cogrinding Method. *Journal of Pharmaceutics*. 2013; 2013: 1–9.
- Pitt, C.G. Poly ( $\epsilon$ -caprolactone) and its co-polymers. In: *Biodegradable Polymers as Drug Delivery Systems*, Chasin, M. & Langer, R. (Editors). 1990; Marcel Decker, New York, p. 71–120.

- Poole, K.E.S., van Bezooijen, R.L., Loveridge, N., Hamersma, H., Papapoulos, S.E., Löwik, C.W. & Reeve, J. Sclerostin is a delayed secreted product of osteocytes that inhibits bone formation. *The FASEB journal*. 2005; 19: 1842–1844.
- Prakash, S.J., Santhiagu, A. & Jasemine, S. Preparation, Characterization and In Vitro Evaluation of Novel Gellan Gum-Raloxifene HCl Nanoparticles. *Journal of Pharmaceutical and BioSciences*. 2014; 2: 63–71.
- Proiakakis, C.S., Mamouzelos, N.J., Tarantili, P.A., et al. Swelling and hydrolytic degradation of poly(D,L-lactic acid) in aqueous solutions. *Polymer degradation and stability*. 2006; 91(3): 614–619.
- Rachner, T.D., Khosla, S. & Hofbauer, L.C. Osteoporosis: now and the future. *Lancet*. 2011; 377(9773): 1276–1287.
- Ramtoola, Z., Corrigan, O.I. & Barrett, C.J. Release kinetics of fluphenazine from biodegradable microspheres. *Journal of microencapsulation*. 1992; 9(4): 415–423.
- Ravn, P., Hosking, D., Thompson, D., et al. Monitoring of alendronate treatment and prediction of effect on bone mass by biochemical markers in the early postmenopausal intervention cohort study. *The Journal of clinical endocrinology and metabolism*. 1999; 84(7): 2363–2368.
- Recker, R.R. Embryology, anatomy, and microstructure of bone. In: *Disorders of Bone and Mineral Metabolism*, Coe, F.L. & Favus, M.J. (Editors). 1992; New York, Raven Press, p. 219–240.
- Reginster, J.Y. & Burlet, N. Osteoporosis: A still increasing prevalence. *Bone*. 2006; 38: S4–S9.

- Reginster, J.Y., Seeman, E., De Vernejoul, M.C., et al. Strontium ranelate reduces the risk of nonvertebral fractures in postmenopausal women with osteoporosis: Treatment of Peripheral Osteoporosis (TROPOS) study. *The Journal of clinical endocrinology and metabolism*. 2005; 90: 2816–2822.
- Riggs, B.L. & Melton, L.J. 3<sup>rd</sup>. The worldwide problem of osteoporosis: Insights afforded by epidemiology. *Bone*. 1995; 17(5): 505S–511S.
- Riggs, B.L., Wahner, H.W., Dunn, W.L., Mazess, R.B., Offord, K.P. & Melton, L.J. Differential changes in bone mineral density of the appendicular and axial skeleton with aging. Relationship to spinal osteoporosis. *Journal of Clinical Investigation*. 1981; 67: 328–335.
- Rodan, G.A. Introduction to Bone Biology. *Bone*. 1992; 13: S3–S6.
- Rodan, G.A. & Martin, T.J. Therapeutic Approaches to Bone Diseases. *Science*. 2000; 289(5484): 1508–1514.
- Rogers, T.L., Hu, J., Yu, Z., Johnston, K.P. & Williams III, R.O. A novel particle engineering technology: Spray freezing into liquid. *International journal of pharmaceutics*. 2002; 242: 93–100.
- Rutanen, E.M., Heikkinen, J., Halonen, K., Komi, J., Lammintausta, R. & Ylikorkala, O. Effects of ospemifene, a novel SERM, on hormones, genital tract, climacteric symptoms, and quality of life in postmenopausal women: a double-blind, randomized trial. *Menopause*. 2003; 10: 433–439.
- Sambrook, P. & Cooper, C. Osteoporosis. *Lancet*. 2006; 367: 2010–2018.
- Sato, M., Rippey, M.K. & Bryant, H.U. Raloxifene, tamoxifen, nafoxidine, or estrogen effects on reproductive and nonreproductive tissues in ovariectomized rats. *FASEB journal*. 1996; 10(8): 905–912.

- Sawaki, M., Wada, M., Sato, Y., et al. High-dose toremifene as firstline treatment of metastatic breast cancer resistant to adjuvant aromatase inhibitor: A multicenter phase II study. *Oncology Letters*. 2012; 3: 61–65.
- Seeman, E. & Delmas, P.D. Bone quality-The material and structural basis of bone strength and fragility. *The New England journal of medicine*. 2006; 354: 2250–2261.
- Shi, D. & Wen, X. Bioactive ceramics: Structure, synthesis and mechanical properties. In: *Introduction to biomaterials*, Shi, D. (Editor). 2006; Tsinghua University Press, China, p. 14–15.
- Shier, D., Butler, J. & Lewis, R. *Human anatomy and physiology*. 1996; Wm. C. Brown Publishers, London, p. 187–190.
- Shin, B.S., Jung, J.H., Lee, K.C. & Yoo, S.D. Nasal absorption and pharmacokinetic disposition of salmon calcitonin modified with low molecular weight polyethylene glycol. *Chemical & pharmaceutical bulletin*. 2004; 52: 957–960.
- Shive, M.S. & Anderson, J.M. Biodegradation and biocompatibility of PLA and PLGA microspheres. *Advanced drug delivery reviews*. 1997; 28(1): 5–24.
- Silverman, S.L., Christiansen, C., Genant, H.K., et al. Efficacy of bazedoxifene in reducing new vertebral fracture risk in postmenopausal women with osteoporosis: results from a 3-year, randomized, placebo-, and active-controlled clinical trial. *Journal of bone and mineral research*. 2008; 23: 1923–1934.
- Silvestroni, L., Menditto, A., Frajese, G. & Gnessi, L. Identification of calcitonin receptors in human spermatozoa. *The Journal of clinical endocrinology and metabolism*. 1987; 65: 742–746.
- Singh, J., Pandit, S., Bramwell, V.W. & Alpar, H.O. Diphtheria toxoid loaded poly-(epsilon-caprolactone) nanoparticles as mucosal vaccine delivery systems. *Methods*. 2006; 38(2): 96–105.

- Sinha, V.R., Bansal, K., Kaushik, R., Kumria, R. & Trehan, A. Poly-epsilon-caprolactone microspheres and nanospheres: an overview. *International journal of pharmaceutics*. 2004; 278(1): 1–23.
- Skerry, T.M., Bitensky, L., Chayen, J. & Lanyon, L.E. Early strain-related changes in enzyme activity in osteocytes following bone loading in vivo. *Journal of bone and mineral research*. 1989; 4(5): 783–788.
- Smith, D.M., Khairi, M.R.A. & Johnston, C.C.J. The loss of bone mineral with aging and its relationship to risk of fracture. *Journal of Clinical Investigation*. 1975; 56: 311–318.
- Sommerfeldt, D.W. & Rubin, C.T. Biology of bone and how it orchestrates the form and function of the skeleton. *European spine journal*. 2001; 10 Suppl 2: S86–95.
- Stevenson, J.C. & Evans, I.M. Pharmacology and therapeutic use of calcitonin. *Drugs*. 1981; 21: 257–272.
- Taluja, A. & Bae, Y.H. Role of a novel excipient poly(ethylene glycol)-b-poly(L-histidine) in retention of physical stability of insulin at aqueous/organic interface. *Molecular pharmaceutics*. 2007; 4(4): 561–570.
- Talukder, R., Connelly, K., Dürig, T. & Fassihi, R. Dissolution Rates Enhancement of Raloxifene HCl using Binary PEG Mixtures (poster presentation).
- Tankó, L.B., Bagger, Y.Z., Alexandersen, P., et al. Safety and efficacy of a novel salmon calcitonin (sCT) technology-based oral formulation in healthy postmenopausal women: acute and 3-month effects on biomarkers of bone turnover. *Journal of bone and mineral research*. 2004; 19(9): 1531–1538.
- Taranta, A., Brama, M., Teti, A., De luca, V., Scandurra, R., et al. The selective estrogen receptor modulator raloxifene regulates osteoclast and osteoblast activity in vitro. *Bone*. 2002; 30(2): 368–376.

- Teeter, J.S. & Meyerhoff, R.D. Environmental fate and chemistry of raloxifene hydrochloride. *Environmental toxicology and chemistry*. 2002; 21(4): 729–736.
- Torrado, J.J., Illum, L. & Davis, S.S. Particle size and size distribution of albumin microspheres produced by heat and chemical stabilization. *International Journal of Pharmaceutics*. 1989; 51: 85–93.
- Tran, T.H., Poudel, B.K., Marasini, N., Chi, S.-C., Choi, H.-G., Yong, C.S. & Kim, J.O. Preparation and evaluation of raloxifene-loaded solid dispersion nanoparticle by spray-drying technique without an organic solvent. *International journal of pharmaceutics*. 2013; 443(1-2): 50–57.
- Tripathi, A., Gupta, R. & Saraf, S.A. PLGA Nanoparticles of Anti Tubercular Drug : Drug Loading and Release Studies of a Water In-Soluble Drug. *International Journal of PharmTech Research*. 2010; 2(3): 2116–2123.
- Uhrich, K.E., Cannizzaro, S.M., Langer, R.S. & Shakesheff, K.M. Polymeric Systems for Controlled Drug Release. *Chemical Reviews*. 1999; 99(11): 3181–3198.
- Van Nijlen, T., Brennan, K., Van den Mooter, G., Blaton, N., Kinget, R. & Augustijns, P. Improvement of the dissolution rate of artemisinin by means of supercritical fluid technology and solid dispersion. *International journal of pharmaceutics*. 2003; 254(2): 173–181.
- Vassilopoulou-Sellin, R. Breast cancer and hormonal replacement therapy. *Annals of the New York Academy of Sciences*. 2003; 997: 341–350.
- Vogel, V.G., Costantino, J.P., Wickerham, D.L., et al. Effects of tamoxifen vs raloxifene on the risk of developing invasive breast cancer and other disease outcomes: the NSABP Study of Tamoxifen and Raloxifene (STAR) P-2 trial. *JAMA*. 2006; 295: 2727–2741.
- Wang, D., Miller, S.C., Kopecková, P. & Kopecek, J. Bone-targeting macromolecular therapeutics. *Advanced drug delivery reviews*. 2005; 57(7): 1049–1076.

Warshawsky, H., Goltzman, D., Rouleau, M.F. & Bergeron, J.J.M. Direct in vivo demonstration by radioautography of specific binding sites for calcitonin in skeletal and renal tissues of the rat. *The Journal of cell biology*. 1980; 85: 682–694.

Weiner, S. & Wagner, H.D. The Material Bone: Structure-Mechanical Function Relations. *Annual Review of Materials Science*. 1998; 28(1): 271–298.

Wischke, C. & Schwendeman, S.P. Principles of encapsulating hydrophobic drugs in PLA/PLGA microparticles. *International journal of pharmaceutics*. 2008; 364(2): 298–327.

[www.sigmaaldrich.com](http://www.sigmaaldrich.com) (last visited on August 2014).

[www.sigmaaldrich.com/life-science/metabolomics/enzyme-explorer/analytical-enzymes/alkaline-phosphatase.html](http://www.sigmaaldrich.com/life-science/metabolomics/enzyme-explorer/analytical-enzymes/alkaline-phosphatase.html) (last visited on August 2014).

Zacchigna, M., Cateni, F., Drioli, S., Procida, G. & Altieri, T. PEG-Ursolic Acid Conjugate: Synthesis and In Vitro Release Studies. *Scientia pharmaceutica*. 2014; 82(2): 411–421.



# APPENDIX A

## ETHICAL COMMITTEE REPORT

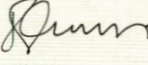
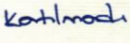
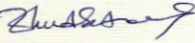
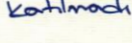
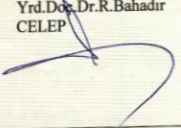


T.C.  
AFYON KOCATEPE ÜNİVERSİTESİ  
Hayvan Deneyleri Yerel Etik Kurulu  
(AKUHADYEK)

Sayı: 49533702/ 405  
Konu: AKUHADYEK-278-13-Referans nolu araştırma  
Doç.Dr. Z. Korhan ALTUNBAŞ  
A.K. Ü. Veteriner Fakültesi Histoloji ve Embriyoloji AD.  
Afyonkarahisar

Tarih : 21/11/2013

Üniversitemiz Hayvan Deneyleri Yerel Etik Kurulu'na sunmuş olduğunuz "Raloksifen ve Raloksifen-Polietilen Glikol Yüklü Mikroküreler ile Mezenkimal Kök Hücreleri İçeren Jel Sisteminin Kemik Defektlerini İyileştirme Potansiyelinin İncelenmesi" isimli araştırma projesi AKUHADYEK yönetmeliğine ve evrensel etik ilkelere uyumlu olduğuna karar verilmiş ve **onaylanmıştır**.

Görevi	Adı	İmza	Görevi	Adı	İmza
Başkan	Prof. Dr. Yahya KUYUCUOĞLU		Üye	Doç. Dr. Bülent ELİTOK	
Üye	Prof. Dr. Hatice ÇİÇEK		Üye	Vet. Hekim Engin GÖKSEL	
Üye	Doç.Dr. Z. Kadir SARITAŞ		Üye	(sivil toplum kuruluş üyesi) Halil KARGA	
Üye	Doç. Dr. Roha DEMREL		Üye	(Halk üyesi) Yunus DOLU	
Üye	Yrd.Doç.Dr.R.Bahadır CELEP				

Gazlıgöl yolu üzeri A.N.S kampüsü 03200 AFYONKARAHİSAR Tel : (272) 214 96 70



## APPENDIX B

### CHROMATOGRAMS & CALIBRATION CURVES USED DURING RELEASE STUDIES

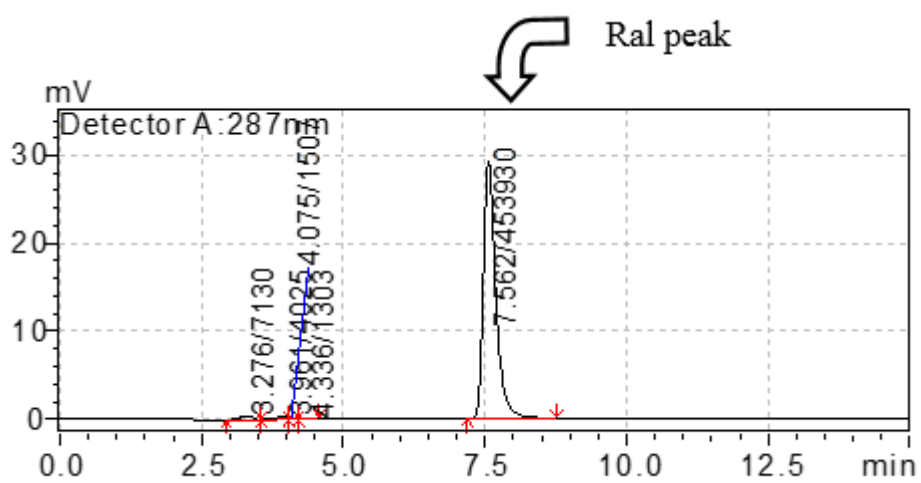


**Figure 58.** Chromatogram of 5  $\mu\text{g/mL}$  Ral in MeOH:PBS (1:1) obtained by HPLC.

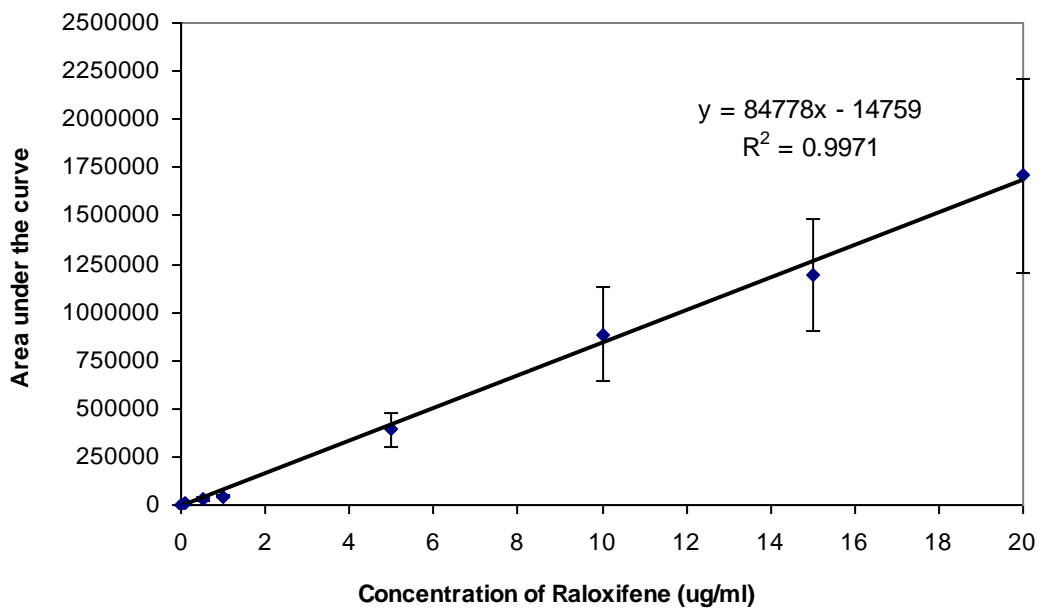


**Figure 59.** Calibration curve of Ral in MeOH:PBS (1:1) obtained by HPLC for release studies.

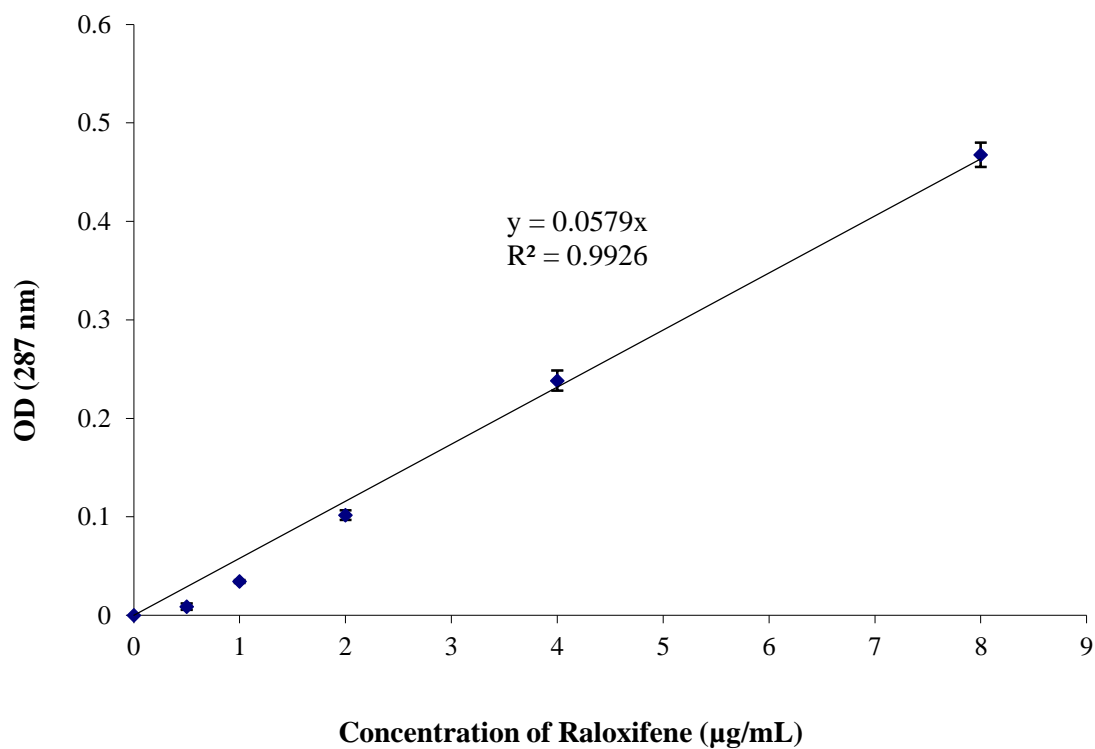


**Figure 60.** Calibration curve of Ral in MeOH:PBS (1:1) obtained by spectrophotometry for release studies.



## APPENDIX C

### CALIBRATION CURVE USED DURING ENCAPSULATION EFFICIENCY ANALYSES

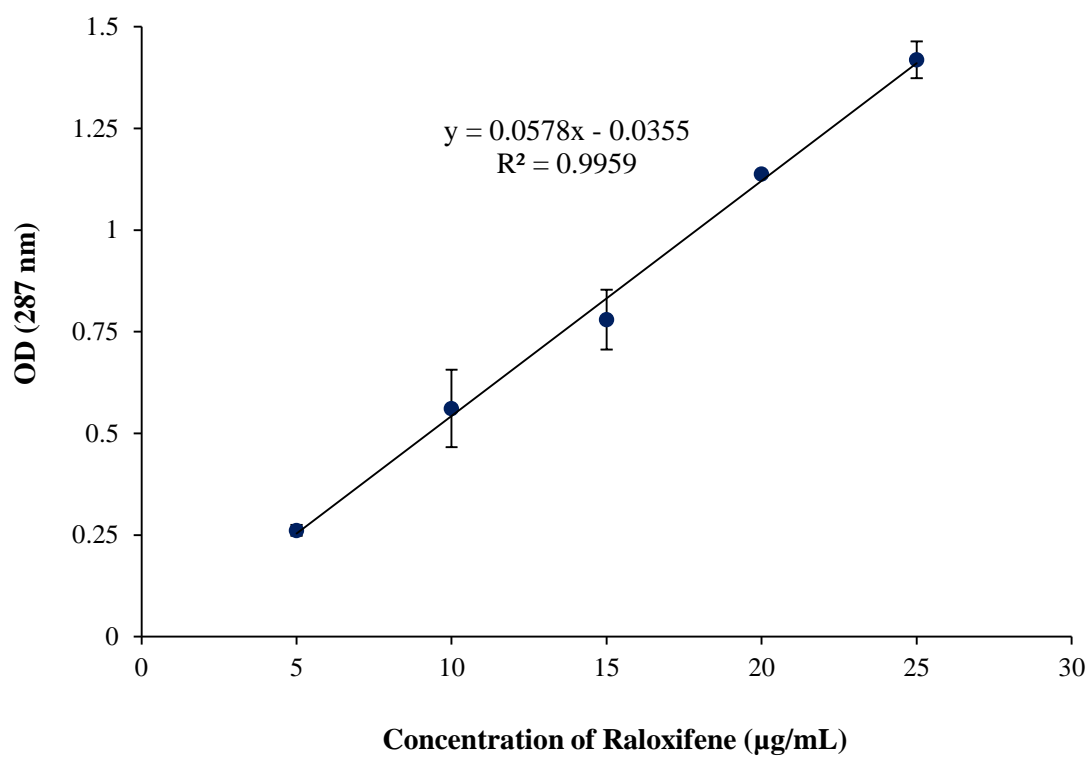


**Figure 61.** Calibration curve of Ral in DCM:MeOH (1:1) obtained by spectrophotometry for determination of Ral encapsulated in the microspheres.



## APPENDIX D

### CALIBRATION CURVE USED DURING ALP ACTIVITY ANALYSES

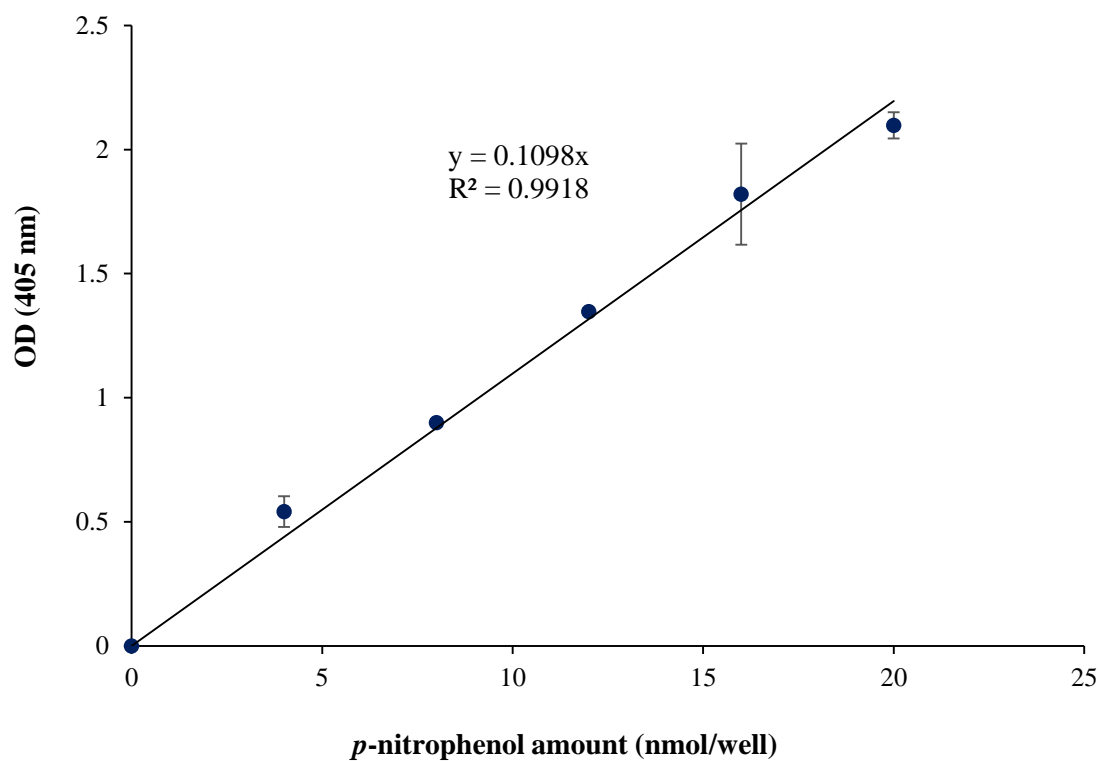


**Figure 62.** Calibration curve of *p*-nitrophenol (nmol/well) for determination of ALP activity of the cells.



# CURRICULUM VITAE

## PERSONAL INFORMATION

Surname, Name: Kavas, Ayşegül  
Nationality: Turkish (TC)  
Date and Place of Birth: 03 August 1980, Tokat  
Marital Status: Single  
Phone: +90 312 285 33 77  
email: aysegul\_kavas@yahoo.com

## EDUCATION

Degree	Institution	Year of Graduation
MS	METU, Engineering Sciences	2007
BS	METU, Chemical Engineering	2003
High School	Ankara Atatürk Anadolu High School, Ankara	1998

## WORK EXPERIENCE

Year	Place	Enrollment
2005-2013	METU Department of Engineering Sciences	Research Assistant
2002 August	Anadolu Refinery Inc. Co., Commercial Depart.	Intern Engineering Student
2001 August	Sugar Factory, Production and Laboratory Depart.	Intern Engineering Student

## FOREIGN LANGUAGES

Advanced English, Basic German

## PUBLICATIONS

1. Kavas A., Cagatay S.T., Banerjee S., Keskin D., Tezcaner A. Potential of Raloxifene in reversing osteoarthritis-like alterations in rat chondrocytes: an in vitro model study. *Journal of Biosciences*. 2013; 38(1): 135-147.
2. Kavas A., Ozdemir M., Gürses S., Keskin D., Tezcaner A. In vitro investigation and biomechanical modeling of the effects of PLF-68 on osteoarthritis in a three-dimensional model. *Biomechanics and modeling in mechanobiology*. 2011; 10(5): 641-650.

3. Akpinar O., Ak O., Kavas A., Bakir U., Yilmaz L. Enzymatic production of xylo-oligosaccharides from cotton stalks. *Journal of Agricultural and Food Chemistry*. 2007; 55: 5544-5551.

## **HOBBIES**

Music, Photography, Swimming, Travelling